Fire Ecology

Fire regime assumptions can drastically influence pyrodiversity-biodiversity relationships in heterogeneous forest landscapes

Ceres Barros[1,2,3*], Cameron E. Naficy[4,5], David W. Andison[6], Ian M. S. Eddy[1], Alex M. Chubaty[7], Tatiane Micheletti[2,8], Steven G. Cumming[3], J. John Stadt[9], Eliot J. B. McIntire[1,2]

[1]Pacific Forestry Centre, Canadian Forest Service, Natural Resources Canada, 506 Burnside Road West, Victoria, BC, V8Z 1M5, Canada.
[2]Department of Forest Resources Management, University of British Columbia, 2424 Main Mall, Vancouver, V6T 1Z4, BC, Canada
[3]Faculté de Foresterie, de Géographie et de Géomatique, Département des Sciences du Bois et de la Forêt, Pavillon Abitibi-Price, 2405, rue de la Terrasse, Université Laval, Québec, G1V 0A6, Canada
[4]Forest and Conservation Sciences, University of British Columbia, 2424 Main Mall, Vancouver, BC, V6t 1Z4, Canada
[5]Department of Forestry, Division of Natural Resources & Sciences, Salish Kootenai College, Pablo MT 59855, USA
[6]Bandaloop Landscape Ecosystem Services Ltd. 6552 Littlewood Road, Nelson, BC. L1V 6S1, Canada.
[7]FOR-CAST Research & Analytics, PO Box 96026 RPO West Springs, Calgary, AB, T3H 0L3, Canada
[8]Helmholtz Centre for Environmental Research—UFZ, Permoserstraße 15, Leipzig, Saxony, 04318, Germany
[9]Forestry Division, Alberta Forestry and Parks, 7000-113 Street NW, Edmonton, AB, T6H 5T6, Canada

***Corresponding author's email address:** ceres.barros@nrcan-rncan.gc.ca

ORCID IDs

C. Barros: 0000-0003-4036-977X

C. E. Naficy: 0000-0001-5733-1300

D. W. Andison: 0000-0001-7135-7160

I. M. S. Eddy: 0000-0001-7397-2116

A. M. Chubaty: 0000-0001-7146-8135

T. Micheletti: 0000-0003-4838-8342

S. G. Cumming: 0000-0002-7862-2913

J. J. Stadt: 0000-0003-3398-5646

E. J. B. McIntire: 0000-0002-6914-8316

Word count: 7579

Abstract

Background. Higher spatio-temporal variation in fire regime attributes in fire-dominated landscapes (pyrodiversity) is thought to promote higher levels of biodiversity – the pyrodiversity-biodiversity hypothesis – yet this effect likely varies across taxa and systems. As a result, ecosystem-based management in heterogenous, fire-dominated forests requires understanding the strength and shape of local pyrodiversity-biodiversity relationships (PBRs). Landscape simulation models can be an effective tool for quantifying the PBR, but they require evaluation of key assumptions. Using LandR, a forest landscape model, evaluated against a dendroecological dataset of historical fire regimes and age structure, we investigated the PBR across forest types of the Montane subregion of the southwestern Alberta Foothills, Canada. We used *n*-dimensional hypervolumes as a multivariate measurement of pyrodiversity and forest diversity and examined how the PBR changed under two modelling assumptions about fire-caused tree mortality – partial mortality (mixed-severity model) and complete mortality (stand-replacing model).

Results. Comparisons against dendroecological data showed that the mixed-severity model provided better estimates of fire intervals, and of old growth and forest diversity under the observed short fire intervals. However, it overestimated *Pseudotsuga menziesii* dominance and age across the landscape. Both models showed little support for positive PBRs in this area and

revealed that PBR strength and direction varied between models, scales and forest types. These results highlight the context-dependency of this relationship.

Conclusions. Our findings underscore how fire severity modelling assumptions that support land management frameworks can have serious consequences for forest diversity and old growth. We also caution against extrapolating observed PBRs across systems and fire regimes, especially in heterogeneous landscapes.

Keywords: pyrodiversity-biodiversity hypothesis; forest landscape model; LandR; mixed-severity; stand-replacement; n-dimensional hypervolumes; natural disturbance regime

Background

Wildfires are amongst the most common disturbances in forest ecosystems worldwide (Bowman et al. 2009). They play an important role in forest succession, biodiversity and, consequently, the provisioning of ecosystem services (He et al. 2019). Fire regime attributes, such as fire frequency, size, return interval, and severity, influence spatio-temporal patterns of landscape vegetation, forest regeneration and extent, and successional trajectories and diversity of the whole ecosystem (Kozlowski 1974; Bond and van Wilgen 1996). Changes in fire regime attributes, due to climate change or land management decisions (Barros et al. 2021), are therefore likely to trigger cascading effects on biodiversity and will also affect the economy of forestry-dependent industries and communities (Brockerhoff et al. 2017). Hence, in wildfire-prone areas, natural disturbance-based forest management that aims to support biodiversity and ecosystem services should emulate the historical fire regimes with which forests co-evolved (Kuuluvainen and Grenfell 2012). Doing so requires understanding how local fire regimes interact with biodiversity, and how both respond to land and fire management decisions (Kelly et al. 2017).

The pyrodiversity-biodiversity hypothesis (PBH) posits a positive relationship between the spatio-temporal variation in fire regime attributes in a landscape ('pyrodiversity' sensu Steel et al. 2021) and biodiversity (usually measured as species richness; Jones and Tingley 2021). It provides a useful and testable framework that can guide and inform forest management in response to the changing fire regimes that many places are experiencing (Kelly et al. 2017). Since Martin & Sapsis (1992) first presented the PBH, studies have provided conflicting evidence of the sign and strength of this relationship (see Jones and Tingley 2021; Jones et al. 2022). These conflicts stem largely from the eco-evolutionary context (Kelly et al. 2017; Steel et al. 2021), but also from scale and measurement issues (Jones and Tingley 2021). For instance, as both pyrodiversity and biodiversity generally scale with spatial and temporal extent (Lawton 1999; He et al. 2019), the PBR can change depending on the scale of analysis (Jones and

Tingley 2021). Also, despite encompassing the variation of multiple fire regime attributes, pyrodiversity is often defined as variation in a single fire regime attribute (often fire severity; Steel et al. 2024). This can be problematic as different fire regime attributes can have different relationships with biodiversity (Gordijn and O'Connor 2021), and a similar issue likely arises from different biodiversity metrics (Giljohann et al. 2015).

Fire severity – here, the degree of aboveground vegetation mortality caused by fire – is an important aspect of pyrodiversity and the PBR. Variation in fire severity is a common proxy for pyrodiversity (Stillman et al. 2019; Steel et al. 2021), as its role in creating spatio-temporal variation in fuel properties and vegetation conditions (McIntire et al. 2005; Perrault-Hébert et al. 2017; Rainsford et al. 2021) should lead to increased variation in other fire regime attributes (Lertzman et al. 1998; Agee 2005). In mixed-severity fire regimes, where severity varies significantly within and/or between fires, this higher fire regime variability (i.e. pyrodiversity) generates higher diversity in forest structures and compositions, which in turn reinforces pyrodiversity via variable fuel conditions (Halofsky et al. 2011). On the other hand, a high-severity fire regime characterised by high mortality stand-replacing fires may generate more homogeneous fuel properties and fire attributes (Marcoux et al. 2013), from which lower forest diversity and pyrodiversity may arise.

Nevertheless, this does not preclude positive PBRs under stand-replacing fire regimes. High-severity fires can also generate biodiversity by creating diverse post-fire understory assemblages (Coop et al. 2010), successional trajectories, and fuel conditions (see Turner and Romme 1994), and can be associated with high pyrodiversity when combined with variable combinations of fire return interval. Here, the spatial scale of analysis will have an important effect on perceived and measured pyrodiversity (He et al. 2019), since the captured spatio-temporal variation in fire frequency and patch size will increase with spatial scale. Given these complex relationships between the PBR, scale and severity patterns across fire regime

121 gradients, quantifying how the PBR responds to varying levels of fire severity and whether these
122 effects change across forest types remains a challenge.
123 Overcoming this challenge is essential if the PBR is to be used to guide disturbance-based
124 forest management (Parr and Andersen 2006). Yet, empirically assessing PBRs under varying
125 fire regimes and severity patterns is difficult. Both experimental fire treatments and
126 observational studies can be logistically challenging and fail to capture the full range of fire
127 regime conditions and post-fire forest succession pathways that occur over multi-decadal
128 timescales. Ecological simulation models can be used to explore beyond these limits when
129 formulated to represent multiple spatial ecological processes in complex systems (Kelly et al.
130 2020) and over extended time series (Kimmins et al. 2008). If calibrated and evaluated against
131 observed data, these models can be used to evaluate how pyrodiversity, forest diversity and
132 their relationship respond to fire regimes with different severity dynamics, and to potentially
133 inform forest management.
134 This is especially important in heterogeneous landscapes, such as southwestern Rocky
135 Mountains of Alberta, Canada. Until recently, forest management frameworks in this area have
136 implicitly assumed stand-replacing fire regimes (Johnson and Larsen 1991; Stockdale et al.
137 2016). Yet, mounting evidence supports historically high pyrodiversity with multi-scaled spatial
138 variation in severity across portions of this region (Amoroso et al., 2011; Naficy & Daniels, 2020;
139 Rogeau et al., 2016). Assumptions about historical patterns of fire severity can determine
140 annual allowable cuts and harvest practices aiming to emulate natural disturbances
141 (Government of Alberta 2021), impacting the diversity of forest structures and compositions and,
142 consequently, biodiversity. For instance, clear-cutting (the removal of all or almost all
143 merchantable forest volume within a cutblock) is still the dominant forest harvest approach
144 across Alberta (Government of Alberta 2017), yet it more closely reproduces stand-replacing
145 fires and fire regimes (Bergeron et al. 2002). If mixed-severity fire regimes dominate the SW
146 Canadian Rockies and are associated with higher pyrodiversity and forest diversity, forest

147 management that emulates stand-replacing fires may not be effective in achieving desired
148 outcomes. By exploring model outputs from different fire severity regimes and validating them
149 against observed data, we can better understand their implications for pyrodiversity, forest
150 diversity and their relationship, and ultimately inform ecosystem-based management.
151 Here, we use the forest landscape model LandR (Barros et al. 2023) and dendroecological
152 records to test assumptions of pre-industrial fire regime severity in the heterogeneous forests of
153 the SW Rocky Mountains of Alberta, Canada, and evaluate their impacts on the PBR. Where
154 available, dendroecological records are an opportune empirical data source to inform simulation
155 modelling of fire regimes and forest outcomes, due to their long time series which capture broad
156 variability of fire regime attributes (e.g. frequency, severity), drivers, and forest attributes (e.g.
157 stand age). Our objectives were two-fold. First, we used dendroecological data to evaluate the
158 relative support for two fire severity models in the study area: a model allowing for partial fire-
159 caused mortality (hereafter 'mixed severity') and a model simulating only complete fire-caused
160 mortality (hereafter 'stand-replacement'). Second, we evaluated how the two models differed in
161 terms of generated pyrodiversity and forest diversity (a surrogate for biodiversity), and the
162 resulting PBRs at two spatial scales: the landscape scale (i.e. across forest types) and the
163 forest-type scale (within a given forest type). We used multidimensional measures of
164 pyrodiversity and of forest diversity that respectively integrated various fire regime and forest
165 attributes, as this should be more appropriate to assess the PBR at the community or
166 ecosystem level (Steel et al. 2024). We hypothesised that stand-replacing fire regimes would
167 generate lower pyrodiversity and lower forest diversity than mixed-severity fire regimes, due to
168 lower spatio-temporal variation in post-fire mortality. We also expected the stand-replacement
169 model to generate lower variation in pyrodiversity and forest diversity values and, consequently,
170 generally weaker PBRs.
171

Methods

Study area

Our study area (~2 000 000 ha) is situated in the Rocky Mountain, Parkland and Grassland natural regions of SW Alberta, Canada (Fig. 1; Downing and Pettapiece 2006). It is characterised by strong elevational gradients and ecotones between grasslands, mixed woodlands of *Populus* spp. (aspen) and, less frequently, *Betula* spp. (birch), and pure coniferous forests. In the montane zone (i.e. mid to low elevations), forests are dominated by *Pseudotsuga menziesii* (Mirbel) Franco (Douglas-fir), or by *P. menziesii* and other conifers. In the subalpine zone (i.e. high to mid elevations), *Pinus contorta* Douglas (lodgepole pine) is dominant at mid elevations and warmer sites, while *Picea* spp. (spruces) and *Abies lasiocarpa* (Hooker) Nuttall (subalpine fir) dominate on cooler sites and higher elevations (Johnson and Larsen 1991; Rogeau et al. 2016). The climate is continental with cold winters and warm, dry summers (mean annual temperature = 4°C) and precipitation regimes dominated by winter snowpack and spring monsoons (Calgary International & Kananaskis stations; Environment Canada 2020). High-severity fire regimes dominate the upper and some of the lower subalpine areas (Fryer and Johnson 1988; Rogeau et al. 2016), transitioning into a more spatially heterogeneous regime of high- and mixed-severity fires in the lodgepole pine, Douglas-fir, and mixedwood forests of the montane zone (Amoroso et al. 2011; Rogeau et al. 2016; Naficy and Daniels 2020).

Model overview

LandR is a forest landscape model implemented in *R,* using the SpaDES meta-package (Chubaty and McIntire 2022), as a group of ‘simulation’ and ‘data’ and ‘calibration’ modules (Barros et al. 2023) that can be linked with other SpaDES modules to simulate additional processes, like fire spread (e.g. Micheletti et al. 2023). Here, we used the ‘simulation modules’ *Biomass_core*, *Biomass_regenerationPM* and *Biomass_regeneration* for cohort dynamics and

198 *Biomass_fuelsPFG*, *fireProperties* and *FavierFireSpread,* for fire dynamics. They were linked to
199 the 'data' and 'calibration' modules *Biomass_speciesData*, *Biomass_borealDataPrep* and
200 *Biomass_speciesParameters,* which prepared vegetation-related parameters and landscape
201 initial conditions, and *fireWeather*, *fireSense_DataPrep*, *fireSense_IgnitionFit, and*
202 *fireSense_IgnitionPredict,* which prepared fire-related parameters (Table A.1 Appendix A). Input
203 data and modules were chained in a continuous workflow that allowed for semi-automated
204 parameterisation (Fig. 2). Data modules automatically retrieved and prepared data from FAIR
205 sources (Wilkinson et al. 2016) as much as possible; however, in some cases, we used higher
206 quality proprietary data. Since we aimed to reproduce pre-industrial forest and fire dynamics, we
207 parametrised and initialised the models using climate and vegetation data that best matched a
208 pre-climate change period, while providing sufficient spatial coverage. For climate, we used data
209 from the 1961-1990 normals period, and for vegetation we used forest attributes and land-cover
210 data ranging from 1990 to 2011. See Table A.2 for details on input data, Appendices B and C
211 for full details on data treatment, parameterisation steps and dynamic models.
212 The core forest succession simulation module, *Biomass_core* has been described in
213 detail in Barros *et al*. (2023) and the online manual (Barros et al. 2022). Briefly, it simulates
214 yearly aboveground biomass dynamics of tree cohorts (unique combinations of species and
215 age), arising from cohort growth, mortality, competition (for space and light), recruitment (local
216 and dispersal) at the pixel level (Fig. 2). Cohort age is measured in years and cohort biomass in
217 g/m^2. The *Biomass_regenerationPM* ("partial mortality") and *Biomass_regeneration* modules
218 simulate cohort responses to fire by removing entire cohorts within burnt pixels (mortality) and
219 activating serotiny and resprouting for entirely or partially killed species that have these traits.
220 They differ in their ability to simulate partial fire-caused mortality. *Biomass_regenerationPM*
221 determines cohort mortality as a function of a pixel-level fire severity class, cohort age and the
222 species fire tolerance, following the approach in LANDIS-II Dynamic Fire System v3.0
223 (Sturtevant et al. 2018; Appendix B). *Biomass_regeneration* always simulates stand-replacing

fires, killing all cohorts in a burnt pixel. Both modules calculate 'actual' pixel-level fire severity as raw and relative biomass burnt (the total amount biomass lost, in g/m^2, and its ratio to pre-fire total biomass). Here, we used relative biomass burnt as the chosen fire severity metric in all analyses.

Fire dynamics were simulated by the *FavierFireSpread* module as a three-stage process, fire ignition, escape and spread, in all vegetated pixels (forested and non-forested). All three processes depended on pixel-level weather, fuels and topography. Daily weather for the 1961-1990 period was generated by BioSIM (Régnière et al. 2017) using corresponding climate normals; initial fuel conditions were derived from species and land-cover data and dynamically updated every year by *Biomass_core* and *Biomass_fuelsPFG*; elevation, aspect and slope were derived from a digital elevation model (Table A.2; Appendices B and C).

Fire ignition depended on ignition probability, which was estimated by the *fireSense_IgnitionFit* module and projected every year by *fireSense_IgnitionPredict*. Ignition probabilities were calculated from the relationship between fire occurrences (fire point data), daily weather and fuel conditions (Marchal et al. 2017) in the study area between 1961 and 1990 (i.e. a "pre-climate-change" period). To simulate fire at each year, we re-estimated ignition probabilities using randomly drawn 'fire day' (FWI >= 19; Podur and Wotton 2011) from the entire 1961-1990 period and the updated fuels; fires ignition success was assessed with binomial random drawn conditional on spread probability (Appendices B and C). A fire then escaped to a neighbouring pixel if its spread probability, p, was larger than a randomly generated number in the [0,1] range. Subsequent spread was modelled using Favier's (2004) fire percolation model, whereby spread to neighbouring pixels also depended on p and could re-occur depending on the persistence probability, q, which determined whether fire persisted in a given pixel for another iteration and potentially spread again. Both p and q were conditional on fire behaviour properties (calculated by *fireProperties*), which depended on the spatiotemporally varying weather and fuels, and topography conditions. We could not calibrate p and q based on

data, as only four fires occurred in the study area between 1961 and 1990 (Canadian Forest Service 2019). Instead, we used a simple multiplicative relationship between fire behaviour properties to calculate *p* and *q* values, and rescaled and bounded their values to allow realistic fire spread and size patterns (*p* in [0.25; 0.25] and *q* in [0,1]; Appendix B). Four fire perimeters were also insufficient to statistically estimate maximum fire size. Instead, we used a constant maximum fire size equal to the largest fire recorded in the area between 1919 and 2019 (Canadian Forest Service 2019).

Simulation setup and model runs

We ran simulations using two alternative fire regime models and weather from the 1961-1990 period, to test which fire severity regime best matched the pre-industrial fire regime of the study area: a mixed-severity model (M_{MS}) using the *Biomass_regenerationPM* module, and a stand-replacing model (M_{SR}) using the *Biomass_regeneration* module.

In both models, vegetation dynamics were simulated in forested pixels only (identified as forest land-cover classes in the Land Cover Map of Canada 2010; Fig. A.1, Appendix A). Fire dynamics were simulated in all vegetated pixels, but in non-forested pixels (e.g. shrublands and grasslands) fuel types were kept constant throughout the simulations. Simulations in forested pixels encompassed six species or species groups: *Abies spp* (representing *A. lasiocarpa* (Hooker) Nuttalland *A. balsamea* (L.) Mill.), *Picea engelmannii* Parry ex Engelm., *Picea glauca* (Moench) Voss, *Pinus spp* (comprising *P. albicaulis* Engelm. and *P. contorta*), a '*Populus/Betula sp*' group (comprising *P. tremuloides*, *P. balsamifera* L., and *Betula papyrifera* Marshall) and *P. menziesii* (Fig. A.2). The landscape was initialised entirely from available data obtained, cleaned and formatted by the *Biomass_speciesData* and *Biomass_borealDataPrep* modules. Species cohorts were "seeded" in forested pixels across the landscape by multiplying the observed species % cover by the observed stand biomass, and assigning the same data-derived stand age to all species in the same pixel (see Table A.1 and Appendix C for details).

Each model was run for 2000 years, to reach quasi-equilibrium with the generated weather, and replicated 5 times to capture variability arising from stochasticity in dispersal, recruitment and fire processes. Cohort biomass and age were saved every five years; fire perimeters and corresponding pixel-level severity class and fire severity (i.e. relative biomass burnt) were saved every year. We used the last 500 years of each replicate (quasi-equilibrium period) in our subsequent analyses and subset pixels to the Montane subregion (Fig. 1), where dendroecological data were available.

Evaluating the mixed-severity and stand-replacing models

Assuming that the simulated quasi-equilibrium dynamics reflect pre-industrial fire regimes and forest dynamics, we tested our two models' ability to reproduce observed stand ages and fire intervals derived from dendroecological reconstructions in our study area (Naficy & Daniels, 2020). Dendroecological samples were collected in 51 forested patches, delineated from historical (1940) aerial imagery (Naficy and Daniels 2020), distributed across geographic, structural, compositional, and biophysical gradients of the montane zone. Within each patch, a representative sample of 20 to 60 increment cores from living trees (>4 cm diameter at breast height, DBH) were collected from multiple (2-6) spatially distributed age structure plots, with larger sample effort in patches with more complex fire histories and age structures. Sampled tree species included *Abies lasiocarpa*, *Picea engelmannii*, *Pinus contorta, Populus tremuloides* and *Populus balsamifera*, and *P. menziesii*. Here, *Populus tremuloides* and *P. balsamifera* records were merged into *Populus spp.* Establishment dates from the age structure records spanned 1568-1991 CE. Fire scar samples were collected from exhaustive surveys conducted within and around each sample patch, resulting in fire history reconstructions spanning 1476-1936 CE, with the most robust record covering the 1717-1936 CE period. All increment cores and fire scar samples were crossdated using master chronologies built from local samples (Naficy & Daniels 2020). To restrict our analyses to the pre-industrial period, we excluded

samples from stands estimated to have been established after 1940, leaving a total of 1979 sampled trees. This also resulted in all patches in the sample having a record of at least one fire event. Stand ages were then calculated as the median age of all trees in a patch, weighted by tree basal area. Summary statistics of the observed dataset are presented in Table 1.

To allow for more direct comparisons between simulated data and observed data, we emulated the field sampling methods described above. First, we classified pixels into different forest types (FTs) using the forest classification method used in the field (Appendix D; for clarity we use species common names when referring to FTs and scientific names when referring to species). In the same way that FTs in the field arise from past fire regimes, the FTs of the last 500 years of simulation arose from fire and vegetation processes in equilibrium with historical climate. Because this is a dynamic equilibrium, species age values in a given pixel can vary temporally and among replicates. Hence, for simulated ages, we i) sampled 5 years from the quasi-equilibrium period using a systematic sampling approach (once every century for each replicate, resulting in 25 sampled years), ii) classified pixels into FTs for each sampled year and iii) calculated ages at the species- or stand-level in each pixel and sampled year. Simulated fire intervals integrated all years of the quasi-equilibrium period, so we classified pixels into FTs at the last year of the simulation and calculated fire intervals as the number of years between subsequent fire events, and the first and last year of the simulation period per pixel (Steel et al., 2021). Non-forested pixels and pixels that did not experience fire events during the quasi-equilibrium period were excluded from the analyses since field methods targeted forested areas with fire evidence. Also, we excluded all cohorts whose ages were lower than age at minimum DBH, i.e., the measurement threshold in our observed data (species-level age ~ DBH relationships were statistically estimated using the observed data; Appendix C).

To evaluate stand ages from model runs, we compared the median biomass-weighted cohort age (calculated as simulated stand ages per pixel, sampled year, replicate and model) with the basal-area weighted patch ages in the observed data. At the species level, raw cohort

ages were evaluated against tree ages reconstructed from dendrochronologies, and calculated species age as the median cohort age, per pixel, sampled year, replicate and model. As for fire interval evaluations, we took the temporally integrated mean fire intervals per pixel, replicate and model and calculated medians per forest type; we compared these with the observed median fire intervals calculated at the patch-level. Model evaluation was done visually by plotting i) the density distributions of simulated and observed ages and fire intervals, ii) the mean absolute deviations (MAD) from observed fire intervals, and iii) the deviations between simulated and observed quantile ages (quantile deviations, QD) as:

$$MAD_{ij} = \frac{\sum_{k=1}^{N}(|FI_{sim_{ijk}} - \underline{FI_{obs_j}}|)}{N} \quad \text{[Eq. 1]}$$

$$QD_{ij} = quantAge_{sim_{ij}} - quantAge_i \quad \text{[Eq. 2]}$$

where FI_{sim} are median fire intervals per FT, *i*, in a given simulation replicate, *j,* and pixel, *k*. *N* is the total number of pixels. $\underline{FI_{obs_j}}$ is observed average median fire internal calculated across all patches within *j*. $quantAge_{sim}$ is the simulated quantile age value calculated across all pixels and sampled years, per species or FT, *i*, and replicate, *j*. $quantAge_{obs}$ is the observed age quantile calculated across all patches for each *i*. We considered the 50%, 75% and 95% quantiles given their relevance to old growth forest management and conservation. Both MAD and QD were also calculated across the landscape (i.e. across species and FTs in the Montane subregion).

Assessing the pyrodiversity-forest-diversity relationship

To assess differences between the two models with respect to generated pyrodiversity and forest diversity and the PBR (our second objective), we used *n*-dimensional hypervolumes to measure pyrodiversity and forest diversity (as a proxy for biodiversity). This follows suggestions by Steel et al. (2021) that pyrodiversity should be quantified using multivariate approaches and by Barros et al. (2016) who suggest using *n*-dimensional hypervolumes for a multivariate assessment of changes in ecosystem structure, and consequently biodiversity. Pyrodiversity

353 hypervolumes were based on three temporally integrated fire properties: fire frequency, mean
354 patch size and mean fire severity (as relative biomass lost). All metrics were calculated per pixel
355 and simulation replicate, and across the full quasi-equilibrium period to represent the simulated
356 fire regime, and following Steel et al. (2021). Forest diversity hypervolumes were based on
357 pixel-level species relative abundances (as in C. Barros et al., 2016), mean and standard
358 deviation of biomass-weighted cohort age, obtained from the same five sampled years used to
359 evaluate the models (see above). We used the full simulated dataset within the Montane region.
360 We calculated hypervolumes at the landscape scale and by FT, per replicate and across
361 years (for pyrodiversity) or per year (for forest diversity). This is, each pixel, or pixel and year
362 combination in the case of forest diversity hypervolumes, constituted a data point entering the
363 hypervolume. We used the same year sample as above for comparisons with observed age
364 data; however, here FTs were classified only at the last year of the quasi-equilibrium period,
365 instead of every year. This is because here we were interested in capturing the variation in
366 attributes over this period that led to a given FT (within a dynamic equilibrium state), regardless
367 of whether its classification changed along with this variation. This is distinct from the
368 comparison exercise above, where we wanted to capture the variation of age compositions over
369 the quasi-equilibrium period within a specific FT. Also, non-forested pixels were included in
370 these hypervolume analyses, as they represent an important component of landscape pyro- and
371 forest-diversity. As in Barros et al. (2016), hypervolumes were calculated on PCA axes
372 coordinates rather than directly on fire and forest variables and replicated thrice to account for
373 variability generated by the hypervolume estimation algorithm (see Appendix D).
374 Hypervolume size was used as a metric of overall diversity, with larger hypervolumes
375 indicating higher variability of fire regimes (higher pyrodiversity) and of forest composition and
376 age structure (higher forest diversity). The PBR was assessed for each model at the landscape
377 and FT levels, by modelling forest diversity as a function of the interaction between pyrodiversity
378 and model type, or the three-way interaction between pyrodiversity, model type and FT. Both

pyrodiversity and forest diversity were logged to meet residual assumptions. In the FT level model, we allowed the variance to differ between model and FT combination using a generalised least squares (GLS) framework. Given that the PBR is likely to be quadratic (He et al., 2019; Steel et al., 2021), we tested model performance with an added quadratic pyrodiversity term. Including a quadratic pyrodiversity term did not improve either model at the landscape or FT level and resulted in patterns that were hard to interpret.

We also analysed the effect of model type on pyrodiversity and on forest diversity, separately. We modelled the response of pyrodiversity and forest diversity to model type (using linear models) and to the interaction between model type and FT (using GLS models with different variance allowed for each model type and FT combination). We used log-hypervolume sizes to meet residual assumptions for forest-diversity hypervolumes, but not for pyrodiversity hypervolumes.

Across all models, we used *post-hoc t*-tests to test differences in estimated marginal means between models, across the landscape and per FT. See Tables S1.3, S1.5-S1.6 (Appendix A) for all model formulae.

Results

General patterns

In general the two models produced similar species ages and biomasses in pixels that never burned during the quasi-equilibrium phase, with the exception of higher *Pinus spp* biomasses resulting from stand-replacing model (M_{SR}) simulations, and slightly higher *Pseudotsuga menziesii* biomasses resulting from mixed-severity model (M_{MS}) simulations (Fig. 3a,c). This can be explained by increased propagule pressure from burned pixels where these species dominated in each model, and by burning legacies from before the quasi-equilibrium phase, as these pixels may have burnt in the preceding 1500 years of simulation.

In pixels that burned during the quasi-equilibrium phase, the M_{SR} produced average species ages that dropped steadily as fire return intervals decreased, and ages that were less variable between and within species. At short fire return intervals of 25-30 years matching the observed median 28-year fire interval (Naficy & Daniels, 2020), the M_{SR} predicted an even-aged landscape (note low variability around 50 years; Fig. 3b) of young and co-dominant *Pinus spp*, *Populus/Betula spp* cohorts, and low to no biomass of other species. The early successional *Pinus spp*, *Populus/Betula spp* dominated burnt pixels up to fire return intervals of 100 years, after which late-successional and longer-lived species like *P. menziesii* and *Picea spp* were able to dominate or co-dominate.

Conversely, the M_{MS} allowed most species to reach overall older ages, and produced larger variability in ages between and within species, especially in *Picea spp* and *P. menziesii* (Fig. 3a,b). These patterns were most evident in the fire tolerant *P. menziesii*, whose old cohorts (> 200 years) were prevalent even at short fire return intervals of 25-30 years. The M_{MS} also created a more diverse and balanced landscape in terms of species composition. *P. menziesii* dominated or co-dominated the landscape across most of the fire return interval range (Fig. 3c,d). This co-dominance was more balanced in pixels that experienced fire intervals between 30-40 years, which created opportunities for both early successional species to establish and the survival of *P. menziesii*, especially in lower severity patches (Fig. 3d). At longer fire intervals, *Pinus spp* and *Populus/Betula spp* stabilized at intermediate biomass levels and were replaced by *Picea spp* as co-dominants; at very short fire intervals *Pinus spp* and *Populus/Betula spp* were the only ones able to grow and colonize quickly after a fire.

Support for the mixed-severity and stand-replacing fire models

Each model's ability to reproduce observed age and fire return interval patterns depended on species and the quantile value analysed in the case of age, and on forest type (FT) in the case of fire return interval. Both models predicted more young cohorts, higher maximum ages for *P.*

menziesii and *Picea engelmannii*, and lower maximum ages for *Pinus spp.*, *Populus/Betula spp.* (Fig. 4a). They showed large deviations (≥ +50 years) from the observed upper age quantiles for *P. menziesii* and *Picea engelmannii* (Fig. 4b). In the case of the M_{MS}, this resulted in large positive age deviations across the landscape, given the large dominance of *P. menziesii* (Fig. A.4). The M_{MS} approximated observed upper quantile ages better for *Pinus spp*, *Populus/Betula spp*, and worse for *P. menziesii*, *Picea engelmannii* and across the landscape. On the other hand, the M_{SR} model under-predicted upper quantile ages for *Pinus spp*, *Populus/Betula spp* and across the landscape. Both models performed similarly for *Abies spp* ages. At the FT scale, both models generally overpredicted stand ages, with the M_{MS} performing worse in stands dominated by *P. menziesii* (dry conifer and Douglas-fir forest) and at the landscape scale – again, due to the large dominance of this species in M_{MS} simulations (Fig. A.3).

Fire intervals were generally overestimated by both models (Fig. 5a), especially in moist-conifer-, spruce- and Douglas-fir-dominated stands. The M_{MS} provided a better or equally good approximation of observed mean fire intervals for all FTs, but not across the landscape (Fig. 5b). Once again, this is due to the large dominance of Douglas-fir stands generated in M_{MS} that drive larger landscape-level deviations, as landscape-level MAD values are equivalent to the average FT-level MAD weighted by the number of pixels in each FT (see Fig. A.4 for number of pixels per FT). In contrast, the M_{SR} simulations generated a large dominance of Pine and dry-conifer stands with overall shorter fire intervals that decreased the landscape-wide average.

Pyrodiversity and forest diversity under mixed-severity and stand-replacing fire models

Unsurprisingly, the M_{MS} model simulated significantly higher pyrodiversity both across the landscape and all FTs, except pine-dominated forests (Fig. 6a,b; Tables A.3 and A.4). Broadleaf, mixed, moist-conifer, spruce and Douglas-fir forests, along with non-forested pixels, had the highest pyrodiversity levels with both models. Dry-conifer and pine-dominated forests had the lowest pyrodiversity levels with the M_{MS}, while dry Douglas-fir forests had the lowest

pyrodiversity levels with M_{SR}. Similarity in pyrodiversity levels, however, did not always mean similar fire regime attribute distributions (Fig. A.5). For example, broadleaf forests had overall smaller patch sizes, shorter fire intervals and higher severities than Douglas-fir forests, but their pyrodiversity levels were comparably high. At the landscape scale, the larger pyrodiversity levels generated by the M_{MS} were associated with larger variation in all three fire regime attributes.

In contrast with pyrodiversity results, whether the M_{MS} or the M_{SR} generated higher or lower forest diversity depended on the forest type and scale (Fig. 6b,d; Tables A.3 and A.5). At the forest type scale, pine, dry-conifer and dry-Douglas-fir forests and non-forested pixels had higher forest diversity with the M_{MS} (Fig. 6b), owing to a combination of higher species diversity (Fig. A.4) and, in dry-conifer forests, more variable stand ages (Fig. A.3a). On the other hand, the M_{SR} model created more diverse mixed forests (Fig. 6b), as the higher relative abundances of early successional species (*Pinus spp* and *Betula/Populus spp*) and of *Picea glauca,* combined with stand-replacing fires, created more variability in species and age compositions between different pixels of this forest type (Fig. A.4). In broadleaf, moist-conifer, spruce and Douglas-fir dominated forests, we found no significant difference in average forest diversity levels generated by M_{MS} and M_{SR}, although the M_{MS} resulted in overall more diverse moist-conifer forests (Fig. A.4). Across the landscape, the M_{MS} generated lower levels of forest diversity (Fig. 6d) associated with the large dominance of Douglas-fir (Fig. A.4).

Across the landscape, we observed a strong negative pyrodiversity-forest-diversity relationship with M_{SR} and a weak positive relationship under the M_{MS} that post-hoc tests revealed was not statistically significant. This pattern, however, was not consistent across forest types (Fig. 7a) and the relationship was more often not statistically significant for any given model (Table A.3). Exceptions were broadleaf and moist conifer forests, where M_{MS} resulted in a strong negative relationship; dry Douglas-fir forests, where M_{SR} resulted in weak and negative

relationship; and spruce forests, where M_{MS} and M_{SR} respectively resulted in negative and positive relationships (Fig. 7a, Table A.3).

Discussion

When compared with observed data, neither of the two models perfectly matched the fire intervals or the species and stand ages reconstructed from dendroecological samples. Both models generally overpredicted fire intervals and the amount of young cohorts, and although the mixed-severity regime model (M_{MS}) resulted in a better approximation of observed fire intervals across forest types, it still overestimated ages for the longer-lived fire tolerant species (*P. menziesii* and *Picea engelmannii*). Together, these deviations indicate that we underestimated fire occurrence and possibly fire severity, which we discuss below in *Future work and considerations for modelling historic fire regimes*.

Two other factors may also explain the young cohort overpredictions. The first is that field methods excluded small (young) trees and, despite our effort to account for this when filtering the simulated data, our estimates of age at minimum DBH may be too low, resulting in including overly young cohorts in the comparisons. The second factor is that LandR likely underestimates mortality of young cohorts. *Populus spp/Betula spp*, for instance, frequently suffer disease- and insect-driven mortality that can significantly reduce stem density at young ages (Peterson and Peterson 1992); yet LandR does not currently simulate these processes, and development-related mortality (i.e. due to intra- and inter-specific competition) is low. Our inability to simulate these additional mortality drivers was also the reason why *Pinus spp* and *Populus/Betula spp* maximum ages were underpredicted, as we set their longevities to values lower than what individual trees can reach to better simulate cohort decay and mortality.

Despite these departures from observed age patterns, the M_{MS} provided a better approximation to the observed fire return intervals and allowed for older cohorts and higher species diversities at comparable fire intervals. Under a stand-replacing regime, median fire

intervals of 30 years produced young cohort ages (ca. 50 years and low variability) and only *Pinus spp* and *Populus/Betula spp* were able to survive in burnt pixels, which does not reflect the diversity of fire-legacy compositions present in the region (Naficy and Daniels 2020). In addition, Naficy and Daniels (2020) reported ca. 30% of fires were low- and moderate-severity in pine-dominated forests, which are usually associated with stand-replacing regimes. In other forest types, proportions of low- and moderate-severity fires were even higher. Taken together with our results, this provides support for the mixed-severity model in this area.

Our analyses of pyrodiversity, forest diversity, and their relationship (PBR) demonstrated how assumptions about fire regime severity influence these diversity metrics, but also how the scale of analysis and forest type (FT) impact the strength and direction of the PBR. At the landscape scale, the mixed-severity simulations did not support a PBR and the stand-replacing simulations supported a negative landscape-wide PBR. Despite generating higher pyrodiversity, the mixed-severity model led to a landscape-wide dominance of *P. menziesii*. This long-lived and fire-tolerant species was able to either dominate or co-exist with other species, lowering dissimilarity between pixels and creating smaller forest diversity hypervolumes. Conversely, the stand-replacing regime frequently re-initiated forest succession and created more heterogeneity in pixel age and species compositions with consequently larger forest diversity hypervolumes at comparably lower pyrodiversity levels.

At the FT scale, the mixed-severity model generated forest diversity values that were generally similar (in four FTs) or higher (in four FTs) than the stand-replacing model's, and the slope of the PBR changed between severity models, as well as between FTs for a given model. For instance, in moist-conifer-dominated forests we obtained no relationship (M_{SR}) or a negative PBR (M_{MS}). These FTs had high pyrodiversity, associated with longer mean fire intervals, moderate to low mean fire severity and larger mean patch sizes (Fig. A.6). Dendroecological analyses showed a predominance of moderate- to high-severity fires in these forests (Naficy and Daniels 2020), indicating that a mixed-severity regime with higher pyrodiversity, but lower-

severity fires, may lead to departures from the historical fire regime and stronger biodiversity reductions, as suggested by our models.

Interestingly, both models showed little support for positive PBR relationships, indicating that in certain landscape, ecological, and fire regime contexts lower pyrodiversity levels may be capable of enhancing diversity, or simply the PBR is not observable. This is not to say that fire regime attributes do not play a role in shaping biodiversity in this landscape, but rather that their spatio-temporal variation may not clearly drive tree diversity responses. Calhoun *et al.* (2025) found a similar pattern, whereby severity level rather than its variability (pyrodiversity) was the main driver of bird and bat diversity, sometimes with a positive effect. Although we did not statistically assess whether individual fire regime attributes explained significantly more forest diversity variation than pyrodiversity, our results suggest that effects depend on the attribute and the scale of analysis (Fig. A.7). Together, our results further support that a) PBRs are likely not universal and depend on fire regime and ecological constraints (He et al. 2019; Miller and Safford 2020; Steel et al. 2021), as well as measurement scale (Jones et al. 2022; Steel et al. 2024); b) contrary to simplistic predictions, the higher pyrodiversity generated by mixed-severity fire regimes may not always relate to higher forest diversity; and c) that higher pyrodiversity generated by stand-replacing regimes can be negatively associated with forest diversity.

We note, however, that the majority of studies explicitly quantifying pyrodiversity and the PBR focused on understory plants and other taxa (Jones and Tingley 2021). We only found one study investigating PBRs that included tree species and that focused on temperate and boreal forest systems (Bell et al. 2026). Also, most of these studies measured pyrodiversity using single fire regime attributes (Steel et al. 2024), which can show different relationships with biodiversity (Greenwood et al. 2024). This and the fact that our pyrodiversity and biodiversity metrics integrate different fire regime and forest attributes, limit our ability to compare our results with other lines of evidence for PBRs. Nonetheless, studies in western Canada have shown both positive and negative severity and understory plant diversity relationships depending on

plant group (Pinno and Errington 2016; Dickson-Hoyle et al. 2024), which again support the context dependency of diversity and fire attribute relationships. Furthermore, although our hypervolume-based measure of forest diversity accounts for tree species diversity, evenness, and age structure in a stand, it is still a narrow view of local plant diversity. For instance, Bell et al. (2026) found that plant diversity measured across all plant and tree species was positively related to pyrodiversity (measured as burn severity variation). Hence, it is likely that other relationships could be observed if we extended our metric to other plant groups and taxa.

Implications for management

Our results have important implications for forest management in the southeastern Canadian Rockies and in other heterogeneous forest landscapes. They raise questions of how to manage pyrodiversity to promote forest diversity and to what extent our assumptions of fire severity can impact our ability to reproduce a 'natural' fire regime and predict pyro- and biodiversity in a fire-dominated landscape.

Forest management across North America and Europe has been shifting towards ecosystem-based management that emulates natural disturbances (Kuuluvainen et al. 2021). This rests on the principle that reproducing 'natural' disturbance regimes promotes the preservation of biodiversity, ecological structure, and ecosystem services (Stockdale et al. 2016). Yet, the success of this undertaking largely depends on the level of understanding of local fire regimes and how they impact forests (Johnson et al. 1998), not to mention how 'natural regimes' are defined given the role of humans in shaping historical fire regimes (Bowman et al. 2011). In the southeastern Canadian Rockies, wildfire has historically been the disturbance with the largest impacts on landscape patterns, forest structure and functioning (Johnson and Larsen 1991; Perbet et al. 2025), including carbon emissions and sequestration (Goetz et al. 2012). In this region, disturbance-based management is therefore focused on reproducing 'natural' fire regimes, yet an assumption of stand-replacing fires often underlines management guidelines.

As we increase our understanding about pre-industrial ('natural') fire regimes in this area, it becomes evident that this assumption is not adequate. Studies have revealed higher fire frequencies in these pre-industrial forests than in post-European settlement periods (Amoroso et al. 2011; Chavardès and Daniels 2016; Davis et al. 2016), likely due to the exclusion of wildfire and Indigenous burning (Rogeau et al. 2016; Naficy and Daniels 2020). Our simulations show that emulating a stand-replacing fire regime across this landscape under these high pre-industrial fire frequencies will lead to younger and less diverse forests. This has important implications for old-growth conservation, whose value has been widely recognized across North America (DellaSala et al. 2022) and the world (Carroll et al. 2025). Regardless of the relative magnitude of their socio-ecological benefits (Jandl et al. 2019), it is generally accepted that the loss of old-growth can negatively impact a number of ecosystem services, from carbon storage to hydrological cycling and biodiversity (Watson et al. 2018; McDowell et al. 2020). According to our results, forest management that emulates mixed-severity fires in the southeastern Canadian Rockies – e.g. with old tree and patch retention – should allow maintaining a better ratio of old to new cohorts and stands and support a wider range of ecosystem services.

We also show that assumptions about the predominant severity of a fire regime strongly impact PBR relationships across scales and FTs. In our case, the M_{SR} generated smaller variation in fire regime attributes at the landscape level (Fig. A.6), from which arose lower pyrodiversity and, when fire intervals were comparable to those in the dendroecological record, lower forest diversity and the lack of old-growth forests. Projected increases in the frequency of stand-replacing fires in this area (Coogan et al. 2019) may then tip it into a negative PBR, with ensuing losses of forest diversity and old growth. Assuming a landscape-wide mixed-severity fire regime should therefore improve disturbance-based forest management aimed at promoting biodiversity in the southeastern Canadian Rockies. Even if fire severity and frequency are likely higher than what our model simulated, the higher spatio-temporal variability in fire severity (and other fire regime attributes) created by emulating a mixed-severity regime can still lead to

distinct post-fire recovery pathways in similar pre-fire FTs, increasing landscape heterogeneity (Perry et al. 2011) and diversity across taxa (Jackson et al. 2015; Lewis et al. 2022).

Finally, it is well known that the effects of pyrodiversity and fire regime can vary widely across taxa and biomes (Geary et al., 2020; Jones & Tingley, 2021; Steel et al., 2021, 2024); here, we add that these relationships can change within the same (heterogenous) landscape and that assumptions about the fire regime, specifically the level of post-fire mortality, can significantly alter our predictions of pyrodiversity effects on biodiversity. Our results thus warn against the extrapolation of PBR relationships across fire regimes, forest types and spatial scales.

Future work and considerations for modelling historic fire regimes

Our results also highlight data and modelling gaps that prevented the best supported model (M_{MS}) from accurately simulating the 'natural range of variation' of fire and forest dynamics (here pertaining to the pre-industrial period). These gaps are common to other similar models (Sturtevant et al. 2009; Keane et al. 2018) and in highlighting them we hope to steer further research into overcoming them.

In particular, the high overestimation of *P. menziesii* dominance that led to the overestimation of cohort and stand ages across the landscape, is related to the overestimation of fire intervals and possibly overly low fire severity. Both are related to important caveats in our model calibration and the observed data used to evaluate it. First, our fire intervals arose from fire frequencies estimated from fire occurrences and climate conditions from 1961 to 1990, and vegetation conditions from 1990 to 2011. This period is climatically different from the pre-industrial period, but also reflects the legacy of fire exclusion and suppression, which likely caused departures from the pre-industrial fire regime and vegetation/fuel conditions in our study area since the early 1900s (Chavardès et al. 2018; Naficy and Daniels 2020) – although we believe that the modern vegetation conditions had a smaller impact on our results, as they still

captured the historical footprint of relative tree species dominance over the last several hundred years. Second, we could not parameterise fire spread, size and severity directly from data due to few fires occurring between 1961 to 1990. Third, it is highly likely that the pre-industrial fire regime in this and similar areas included Indigenous-led fire events of some frequency (Rogeau et al. 2016; Naficy and Daniels 2020; Hoffman et al. 2022). In this area, Indigenous-led fire was likely ignited in the lower foothills closer to the grasslands (Naficy & Daniels, pers. comm.), rather than at higher elevations where lightning activity has been driving recent naturally-ignited fires, and where our models consequently predicted higher ignition probabilities (Figs. B.1 and B.3). Finally, the fourth caveat is that field sampling of dendroecological data was biased towards locations where fire evidence was likely to be found, which may have led to fires appearing on average more frequent across the landscape than they are.

All in all, these caveats limit our ability to reproduce the pre-industrial fire regime captured by the dendroecological data, whose fire history dates back to the 1750s. Future research should focus on improving estimates of 'natural disturbance regimes' using appropriate data. In our case, for instance, the severity estimation mechanism (which currently follows the LANDIS-II Dynamic Fire System) will benefit from adjustments with (or a full conversion to) a data-driven approach, and fire frequencies and locations could be adjusted to reflect pre-industrial fire occurrence patterns.

Conclusions

We echo others in that there is no blanket rule to guide pyrodiversity management with respect to maximising biodiversity. The better fit between observed dendroecological data and our mixed-severity fire model suggests that in the landscapes of the southeastern Canadian Rockies, natural disturbance-based forest management would need to mimic diverse fire regimes to maintain a pyrodiversity condition in line with historic regimes. Despite data limitations, this can be facilitated by bringing together field data and simulation models to test

assumptions, gain understanding of underlying fire regimes and pyrodiversity-biodiversity relationships, as we did here, and by forecasting changes into the future.

Acknowledgements

We acknowledge Prof. L. Daniels who provided insightful comments and discussions throughout the development of this work. We declare the use of AI (Posit Assistant, Anthropic Claude model) to proof-read the final version of this manuscript and signal text flow, grammar and typological issues; all issues were solved by the authors and no text or interpretation were generated by AI.

Author contributions

CB conceptualised the manuscript, conducted all simulations and formal analyses, and led manuscript writing; CEN, DWA, SGC and EJBM significantly contributed to the interpretation of results, with contributions from other co-authors; IMSE, AMC, TM and EJBM supported dynamic modelling code development; DWA, SGC, EJBM, JJS and CB supported funding acquisition. DWA, EJBM and AMC also provided access to computing resources.

Data Availability

Full workflow and analysis code is available at: https://github.com/CeresBarros/LIM_PBH.

Declarations

We acknowledge funding from a Mitacs Accelerate Award no. IT10289 and Mitacs Elevate Fellowship no. IT12391, in partnership with the fRI Research, both awarded to CB, and funding from Alberta Innovates and the Forest Resources Improvement Association of Alberta.

References

Agee, J. K. (2005). The Complex Nature of Mixed-Severity Fire Regimes. In J. Z. Lagene, S. Cadwallader, & B. Hughes (Eds), *Mixed Severity Fire Regimes: Ecology and Management: Volume AFE MISC03*. Washington State University Cooperative Extension Service/The Association for Fire Ecology. https://tinyurl.com/Agee2005

Amoroso, M. M., Daniels, L. D., Bataineh, M., & Andison, D. W. (2011). Evidence of mixed-severity fires in the foothills of the Rocky Mountains of west-central Alberta, Canada. *Forest Ecology and Management*, *262*(12), 2240–2249. https://doi.org/10.1016/j.foreco.2011.08.016

Barros, A. M. G., Day, M. A., Preisler, H. K., Abatzoglou, J. T., Krawchuk, M. A., Houtman, R., & Ager, A. A. (2021). Contrasting the role of human- and lightning-caused wildfires on future fire regimes on a Central Oregon landscape. *Environmental Research Letters*, *16*(6), 064081. https://doi.org/10.1088/1748-9326/ac03da

Barros, C., Chubaty, A., & McIntire, E. (2022). *PredictiveEcology/LandR-Manual: V1.0.3* (Version v1.0.3) [Computer software]. Zenodo. https://doi.org/10.5281/ZENODO.7293682

Barros, C., Luo, Y., Chubaty, A. M., Eddy, I. M. S., Micheletti, T., Boisvenue, C., Andison, D. W., Cumming, S. G., & McIntire, E. J. B. (2023). Empowering ecological modellers with a PERFICT workflow: Seamlessly linking data, parameterisation, prediction, validation and visualisation. *Methods in Ecology and Evolution*, *14*(1), 173–188. https://doi.org/10.1111/2041-210X.14034

Barros, C., Thuiller, W., Georges, D., Boulangeat, I., & Münkemüller, T. (2016). *N*-dimensional hypervolumes to study stability of complex ecosystems. *Ecology Letters*, *19*(7), 729–742. https://doi.org/10.1111/ele.12617

Bell, A. J., Paterson, S. M. A., Van Wilgenburg, S. L., Laroque, C. P., Wardle, D. A., & Phillips, I. D. (2026). Pyrodiversity of boreal lake islands begets biodiversity of beetles, plants, and

birds. *Ecological Applications*, *36*(2), e70218. https://doi.org/10.1002/eap.70218

Bergeron, Y., Leduc, A., Harvey, B., & Gauthier, S. (2002). Natural fire regime: A guide for sustainable management of the Canadian boreal forest. *Silva Fennica*, *36*(1). https://doi.org/10.14214/sf.553

Bond, W. J., & van Wilgen, B. W. (1996). *Fire and Plants*. Springer Netherlands. https://doi.org/10.1007/978-94-009-1499-5

Bowman, D. M. J. S., Balch, J. K., Artaxo, P., Bond, W. J., Carlson, J. M., Cochrane, M. A., D'Antonio, C. M., DeFries, R. S., Doyle, J. C., Harrison, S. P., Johnston, F. H., Keeley, J. E., Krawchuk, M. A., Kull, C. A., Marston, J. B., Moritz, M. A., Prentice, I. C., Roos, C. I., Scott, A. C., … Pyne, S. J. (2009). Fire in the Earth System. *Science*, *324*(5926), 481–484. https://doi.org/10.1126/science.1163886

Brockerhoff, E. G., Barbaro, L., Castagneyrol, B., Forrester, D. I., Gardiner, B., González-Olabarria, J. R., Lyver, P. O., Meurisse, N., Oxbrough, A., Taki, H., Thompson, I. D., van der Plas, F., & Jactel, H. (2017). Forest biodiversity, ecosystem functioning and the provision of ecosystem services. *Biodiversity and Conservation*, *26*(13), 3005–3035. https://doi.org/10.1007/s10531-017-1453-2

Calhoun, K. L., Steel, Z. L., Parker-Shames, P., Oyler, H., & Brashares, J. S. (2025). Severity outweighs pyrodiversity in shaping avian and bat species distributions following an oak woodland megafire. *Ecosphere*, *16*(7), e70263. https://doi.org/10.1002/ecs2.70263

Canadian Forest Service. (2019). *Canadian National Fire Database – Agency Fire Data* [Data set]. Natural Resources Canada, Canadian Forest Service, Northern Forestry Centre, Edmonton, Alberta. http://cwfis.cfs.nrcan.gc.ca/en_CA/nfdb

Carroll, C., Noon, B. R., Masino, S. A., & Noss, R. F. (2025). Coordinating old-growth conservation across scales of space, time, and biodiversity: Lessons from the US policy debate. *Frontiers in Forests and Global Change*, *8*, 1493879. https://doi.org/10.3389/ffgc.2025.1493879

740 Chavardès, R. D., & Daniels, L. D. (2016). Altered mixed-severity fire regime has homogenised
741 montane forests of Jasper National Park. *International Journal of Wildland Fire*, *25*(4),
742 433. https://doi.org/10.1071/WF15048
743 Chavardès, R. D., Daniels, L. D., Gedalof, Z., & Andison, D. W. (2018). Human influences
744 superseded climate to disrupt the 20th century fire regime in Jasper National Park,
745 Canada. *Dendrochronologia*, *48*, 10–19. https://doi.org/10.1016/j.dendro.2018.01.002
746 Chubaty, A. M., & McIntire, E. J. B. (2022). *SpaDES: Develop and run spatially explicit discrete*
747 *event simulation models* [Computer software]. https://CRAN.R-
748 project.org/package=SpaDES
749 Coogan, S. C. P., Robinne, F.-N., Jain, P., & Flannigan, M. D. (2019). Scientists' warning on
750 wildfire—A Canadian perspective. *Canadian Journal of Forest Research*, *49*(9), 1015–
751 1023. https://doi.org/10.1139/cjfr-2019-0094
752 Coop, J. D., Massatti, R. T., & Schoettle, A. W. (2010). Subalpine vegetation pattern three
753 decades after stand-replacing fire: Effects of landscape context and topography on plant
754 community composition, tree regeneration, and diversity. *Journal of Vegetation Science*,
755 *21*(3), 472–487. https://doi.org/10.1111/j.1654-1103.2009.01154.x
756 Davis, E. L., Mustaphi, C. J. C., Gall, A., Pisaric, M. F. J., Vermaire, J. C., & Moser, K. A.
757 (2016). Determinants of fire activity during the last 3500 yr at a wildland—Urban
758 interface, Alberta, Canada. *Quaternary Research*, *86*(3), 247–259.
759 https://doi.org/10.1016/j.yqres.2016.08.006
760 DellaSala, D. A., Mackey, B., Norman, P., Campbell, C., Comer, P. J., Kormos, C. F., Keith, H.,
761 & Rogers, B. (2022). Mature and old-growth forests contribute to large-scale
762 conservation targets in the conterminous United States. *Frontiers in Forests and Global*
763 *Change*, *5*, 979528. https://doi.org/10.3389/ffgc.2022.979528
764 Dickson-Hoyle, S., Stuxwtéws (Bonaparte First Nation), Skeetchestn Natural Resources
765 Corporation, Eatherton, A., Baron, J. N., Tiribelli, F., & Daniels, L. D. (2024). Fire

severity drives understory community dynamics and the recovery of culturally significant plants. *Ecosphere*, *15*(3), e4795. https://doi.org/10.1002/ecs2.4795

Downing, D. J., & Pettapiece, W. W. (with Alberta). (2006). *Natural regions and subregions of Alberta*. Natural Regions Committee.

Environment Canada. (2020). *Past weather and climate—Historical Data* [Data set]. https://climate.weather.gc.ca/historical_data/search_historic_data_e.html

Favier, C. (2004). Percolation model of fire dynamic. *Physics Letters A*, *330*(5), 396–401. https://doi.org/10.1016/j.physleta.2004.07.053

Fontaine, J. B., & Kennedy, P. L. (2012). Meta-analysis of avian and small-mammal response to fire severity and fire surrogate treatments in U.S. fire-prone forests. *Ecological Applications*, *22*(5), 1547–1561. https://doi.org/10.1890/12-0009.1

Fryer, G. I., & Johnson, E. A. (1988). Reconstructing Fire Behaviour and Effects in a Subalpine Forest. *The Journal of Applied Ecology*, *25*(3), 1063. https://doi.org/10.2307/2403766

Geary, W. L., Doherty, T. S., Nimmo, D. G., Tulloch, A. I. T., & Ritchie, E. G. (2020). Predator responses to fire: A global systematic review and meta-analysis. *Journal of Animal Ecology*, *89*(4), 955–971. https://doi.org/10.1111/1365-2656.13153

Giljohann, K. M., McCarthy, M. A., Kelly, L. T., & Regan, T. J. (2015). Choice of biodiversity index drives optimal fire management decisions. *Ecological Applications*, *25*(1), 264–277. https://doi.org/10.1890/14-0257.1

Goetz, S. J., Bond-Lamberty, B., Law, B. E., Hicke, J. A., Huang, C., Houghton, R. A., McNulty, S., O'Halloran, T., Harmon, M., Meddens, A. J. H., Pfeifer, E. M., Mildrexler, D., & Kasischke, E. S. (2012). Observations and assessment of forest carbon dynamics following disturbance in North America: FOREST CARBON AFTER DISTURBANCE. *Journal of Geophysical Research: Biogeosciences*, *117*(G2), n/a-n/a. https://doi.org/10.1029/2011JG001733

Gordijn, P., & O'Connor, T. (2021). Multidecadal effects of fire in a grassland biodiversity

hotspot: Does pyrodiversity enhance plant diversity? *Ecological Applications*. https://doi.org/10.1002/eap.2391

Government of Alberta. (2017). *Area harvested 2016* (Sustainable Forest Management Facts & Statistics). Agriculture and Forestry. https://open.alberta.ca/dataset/72d4f8aa-a493-4773-a5d0-bdaf370f6cfc/resource/404f949c-a66d-4b34-8fee-7ef2036c5ecf/download/af-forest-managment-stats-2016-area-harvested.pdf

Government of Alberta. (2021). *Directive: Impacts of wildfire burned areas on annual allowable cuts*. Agriculture and Forestry. https://open.alberta.ca/dataset/d2a18d66-ad55-4970-b158-0473c2ffcaf2/resource/9902fa89-36dc-4690-8875-45af84e744be/download/af-directive-impacts-wildfire-burned-areas-annual-allowable-cuts-2021.pdf

Greenwood, L., Bliege Bird, R., McGuire, C., Jadai, N., Price, J., Skroblin, A., Van Leeuwen, S., & Nimmo, D. (2024). Indigenous pyrodiversity promotes plant diversity. *Biological Conservation*, *291*, 110479. https://doi.org/10.1016/j.biocon.2024.110479

Halofsky, J. E., Donato, D. C., Hibbs, D. E., Campbell, J. L., Cannon, M. D., Fontaine, J. B., Thompson, J. R., Anthony, R. G., Bormann, B. T., Kayes, L. J., Law, B. E., Peterson, D. L., & Spies, T. A. (2011). Mixed-severity fire regimes: Lessons and hypotheses from the Klamath-Siskiyou Ecoregion. *Ecosphere*, *2*, art40. http://doi.wiley.com/10.1890/ES10-00184.1

He, T., Lamont, B. B., & Pausas, J. G. (2019). Fire as a key driver of Earth's biodiversity. *Biological Reviews*, *94*(6), 1983–2010. https://doi.org/10.1111/brv.12544

Jandl, R., Spathelf, P., Bolte, A., & Prescott, C. E. (2019). Forest adaptation to climate change—Is non-management an option? *Annals of Forest Science*, *76*(2), 48. https://doi.org/10.1007/s13595-019-0827-x

Johnson, E. A., & Larsen, C. P. S. (1991). Climatically Induced Change in Fire Frequency in the Southern Canadian Rockies. *Ecology*, *72*(1), 194–201. https://doi.org/10.2307/1938914

Jones, G. M., Ayars, J., Parks, S. A., Chmura, H. E., Cushman, S. A., & Sanderlin, J. S. (2022).

Pyrodiversity in a Warming World: Research Challenges and Opportunities. *Current Landscape Ecology Reports*, *7*(4), 49–67. https://doi.org/10.1007/s40823-022-00075-6

Jones, G. M., & Tingley, M. W. (2021). Pyrodiversity and biodiversity: A history, synthesis, and outlook. *Diversity and Distributions*, ddi.13280. https://doi.org/10.1111/ddi.13280

Keane, R. E., Loehman, R. A., Holsinger, L. M., Falk, D. A., Higuera, P., Hood, S. M., & Hessburg, P. F. (2018). Use of landscape simulation modeling to quantify resilience for ecological applications. *Ecosphere*, *9*(9), e02414. https://doi.org/10.1002/ecs2.2414

Kelly, L. T., & Brotons, L. (2017). Using fire to promote biodiversity. *Science*, *355*(6331), 1264–1265. https://doi.org/10.1126/science.aam7672

Kelly, L. T., Brotons, L., & McCarthy, M. A. (2017). Putting pyrodiversity to work for animal conservation: Pyrodiversity and Animal Conservation. *Conservation Biology*, *31*(4), 952–955. https://doi.org/10.1111/cobi.12861

Kelly, L. T., Giljohann, K. M., Duane, A., Aquilué, N., Archibald, S., Batllori, E., Bennett, A. F., Buckland, S. T., Canelles, Q., Clarke, M. F., Fortin, M.-J., Hermoso, V., Herrando, S., Keane, R. E., Lake, F. K., McCarthy, M. A., Morán-Ordóñez, A., Parr, C. L., Pausas, J. G., … Brotons, L. (2020). Fire and biodiversity in the Anthropocene. *Science*, *370*(6519), eabb0355. https://doi.org/10.1126/science.abb0355

Kimmins, J. P. (Hamish), Blanco, J. A., Seely, B., Welham, C., & Scoullar, K. (2008). Complexity in modelling forest ecosystems: How much is enough? *Forest Ecology and Management*, *256*(10), 1646–1658. https://doi.org/10.1016/j.foreco.2008.03.011

Kozlowski, T. T. (Ed.). (1974). *Fire and Ecosystems*. Elsevier. https://doi.org/10.1016/B978-0-12-424255-5.X5001-9

Kuuluvainen, T., Angelstam, P., Frelich, L., Jõgiste, K., Koivula, M., Kubota, Y., Lafleur, B., & Macdonald, E. (2021). Natural Disturbance-Based Forest Management: Moving Beyond Retention and Continuous-Cover Forestry. *Frontiers in Forests and Global Change*, *4*, 629020. https://doi.org/10.3389/ffgc.2021.629020

Lertzman, K. P., Fall, J., & Dorner, B. (1998). Three kinds of heterogeneity in fire regimes: At the crossroads of fire history and landscape ecology. *Northwest Science*, *72*(4), 23.

Marchal, J., Cumming, S. G., & McIntire, E. J. B. (2017). Exploiting Poisson additivity to predict fire frequency from maps of fire weather and land cover in boreal forests of Québec, Canada. *Ecography*, *40*(1), 200–209. https://doi.org/10.1111/ecog.01849

Marcoux, H. M., Gergel, S. E., & Daniels, L. D. (2013). Mixed-severity fire regimes: How well are they represented by existing fire-regime classification systems? *Canadian Journal of Forest Research*, *43*(7), 658–668. https://doi.org/10.1139/cjfr-2012-0449

Martin, R. E., & Sapsis, D. B. (1992). *Fires as agents of biodiversity: Pyrodiversity promotes biodiversity*. 150–157.

McDowell, N. G., Allen, C. D., Anderson-Teixeira, K., Aukema, B. H., Bond-Lamberty, B., Chini, L., Clark, J. S., Dietze, M., Grossiord, C., Hanbury-Brown, A., Hurtt, G. C., Jackson, R. B., Johnson, D. J., Kueppers, L., Lichstein, J. W., Ogle, K., Poulter, B., Pugh, T. A. M., Seidl, R., … Xu, C. (2020). Pervasive shifts in forest dynamics in a changing world. *Science*, *368*(6494), eaaz9463. https://doi.org/10.1126/science.aaz9463

McIntire, E. J. B., Duchesneau, R., & Kimmins, J. P. (2005). *Seed and bud legacies interact with varying fire regimes to drive long-term dynamics of boreal forest communities*. *35*, 9.

Micheletti, T., Stewart, Frances E. C., Cumming, S. G., Haché, S., Stralberg, D., Tremblay, J. A., Barros, C., Eddy, I. M. S., Chubaty, A. M., Leblond, M., Pankratz, R. F., Mahon, C. L., Van Wilgenburg, S. L., Bayne, E. M., Schmiegelow, F. K. A., & McIntire, E. J. B. (2021). Assessing pathways of climate change effects in SpaDES: an application to boreal landbirds of Northwest Territories Canada. *Frontiers in Ecology and Evolution*. https://doi.org/10.3389/fevo.2021.679673

Miller, J. E. D., & Safford, H. D. (2020). Are plant community responses to wildfire contingent upon historical disturbance regimes? *Global Ecology and Biogeography*, *29*(10), 1621–1633. https://doi.org/10.1111/geb.13115

Naficy, C. E., & Daniels, L. D. (2020). *Final Report fRI Research, Landscapes in Motion: Fire Regime Dynamics of the Southwestern Alberta Foothills* (p. 59). fRI Research. https://www.landscapesinmotion.ca/resources/2020/10/20/report-fire-regime-dynamics

Parr, C. L., & Andersen, A. N. (2006). Patch Mosaic Burning for Biodiversity Conservation: A Critique of the Pyrodiversity Paradigm. *Conservation Biology*, *20*(6), 1610–1619. https://doi.org/10.1111/j.1523-1739.2006.00492.x

Perrault-Hébert, M., Boucher, Y., Fournier, R., Girard, F., Auger, I., Thiffault, N., & Grenon, F. (2017). Ecological drivers of post-fire regeneration in a recently managed boreal forest landscape of eastern Canada. *Forest Ecology and Management*, *399*, 74–81. https://doi.org/10.1016/j.foreco.2017.05.026

Perry, D. A., Hessburg, P. F., Skinner, C. N., Spies, T. A., Stephens, S. L., Taylor, A. H., Franklin, J. F., McComb, B., & Riegel, G. (2011). The ecology of mixed severity fire regimes in Washington, Oregon, and Northern California. *Forest Ecology and Management*, *262*(5), 703–717. https://doi.org/10.1016/j.foreco.2011.05.004

Peterson, E. B., & Peterson, N. M. (1992). *Ecology, management, and use of aspen and balsam poplar in the prairie provinces, Canada*. Forestry Canada, Northwest Region, Northern Forestry Centre.

Pinno, B., & Errington, R. (2016). Burn Severity Dominates Understory Plant Community Response to Fire in Xeric Jack Pine Forests. *Forests*, *7*(4), 83. https://doi.org/10.3390/f7040083

Podur, J., & Wotton, B. M. (2011). Defining fire spread event days for fire-growth modelling. *International Journal of Wildland Fire*, *20*(4), 497. https://doi.org/10.1071/WF09001

Rainsford, F. W., Kelly, L. T., Leonard, S. W. J., & Bennett, A. F. (2021). Post-fire habitat relationships for birds differ among ecosystems. *Biological Conservation*, *260*, 109218. https://doi.org/10.1016/j.biocon.2021.109218

Régnière, J., Saint-Amant, R., Béchard, A., & Moutaoufik, A. (2017). *BioSIM 11 USER'S*

MANUAL (Version v11) [Computer software].

Rogeau, M.-P., Flannigan, M. D., Hawkes, B. C., Parisien, M.-A., & Arthur, R. (2016). Spatial and temporal variations of fire regimes in the Canadian Rocky Mountains and Foothills of southern Alberta. *International Journal of Wildland Fire*, *25*(11), 1117. https://doi.org/10.1071/WF15120

Steel, Z. L., Collins, B. M., Sapsis, D. B., & Stephens, S. L. (2021). Quantifying pyrodiversity and its drivers. *Proceedings of the Royal Society B: Biological Sciences*, *288*(1948), rspb.2020.3202, 20203202. https://doi.org/10.1098/rspb.2020.3202

Steel, Z. L., Miller, J. E. D., Ponisio, L. C., Tingley, M. W., Wilkin, K., Blakey, R., Hoffman, K. M., & Jones, G. (2024). A roadmap for pyrodiversity science. *Journal of Biogeography*, *51*(2), 280–293. https://doi.org/10.1111/jbi.14745

Stillman, A. N., Siegel, R. B., Wilkerson, R. L., Johnson, M., & Tingley, M. W. (2019). Age-dependent habitat relationships of a burned forest specialist emphasise the role of pyrodiversity in fire management. *Journal of Applied Ecology*, *56*(4), 880–890. https://doi.org/10.1111/1365-2664.13328

Stockdale, C., Flannigan, M., & Macdonald, E. (2016). Is the END (emulation of natural disturbance) a new beginning? A critical analysis of the use of fire regimes as the basis of forest ecosystem management with examples from the Canadian western Cordillera. *Environmental Reviews*, *24*(3), 233–243. https://doi.org/10.1139/er-2016-0002

Sturtevant, B. R., Miranda, B. R., Scheller, R. M., & Shinneman, D. (2018). *LANDIS-II Dynamic Fire System Extension v3.0 – User Guide* (Version v3.0) [Computer software]. https://github.com/475aada6-c0c3-4d6b-a178-8530ce846e62

Sturtevant, B. R., Scheller, R. M., Miranda, B. R., Shinneman, D., & Syphard, A. (2009). Simulating dynamic and mixed-severity fire regimes: A process-based fire extension for LANDIS-II. *Ecological Modelling*, *220*(23), 3380–3393. https://doi.org/10.1016/j.ecolmodel.2009.07.030

Turner, M. G., & Romme, W. H. (1994). Landscape dynamics in crown fire ecosystems. *Landscape Ecology*, *9*(1), 59–77. https://doi.org/10.1007/BF00135079

Watson, J. E. M., Evans, T., Venter, O., Williams, B., Tulloch, A., Stewart, C., Thompson, I., Ray, J. C., Murray, K., Salazar, A., McAlpine, C., Potapov, P., Walston, J., Robinson, J. G., Painter, M., Wilkie, D., Filardi, C., Laurance, W. F., Houghton, R. A., … Lindenmayer, D. (2018). The exceptional value of intact forest ecosystems. *Nature Ecology & Evolution*, *2*(4), 599–610. https://doi.org/10.1038/s41559-018-0490-x

Wilkinson, M. D., Dumontier, M., Aalbersberg, Ij. J., Appleton, G., Axton, M., Baak, A., Blomberg, N., Boiten, J.-W., da Silva Santos, L. B., Bourne, P. E., Bouwman, J., Brookes, A. J., Clark, T., Crosas, M., Dillo, I., Dumon, O., Edmunds, S., Evelo, C. T., Finkers, R., … Mons, B. (2016). The FAIR Guiding Principles for scientific data management and stewardship. *Scientific Data*, *3*(1), 160018. https://doi.org/10.1038/sdata.2016.18

Tables

Table 1. Summary statistics of species and patch ages recorded in the observed field dataset.

		Median	Mean	Min.	Max.
Age by species	*Pinus spp*	99	112	77	371
	Picea engelmannii	96	109	77	242
	Abies spp	107	115	77	191
	Populus spp	101	104	78	166
	Pseudotsuga menziesii	119	138	77	449
Age by forest type	Broadleaf	72	72	72	72
	Douglas-fir	45	79	31	182
	Dry conif.	30	37	10	61
	Mixed	20	21	12	34
	Moist conif.	21	22	1	35
	Pine	23	35	4	151
	Spruce	62	62	62	62
Median fire interval by forest type	Broadleaf	14	14	14	14
	Douglas-fir	17	16.69	9.5	23
	Dry conif.	42	39.9	27	56
	Mixed	23	20.98	17	27
	Moist conif.	27	25.8	12	47
	Pine	31.25	37.83	10	202
	Spruce	27	27	27	27

Figures

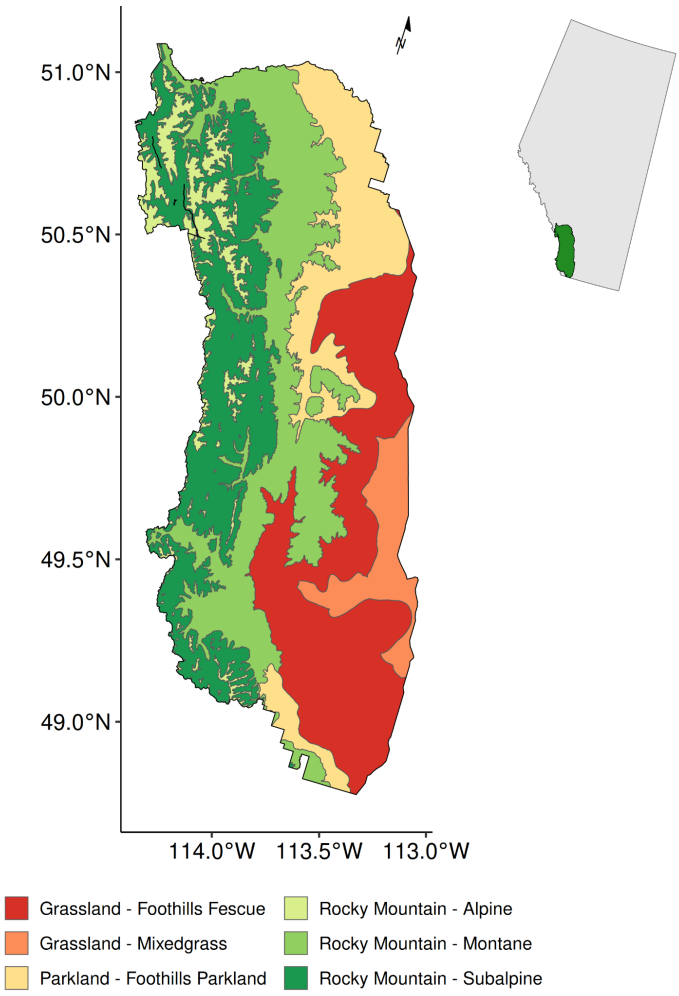

Figure 1. Study area map showing Natural Regions and Subregions of Alberta (Downing & Pettapiece, 2006). We ran simulations across the entire study area, but subset simulation outputs to the Montane subregion. Inset shows the study area within the province of Alberta, Canada.

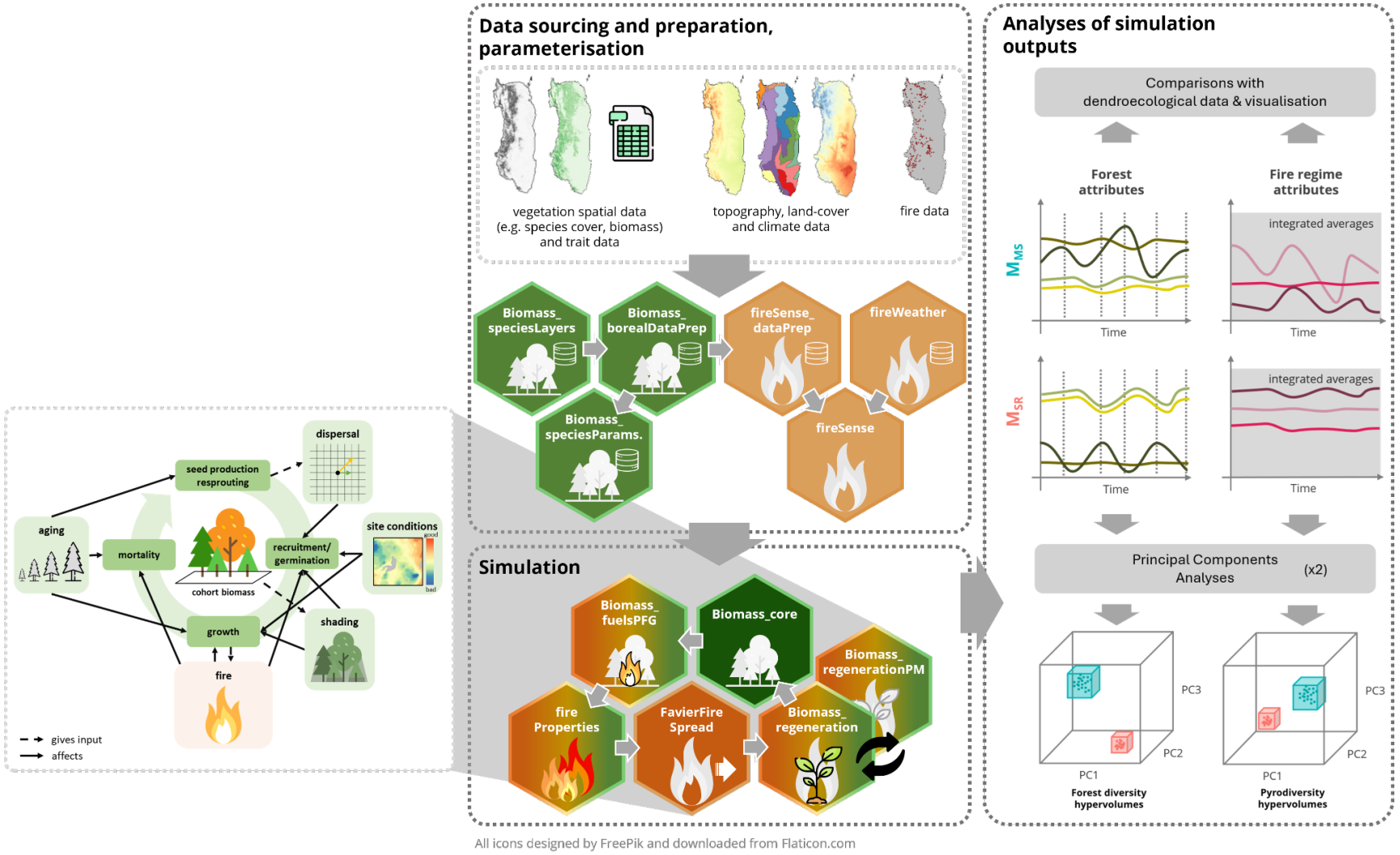

945

946 **Figure 2.** LandR modelling workflow and *post-hoc* analyses. We used a continuous modelling workflow that integrated data retrieval,

947 parameterisation and dynamic simulation steps (centre) to simulate historical forest and fire dynamics (inset to the left) in the

948 southwestern Rockies of Alberta, Canada. We ran two alternative model formulations, a mixed-severity fire model (M_{MS}) and a stand-
949 replacing fire model (M_{SR}), for 2000 years and five replicates. Fire behaviour depended on historical weather data and simulated fuel
950 changes. For post-simulation analyses (right), we used only the last 500 years of simulation (quasi-equilibrium period). Simulated
951 forest attributes (tree species relative biomasses and ages) were taken from five randomly sampled years, per replicate. Simulated
952 fire regime attributes (median fire interval, patch size, and severity) were integrated across the entire quasi-equilibrium. These
953 outputs were evaluated against a dendroecological dataset and fed into two Principal Components Analyses, one for forest attributes
954 and the other for fire regime attributes. Coordinates on the first principal components of each PCA (four and three, respectively) were
955 then used to build hypervolumes for each model, whose sizes were used as metrics of forest diversity and pyrodiversity. Grey arrows
956 indicate the flow of information between modules, arrows on the right indicate the interactions between simulated processes. Data
957 modules are indicated with a database symbol.

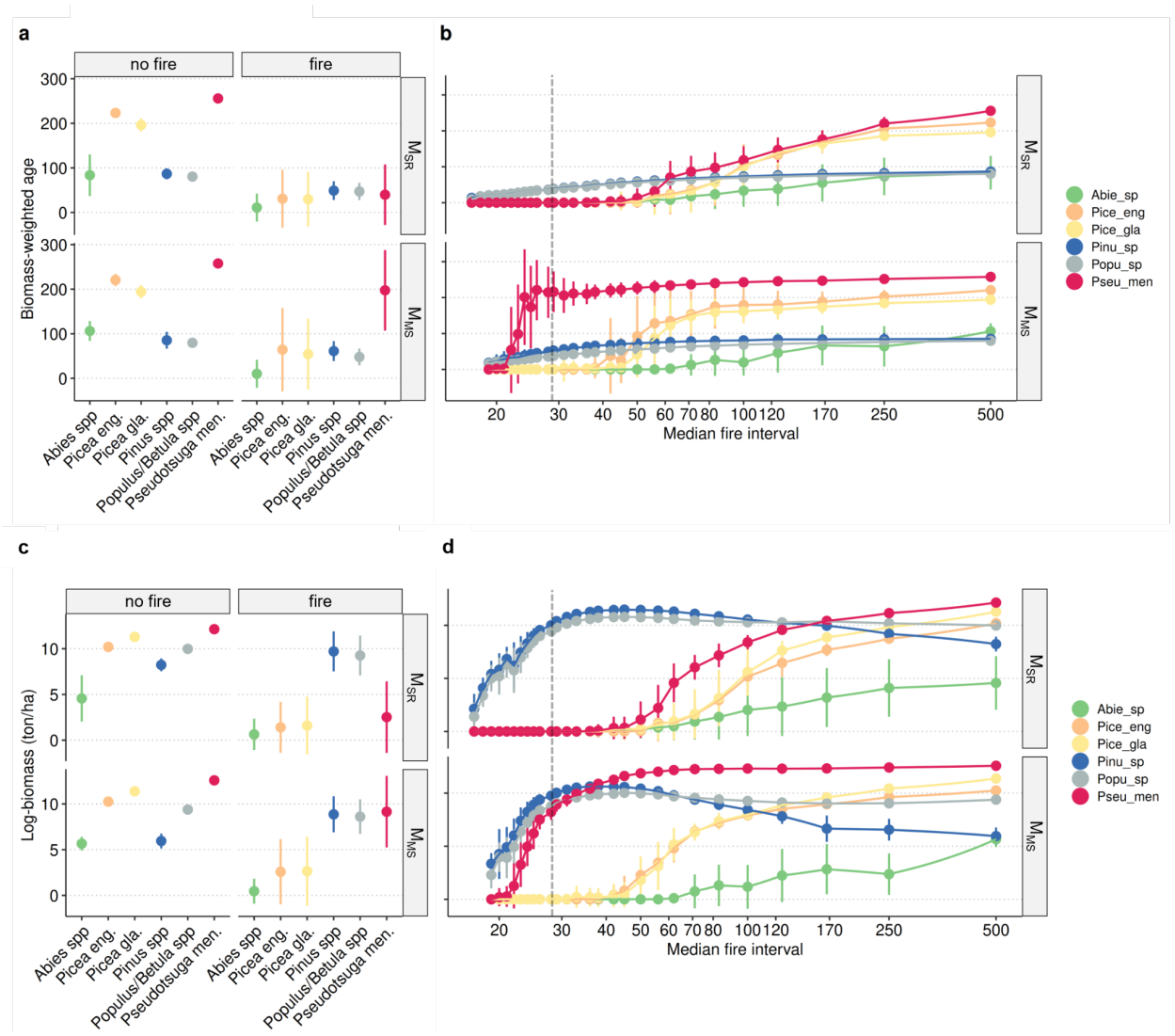

Figure 3. Age and total biomass per species and by fire occurrence and interval. All panels show landscape-wide values of biomass-weighted age (a,b) and total biomass (c,d) per species, averaged across replicates and the five sampled years of the quasi-equilibrium period (error bars show standard deviation). Panels a) and c) break up the data into pixels that never burnt during the quasi-equilibrium period ('no fire') and pixels that burnt at least once ('fire'); panels b) and d) break up the data by median fire interval (calculated over the entire quasi-equilibrium period). Dashed vertical lines in panels b,d show the observed 28-year median fire interval (Naficy & Daniels, 2020).

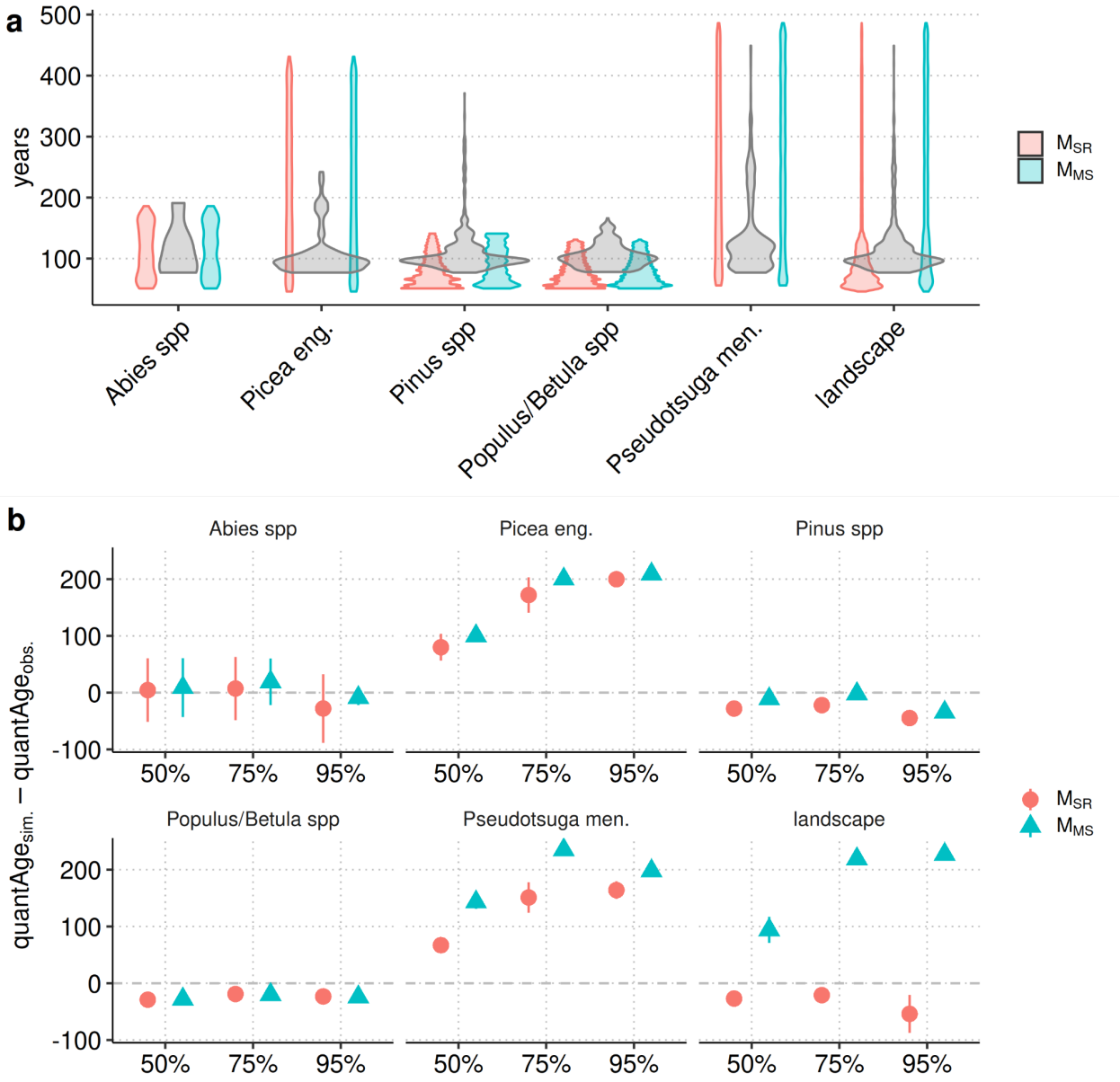

967

968 **Figure 4.** Comparisons between simulated and observed species ages. Panel a) shows density
969 distributions of observed (grey) and simulated species ages of each model. Simulated species
970 ages were calculated per pixel, sampled year and replicate. Panel b) shows simulated quantile
971 deviations from observed quantile ages (averaged across patches) calculated across pixels and
972 sampled years, per replicate (points are means with 95% confidence intervals across
973 replicates). 'Landscape' values were calculated using all pixels/plots in the Montane subregion,

not by averaging values calculated per forest type. 'M_{SR}' stands for 'stand replacement model', and 'M_{MS}' for 'mixed-severity model'.

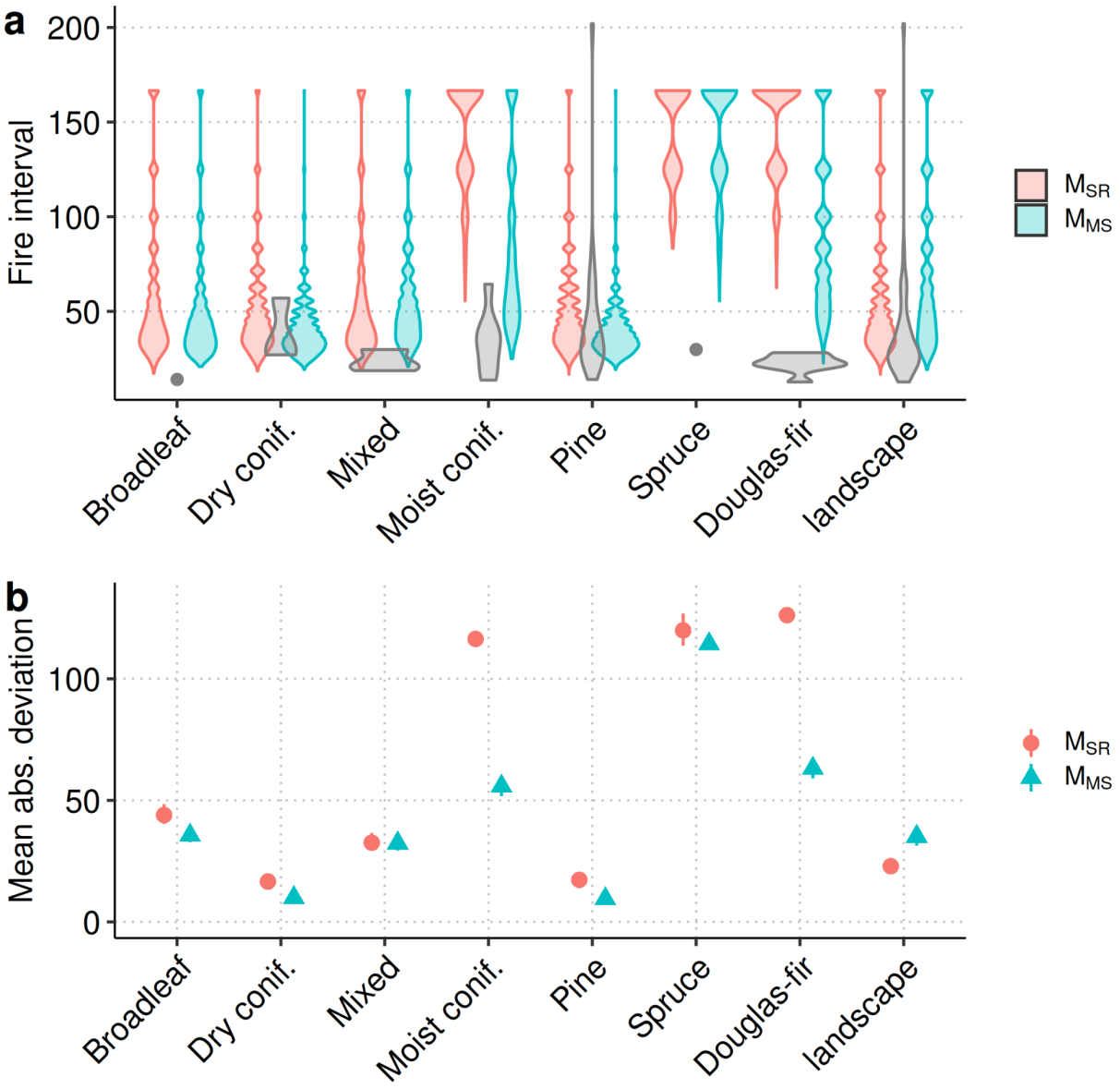

976
977 **Figure 5.** Comparisons between simulated and observed fire intervals. Panel a) shows density
978 distributions of observed (grey) and simulated median fire intervals. Simulated median fire
979 intervals were calculated across the entire quasi-equilibrium period, per pixel and replicate.
980 Panel b) shows simulated mean absolute deviations (MAD) from observed mean fire intervals
981 (averaged across plots), calculated per pixel, per replicate (points are means with 95%
982 confidence intervals across replicates). 'Landscape' values were calculated using all pixels/plots
983 in the Montane subregion, not by averaging values calculated per forest type.

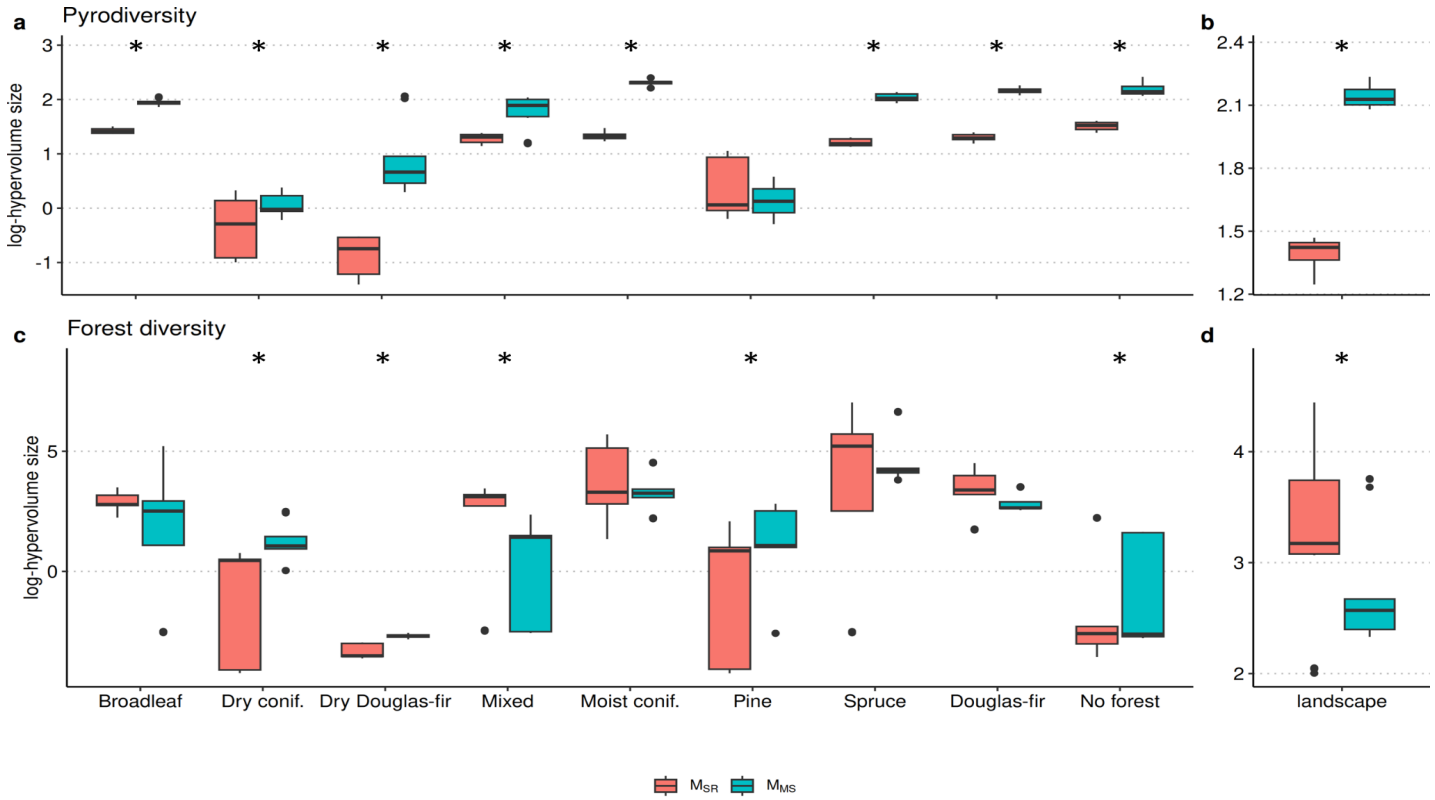

Figure 6. Pyrodiversity and forest diversity levels under each post-fire mortality model, by forest type (a and c) and across the landscape (b and d). Asterisks indicate statistically significant differences (p-value < 0.05) between models per forest type and at the landscape scale (Table A.3).

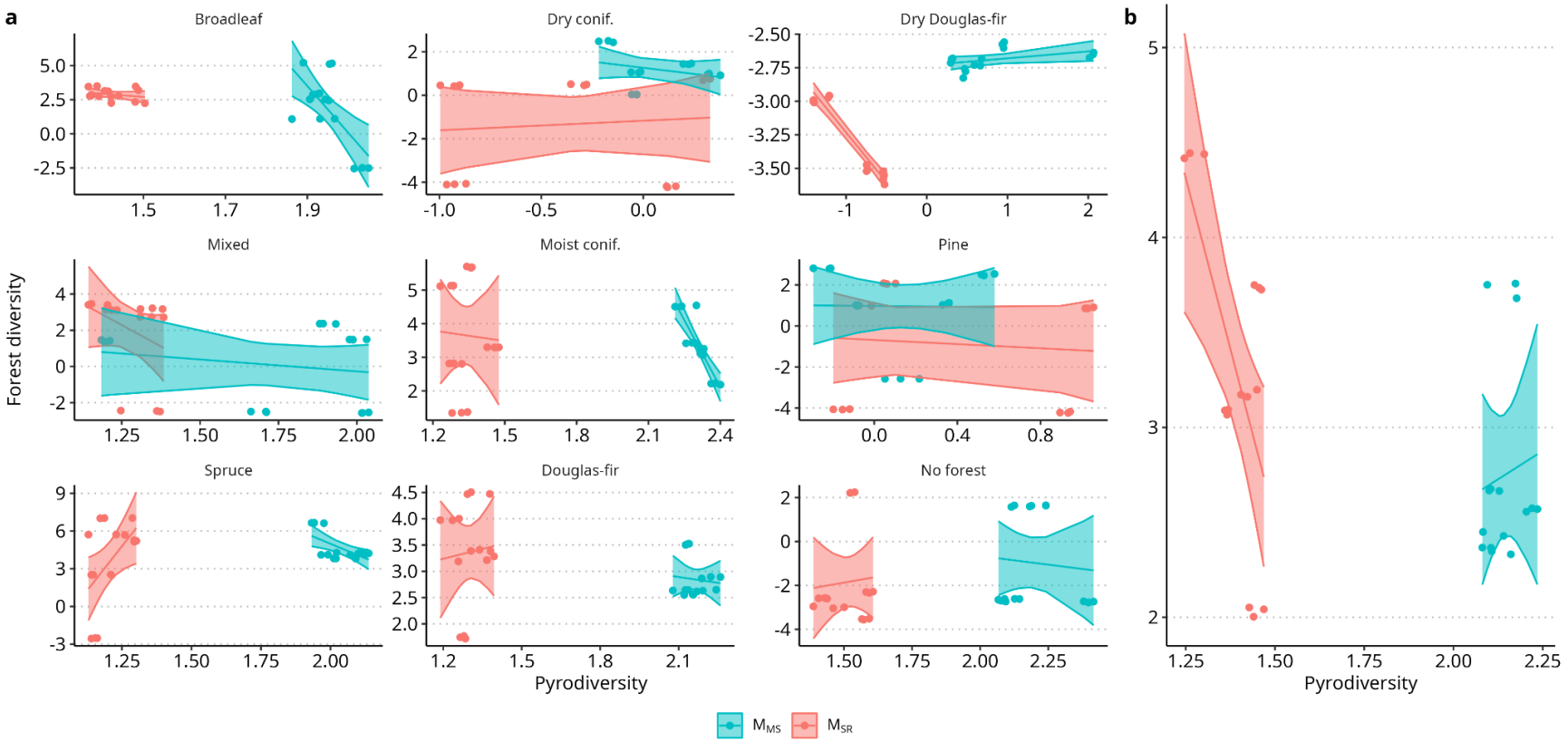

Figure 7. Pyrodiversity-forest-diversity relationships under the mixed-severity model (M_{MS}, blue) and the stand-replacing model (M_{SR}, red), within (a) and across forest types (b). Pyrodiversity and forest diversity were measured as hypervolume size, and their values were log transformed. Each point represents a hypervolume replicate (n = 3) calculated for each simulation replicate (n = 5; total n =

15). Lines show model fitted values and shaded areas are the prediction intervals at a 95% probability level (see Table A.3 for model formulae and coefficients).

Appendix A

Supplementary tables

Table A.1. LandR Biomass modules and other SpaDES modules used in the simulations and their corresponding repositories. Full workflow and data analysis exist at https://github.com/CeresBarros/LIM_PBH.

Module type	Module name/version	Description	Repository URL
Data prep. and calibration modules	*fireSense_DataPrep*	An accessory module to FireSense that prepares fire, weather and fuel data for the statistical fire models	https://github.com/CeresBarros/fireSense_dataPrep/tree/e3194b1d5f7379084d82ebd481a65e8787d3f039
	fireSense_IgnitionFit	Fits an empirical fire ignition probability model based on the statistical relationship between fire occurrences (response), fuel and weather (predictors).	https://github.com/CeresBarros/*fireSense_IgnitionFit*/tree/8ea03bc4557b8136c3797f0711ff16601a26fd4e
	fireWeather	Prepares and summarises weather data into raster layers used by *fireProperties* and by *fireSense_IgnitionFit*.	https://github.com/CeresBarros/fireWeather/tree/bb91c9ea1c663ea2d30f1a0b96527f56572f8921
	LandR *Biomass_borealDataPrep* v1.5.4	Prepares multiple inputs and parameters used by *Biomass_core*; customised for Western Canadian boreal and montane forests.	https://github.com/CeresBarros/Biomass_borealDataPrep/tree/7f5c807a978aadeffd6bf7a0db830eca233fe7a5
	LandR *Biomass_speciesData* v1.0.0	Prepares species input layers from multiple data sources.	https://github.com/CeresBarros/*Biomass_speciesData*/tree/55e35c845231752878b2cd71caff1eeb67d61fde
	LandR *Biomass_speciesParameters*	Estimates invariant species traits (growth and mortality-related life-history traits) and adjusts spatially varying species traits (*maxB* and *maxANPP)* used by *Biomass_core* from permanent sample plot data	https://github.com/CeresBarros/Biomass_speciesParameters/tree/5e4653870a015fc7bcd251d8f9c12c12555988ac

Vegetation and fire simulation modules	*fireProperties* v1.0.0	Calculates fire (behaviour) properties in function of vegetation (fuels), climate and topography conditions, using the Canadian Forest Fire Behaviour Prediction System.	https://github.com/CeresBarros/fireProperties/tree/ddb69ade07dccc8b0e609d708a312ee5b7737fa1
	FavierFireSpread	Ignites and spreads fire in function of fire behaviour properties calculated by *fireProperties*. Spreading follows the fire percolation model by Favier (2004)	https://github.com/CeresBarros/FavierFireSpread/tree/bd9f4f0161ee49be6627b9f92702fcd4fef0a88c
	fireSense_IgnitionPredict	Uses the model fitted by *fireSense_IgnitionFit* to predict fire probabilities across the landscape, every year, under changing conditions of covariates (fuels and weather).	https://github.com/CeresBarros/*fireSense_IgnitionPredict*/tree/cc17b15e10b843381b23d64ec24b11464ba1d482
	LandR *Biomass_core* v1.3.9	Simulates vegetation growth, mortality, ageing, and dispersal. Updates biomass following other modules' events, and produces summary figures and tables.	https://github.com/CeresBarros/Biomass_core/tree/9b209fe8b80388c1451c53631bb4f2df423d1768
	LandR *Biomass_regeneration* v0.1.9000	Simulates post-disturbance (fire) biomass regeneration assuming 100% post-disturbance mortality	https://github.com/CeresBarros/Biomass_regeneration/tree/2bdd1d4cbe645e5a021e5eee7bdef741ddc29b68
	LandR *Biomass_regenerationPM* v0.2.0	Simulates post-disturbance (fire) biomass regeneration assuming partial mortality (PM) following a disturbance	https://github.com/CeresBarros/*Biomass_regenerationPM*/tree/3529d5158519552ca7630b49105cc7a6f592a3c5
	LandR *Biomass_fuelsPFG* v1.0.0	Converts cohort biomasses generated by LandR *Biomass_core* into fire fuels, using fuel type classification from Canadian Forest Fire Behaviour Prediction System, adapted to the study area forest systems.	https://github.com/CeresBarros/Biomass_fuelsPFG/tree/69dd95573b8d102ab5a44203a4d31b556f0ff97e

Table A.2. Data used to parametrize vegetation and fire dynamics.

Data	Used for	Data type	Data source(s)
Species % cover	- initialising species in the landscape (location and biomass) - estimating spatially varying species traits	Spatial raster layers	In increasing order of data quality: National Forest Inventory, Natural Resources Canada, Canadian Forest Service (Beaudoin et al. 2017); https://open.canada.ca/data/en/dataset/ec9e2659-1c29-4ddb-87a2-6aced147a990) CASFRI v4 (2016; Cosco 2011) Pickell Forest Resource Inventory (LandWeb project partners, prepared by Silvacom)
Stand age, stand biomass	- initialising species in the landscape (age and biomass) - estimating spatially varying species traits	Spatial raster layers	National Forest Inventory, Natural Resources Canada, Canadian Forest Service (Beaudoin et al. 2017); https://open.canada.ca/data/en/dataset/ec9e2659-1c29-4ddb-87a2-6aced147a990)
Ecological zonation	- defining ecolocations (by combining with land cover) - estimating spatially varying species traits	Spatial polygons layer	Natural Regions and Subregion of Alberta (https://www.albertaparks.ca/media/429607/natural_regions_subregions_of_alberta.zip)
Land cover	- defining ecolocations (combined with ecological zonation) - estimating spatially varying species traits	Spatial raster layers	Land Cover of Canada 2010, Canada Centre for Remote Sensing (CCRS), Earth Sciences Sector, NRCan (http://ftp.maps.canada.ca/pub/nrcan_rncan/Land-cover_Couverture-du-sol/canada-landcover_canada-couverture-du-sol/CanadaLandcover2010.zip)
Elevation, aspect, slope	- calculation of fire behaviour properties	Spatial raster layers	Derived from a digital elevation model (DEM) raster layer covering the study area (https://open.canada.ca/data/en/dataset/7f245e4d-76c2-4caa-951a-45d1d2051333)
Permanent sample plot data	- estimating/adjusting invariant species traits	Tables	Proprietary provincial data.

Simulated species growth curves	- estimating invariant species traits (growth and mortality curve parameters) - adjusting and estimating spatially varying species traits (adjusting maxB and estimating maxANPP)	Tables	
Invariant species traits, ecolocation-specific parameters		Tables	Dominic Cyr's LANDIS-II traits (https://raw.githubusercontent.com/dcyr/LANDIS-II_IA_generalUseFiles/master/speciesTraits.csv) LANDIS-II default inputs (https://raw.githubusercontent.com/LANDIS-II-Foundation/Extensions-Succession/master/biomass-succession-archive/trunk/tests/v6.0-2.0/biomass-succession-dynamic-inputs_test.txt and https://github.com/LANDIS-II-Foundation/Extensions-Succession-Archive/blob/master/biomass-succession-archive/trunk/tests/v6.0-2.0/biomass-succession_test.txt)
Weather data	- estimating average number of fires per pixel - calculating fire behaviour properties during the simulation	Table	Daily weather data (Jan. 1st 1961 to Dec. 31st 1990), generated with BioSIM (Régnière et al., 2017) using Canada-US climate normals 1961-1990 (ftp://ftp.cfl.scf.rncan.gc.ca/regniere/Data11/Weather/Normals/past/Canada-USA_1961-1990.zip)
Fire point data	- estimating average number of fires per pixel	Spatial points layer	Canadian National Fire Database – Agency Fire Data (2019). https://cwfis.cfs.nrcan.gc.ca/downloads/nfdb/fire_pnt/current_version/NFDB_point.zip
Fire polygon data	- estimating largest fire size between 1919 and 2019	Spatial polygons layer	Canadian National Fire Database – Agency Fire Data (2019).

	https://cwfis.cfs.nrcan.gc.ca/downloads/nfdb/fire_poly/current_version/NFDB_poly.zip

Table A.3. Effects of simulation model on mean pyrodiversity and mean forest diversity estimates (i.e., log-volume) and on the effect of pyrodiversity on forest diversity, within and across forest types (i.e., landscape). Bold values in the M_{SR} and M_{MS} columns indicate where the effect estimates were significantly different from 0 (i.e. confidence intervals did not overlap 0). The last column indicates where post-hoc tests indicated a significant difference between M_{SR} and M_{MS} effect estimates (+ p-value ≤ 0.05, * p-value ≤ 0.01, ** p-value ≤ 0.001, *** p-value ≤ 0.0001). Symbols: 'HVs' stands for hypervolumes. 'M_{SR}' and 'M_{MS}' stand for stand-replacing and mixed-severity models respectively.

			M_{SR}	**M_{MS}**	**Difference between models**
Pyrodiversity hypervolumes	Mean log-volume estimate	landscape	**4.030**	**8.520**	***
		No forest	**4.56**	**9.017**	***
		Broadleaf	**4.145**	**7.028**	***
		Dry conif.	**0.807**	**1.083**	+
		Dry Douglas-fir	**0.439**	**3.039**	*
		Mixed	**3.612**	**6.08**	***
		Moist conif.	**3.811**	**10.094**	***
		Pine	**1.644**	**1.197**	
		Spruce	**3.351**	**7.717**	***
		Douglas-fir	**3.684**	**8.708**	***
Forest diversity hypervolumes	Mean log-volume estimate	landscape	**3.290**	**2.750**	+
		No forest	**-1.8407**	-0.9639	***
		Broadleaf	**2.8917**	**1.8293**	
		Dry conif.	**-1.3238**	**1.1934**	*
		Dry Douglas-fir	**-3.3171**	**-2.6862**	***

		Mixed	**1.9975**	0.0403	+
		Moist conif.	**3.655**	**3.2955**	
		Pine	-0.8687	0.9609	+
		Spruce	**3.5882**	**4.6078**	
		Douglas-fir	**3.3662**	**2.8453**	
Effect of pyrodiversity	Coefficient estimate	landscape	**-7.200**	1.190	+
		No forest	2.1863	-1.5723	
		Broadleaf	-2.354	**-34.3312**	*
		Dry conif.	0.4385	-1.1313	
		Dry Douglas-fir	**-0.7418**	0.0512	***
		Mixed	-9.4352	-1.3149	
		Moist conif.	-1.0436	**-13.2733**	
		Pine	-0.5069	-0.097	
		Spruce	**28.1517**	**-9.2331**	*
		Douglas-fir	1.2454	-0.7298	

Table A.4. Pyrodiversity as a function of scenario and vegetation type. Pyrodiversity was measured as hypervolume size (i.e. volume) and modelled in the log scale. We fit separate models at the landscape scale and at the forest type scale. In the latter, we used a generalised least squares model allowing for different variance between combinations of scenario and forest type ('forestType'). Symbols indicate the significance level of t-tests evaluating coefficient differences with respect to the reference levels 'model (SR)' (stand-replacing) and 'forestType (No forest)' (+ p-value ≤ 0.05, * p-value ≤ 0.01, ** p-value ≤ 0.001, *** p-value ≤ 0.0001). 'MS' stands for mixed-severity.

Model	Coefficient	Value	Std.Error	t-value
log(volume) ~ model	(Intercept)	4.559517	0.0853253	53.44***
	model (MS)	4.457172	0.3034743	14.69***
log(volume) ~ model + forestType	forestType (Broadleaf)	-0.414465	0.0995394	-4.16***
with variance function:	forestType (Dry conif.)	-3.75255	0.1355076	-27.69***
~1 | model * forestType	forestType (Dry Douglas-fir)	-4.120892	0.0934865	-44.08***
	forestType (Mixed)	-0.948003	0.1156559	-8.2***
	forestType (Moist conif.)	-0.748282	0.1116409	-6.7***
	forestType (Pine)	-2.915505	0.240104	-12.14***
	forestType (Spruce)	-1.208232	0.1024646	-11.79***
	forestType (Douglas-fir)	-0.87537	0.1022839	-8.56***
	model (MS):forestType (Broadleaf)	-1.573772	0.3221566	-4.89***
	model (MS):forestType (Dry conif.)	-4.181168	0.3260958	-12.82***
	model (MS):forestType (Dry Douglas-fir)	-1.856466	0.709051	-2.62*
	model (MS):forestType (Mixed)	-1.988294	0.524964	-3.79**

	model (MS):forestType (Moist conif.)	1.825266	0.3381605	5.4***
	model (MS):forestType (Pine)	-4.904078	0.3881529	-12.63***
	model (MS):forestType (Spruce)	-0.091432	0.3393638	-0.27
	model (MS):forestType (Douglas-fir)	0.567162	0.3288539	1.72

Table A.5. Forest diversity as a function of scenario and vegetation type. Forest diversity was measured as hypervolume size (i.e. volume) and modelled in the log scale. We fit separate models at the landscape scale and at the forest type scale. In the latter, we used a generalised least squares model allowing for different variance between combinations of scenario and forest type ('forestType'). Symbols indicate the significance level of t-tests evaluating coefficient differences with respect to the reference levels 'model (SR)' (stand-replacing) and 'forestType (No forest)' (+ p-value ≤ 0.05, * p-value ≤ 0.01, ** p-value ≤ 0.001, *** p-value ≤ 0.0001). 'MS' stands for mixed-severity.

Model	Coefficient	Value	Std.Error	t-value
log(volume) ~ model	(Intercept)	-1.840703	0.554357	-3.32**
	model (MS)	0.876771	0.790841	1.11
log(volume) ~ model * forestType	forestType (Broadleaf)	4.732395	0.564774	8.38***
with variance function:	forestType (Dry conif.)	0.516856	0.829057	0.62
~1 | model * forestType	forestType (Dry Douglas-fir)	-1.476391	0.559221	-2.64*
	forestType (Mixed)	3.838229	0.815986	4.7***
	forestType (Moist conif.)	5.495674	0.696157	7.89***
	forestType (Pine)	0.971959	0.910569	1.07
	forestType (Spruce)	5.428912	1.06207	5.11***
	forestType (Douglas-fir)	5.206867	0.606972	8.58***
	model (MS):forestType (Broadleaf)	-1.93917	1.047409	-1.85
	model (MS):forestType (Dry conif.)	1.640491	1.024615	1.6
	model (MS):forestType (Dry Douglas-fir)	-0.245826	0.794491	-0.31
	model (MS):forestType (Mixed)	-2.833998	1.142864	-2.48+
	model (MS):forestType (Moist conif.)	-1.236196	0.917603	-1.35

	model (MS):forestType (Pine)	0.952827	1.186812	0.8
	model (MS):forestType (Spruce)	0.142804	1.233671	0.12
	model (MS):forestType (Douglas-fir)	-1.397592	0.833952	-1.68

Table A.6. Relationships between forest diversity and pyrodiversity. Forest diversity and pyrodiversity were measured as hypervolume size (i.e. volume) and modelled in the log scale. We fit separate models at the landscape scale and at the forest type scale. In the latter, we used a generalised least squares model allowing for different variance between combinations of simulation model ('model') and forest type ('forestType'). Symbols indicate the significance level of t-tests evaluating coefficient differences with respect to the reference levels 'model (SR)' (stand-replacing) and 'forestType (No forest)' (+ p-value ≤ 0.05, * p-value ≤ 0.01, ** p-value ≤ 0.001, *** p-value ≤ 0.0001). 'MS' stands for mixed-severity.

Model	Coefficient	Value	Std.Error	t-value
logVolume_forest ~ logVolume_fire* model	(Intercept)	13.310	3.077	4.33**
	logVolume_fire	-7.197	2.208	-3.26*
	model (MS)	-13.122	7.385	-1.78
	logVolume_fire:model (MS)	8.392	3.835	2.19+
logVolume_forest ~ logVolume_fire * model * forestType	(Intercept)	-5.152	12.239	-0.42
with variance function:	logVolume_fire	2.186	8.071	0.27
~1 | model * forestType	model (MS)	7.635	16.535	0.46
	forestType (Broadleaf)	11.389	12.690	0.9
	forestType (Dry conif.)	3.980	12.263	0.32
	forestType (Dry Douglas-fir)	1.179	12.239	0.1
	forestType (Mixed)	19.234	15.284	1.26
	forestType (Moist conif.)	10.201	14.871	0.69
	forestType (Pine)	4.470	12.274	0.36
	forestType (Spruce)	-25.249	19.722	-1.28

	forestType (Douglas-fir)	6.896	13.553	0.51
	logVolume_fire:model (MS)	-3.759	9.529	-0.39
	logVolume_fire:forestType (Broadleaf)	-4.540	8.409	-0.54
	logVolume_fire:forestType (Dry conif.)	-1.748	8.163	-0.21
	logVolume_fire:forestType (Dry Douglas-fir)	-2.928	8.071	-0.36
	logVolume_fire:forestType (Mixed)	-11.621	10.771	-1.08
	logVolume_fire:forestType (Moist conif.)	-3.230	10.249	-0.32
	logVolume_fire:forestType (Pine)	-2.693	8.205	-0.33
	logVolume_fire:forestType (Spruce)	25.965	15.125	1.72
	logVolume_fire:forestType (Douglas-fir)	-0.941	9.224	-0.1
	model (MS):forestType (Broadleaf)	54.859	26.310	2.09+
	model (MS):forestType (Dry conif.)	-5.200	16.555	-0.31
	model (MS):forestType (Dry Douglas-fir)	-6.393	16.536	-0.39
	model (MS):forestType (Mixed)	-19.359	19.200	-1.01
	model (MS):forestType (Moist conif.)	21.283	19.176	1.11
	model (MS):forestType (Pine)	-5.97822	16.572	-0.36
	model (MS):forestType (Spruce)	46.21904	23.615	1.96
	model (MS):forestType (Douglas-fir)	-4.95554	18.071	-0.27
	logVolume_fire:model (MS):forestType (Broadleaf)	-28.21859	14.269	-1.98+
	logVolume_fire:model (MS):forestType (Dry conif.)	2.18887	9.670	0.23
	logVolume_fire:model (MS):forestType (Dry Douglas-fir)	4.55167	9.529	0.48
	logVolume_fire:model (MS):forestType (Mixed)	11.87889	12.052	0.99

	logVolume_fire:model (MS):forestType (Moist conif.)	-8.47112	11.61854	-0.73
	logVolume_fire:model (MS):forestType (Pine)	4.16847	9.821908	0.42
	logVolume_fire:model (MS):forestType (Spruce)	-33.62613	16.28581	-2.06
	logVolume_fire:model (MS):forestType (Douglas-fir)	1.78346	10.71654	0.17

Supplementary figures

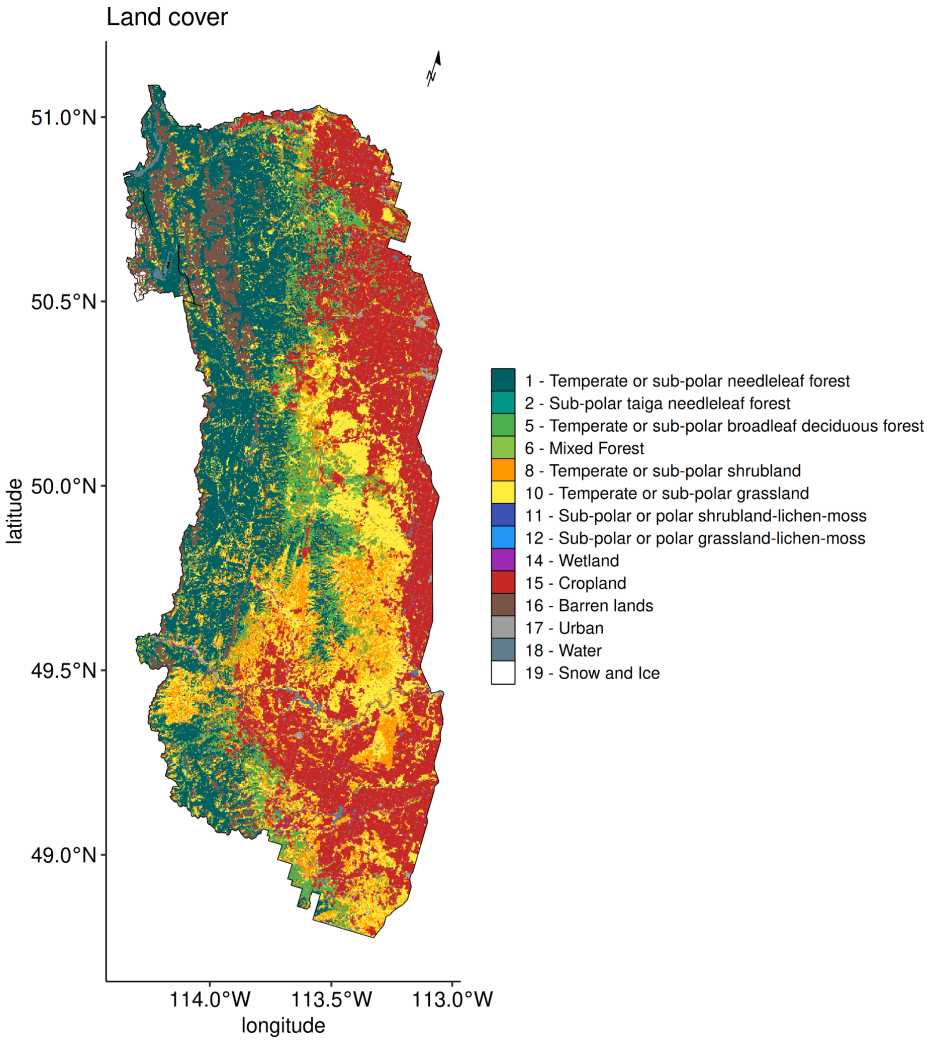

Figure A.1. Land-cover classes used to define ecolocations, derived from the Land Cover Map of Canada 2010 (see Table A.2). Only pixels in forested land-cover classes (1, 2, 5 and 6) were used to simulate vegetation dynamics; non-forested classes 8, 10-12 and 16 were included as non-forested pixels where fire spread dynamics could occur (see Appendix C).

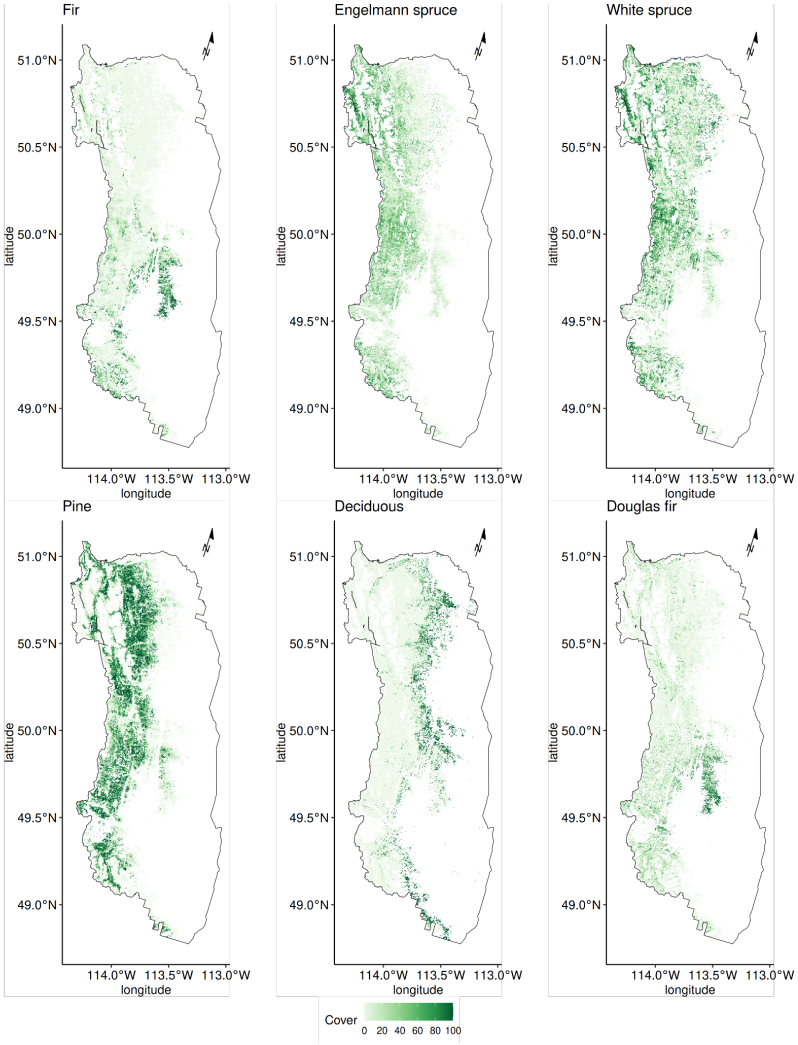

Figure A.2. Percent cover of species entering the simulation model. Fir comprises all *Abies* species found in the study area, Pine comprises all *Pinus* species in the area (mostly *Pinus contorta*), Deciduous comprises *Populus tremuloides*, *P. balsamifera* and *Betula papyrifera*. Douglas-fir is *Pseudotsuga menziesii*. See Table A.2 for data sources.

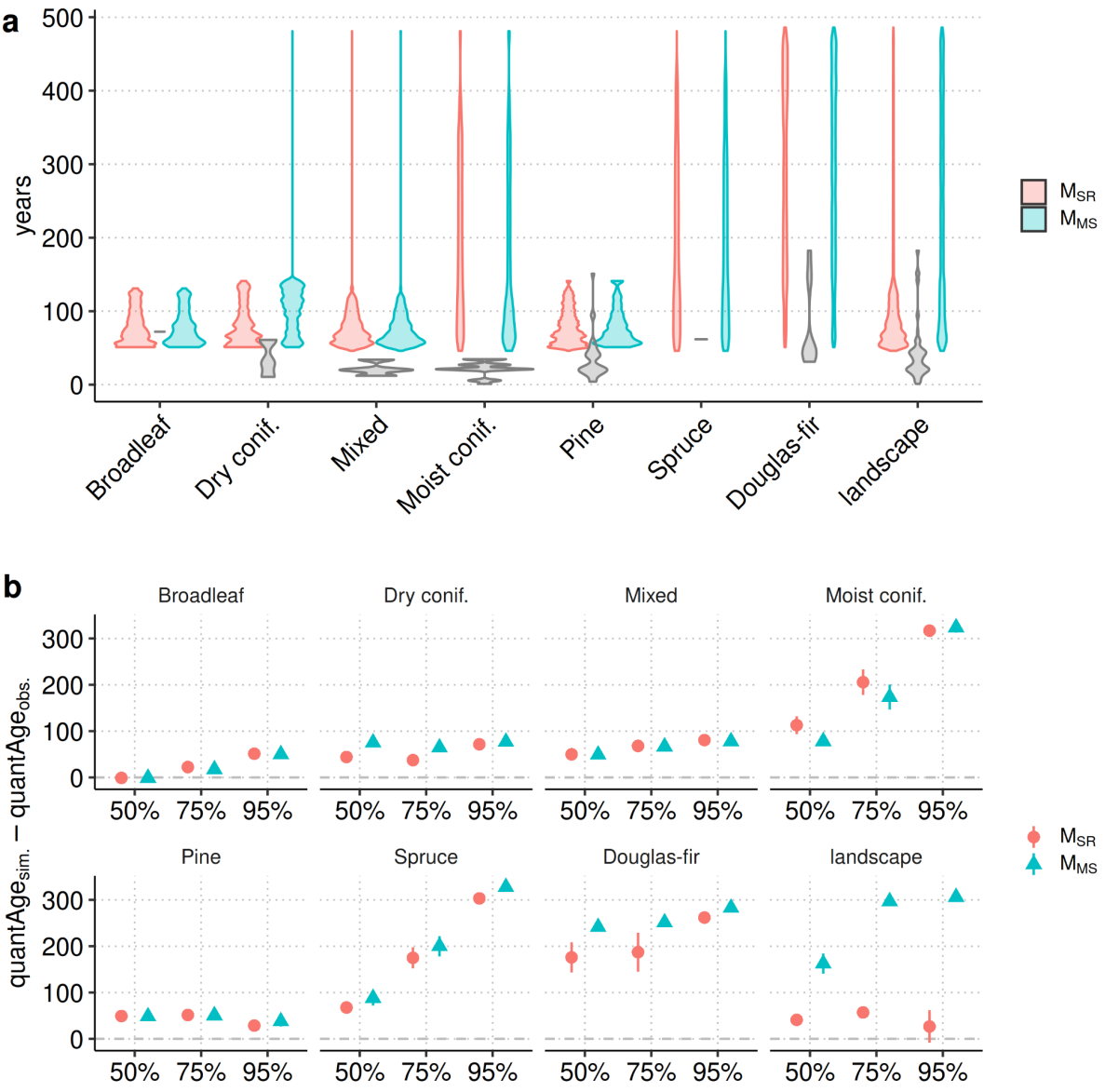

Figure A.3. Comparisons between simulated and observed ages. Panel a) shows density distributions for each model across pixels, years and replicates by forest type and across forest types (i.e., landscape). Panel b) shows simulated quantile deviations from observed quantile ages (averaged across patches) calculated across pixels and sampled years, per replicate (points are means with 95% confidence intervals across replicates). Forest types are: dry-mixed conifer ('Dry conif.'), Douglas-fir-dominated ('Douglas-fir'), moist conifer ('Moist conif.'), pine-dominated ('Pine'), spruce-dominated ('Spruce'), broadleaf-dominated ('Broadleaf') and mixedwood forests ('Mixed'). Only pixels (and field plots) with simulated

(and observed) fire events were included. Forest types that were simulated but not sampled in the field are not shown here, as they have no observed data to compare to.

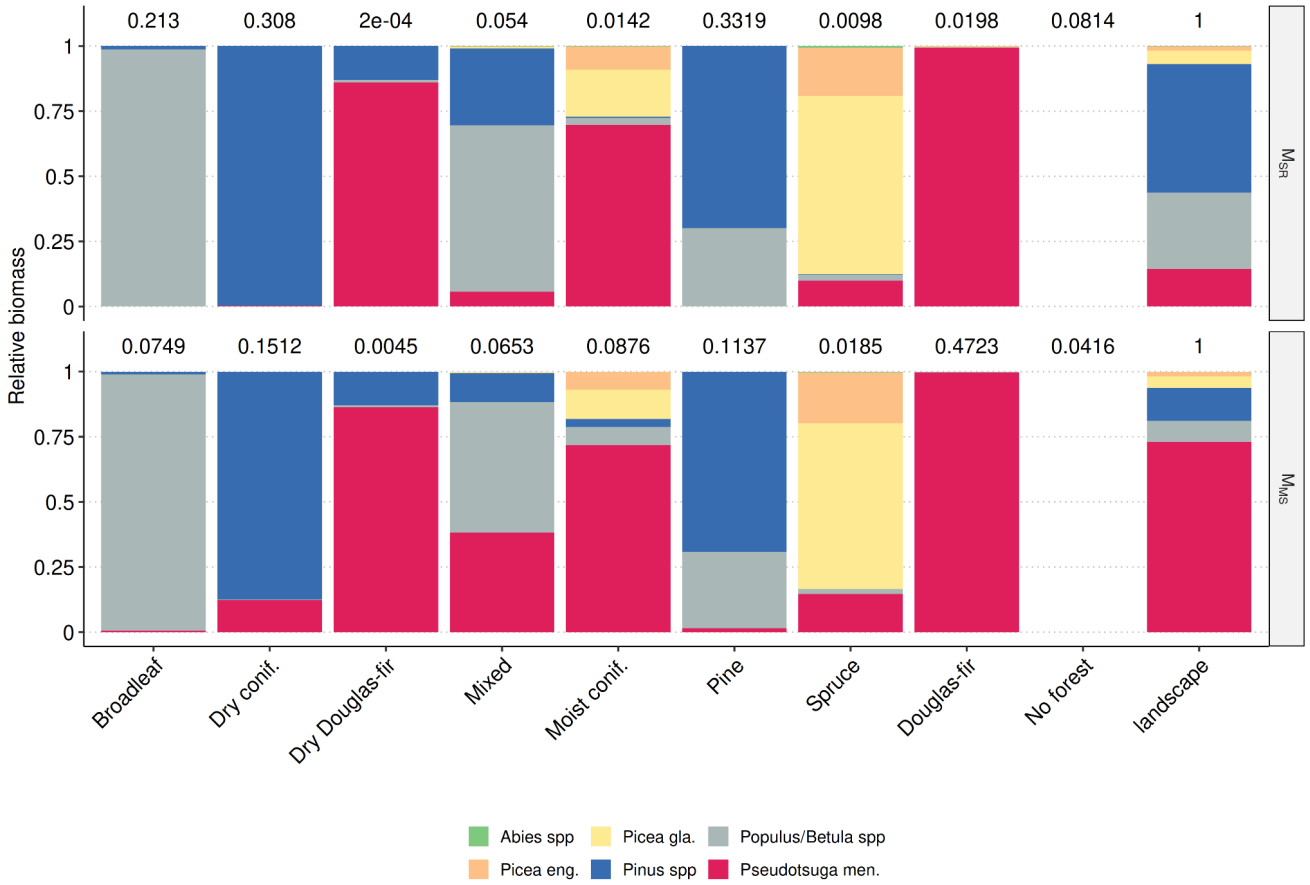

Figure A.4. Species relative biomass per forest type. Species relative biomass was calculated as a species' proportion of the total biomass summed across all pixels within a forest type, per sampled year and simulation replicate. Stacked bars show averages across sampled years

and replicates. Annotated numbers show the relative number of pixels within each forest type, averaged across sampled years and replicates. Note that five years were sampled from each replicate's quasi-equilibrium period. Only burnt pixels were considered here.

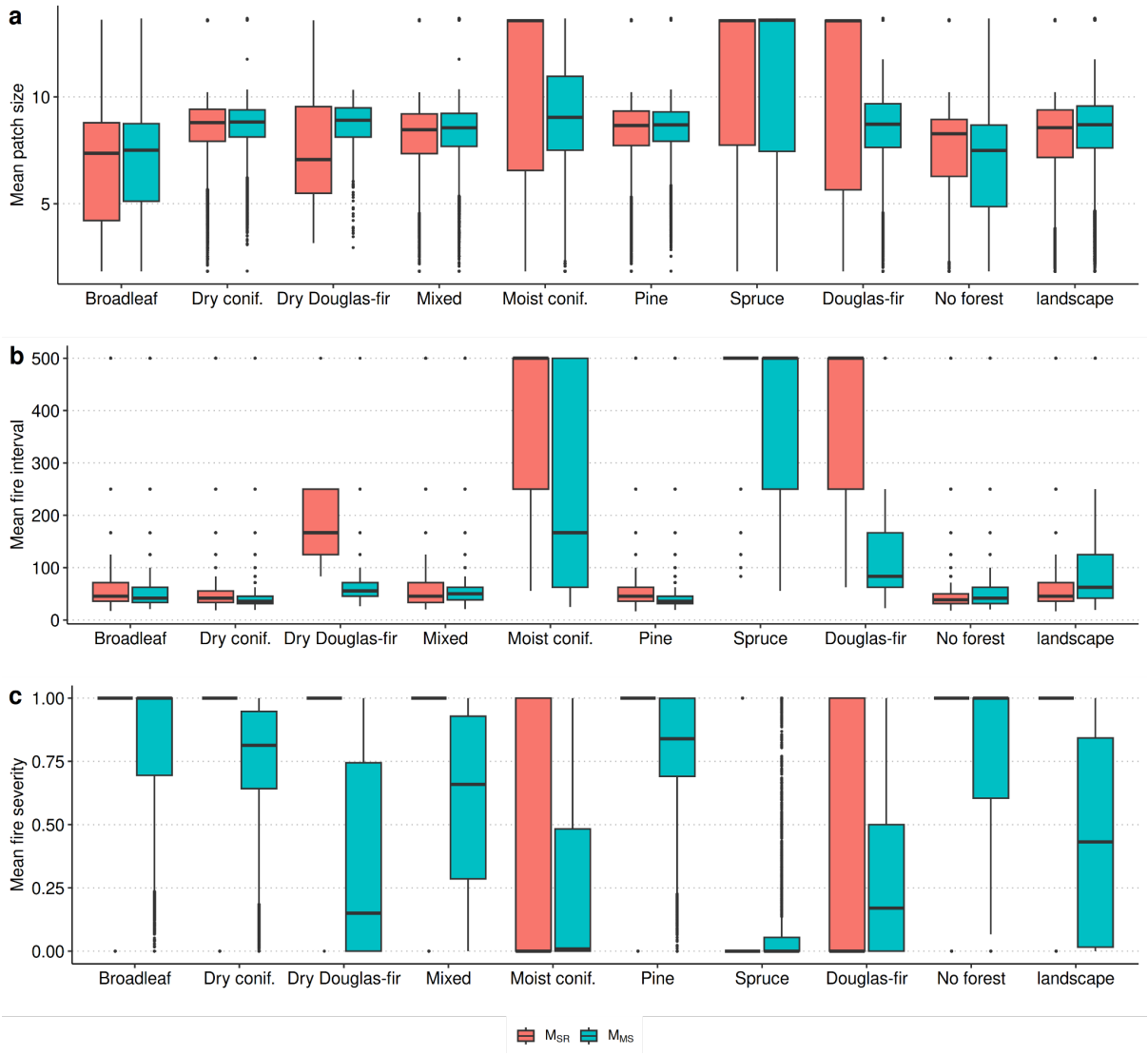

Figure A.5. Temporally integrated fire attribute values per forest type and across the landscape; fire attribute calculations follow Steel et al. (2021).

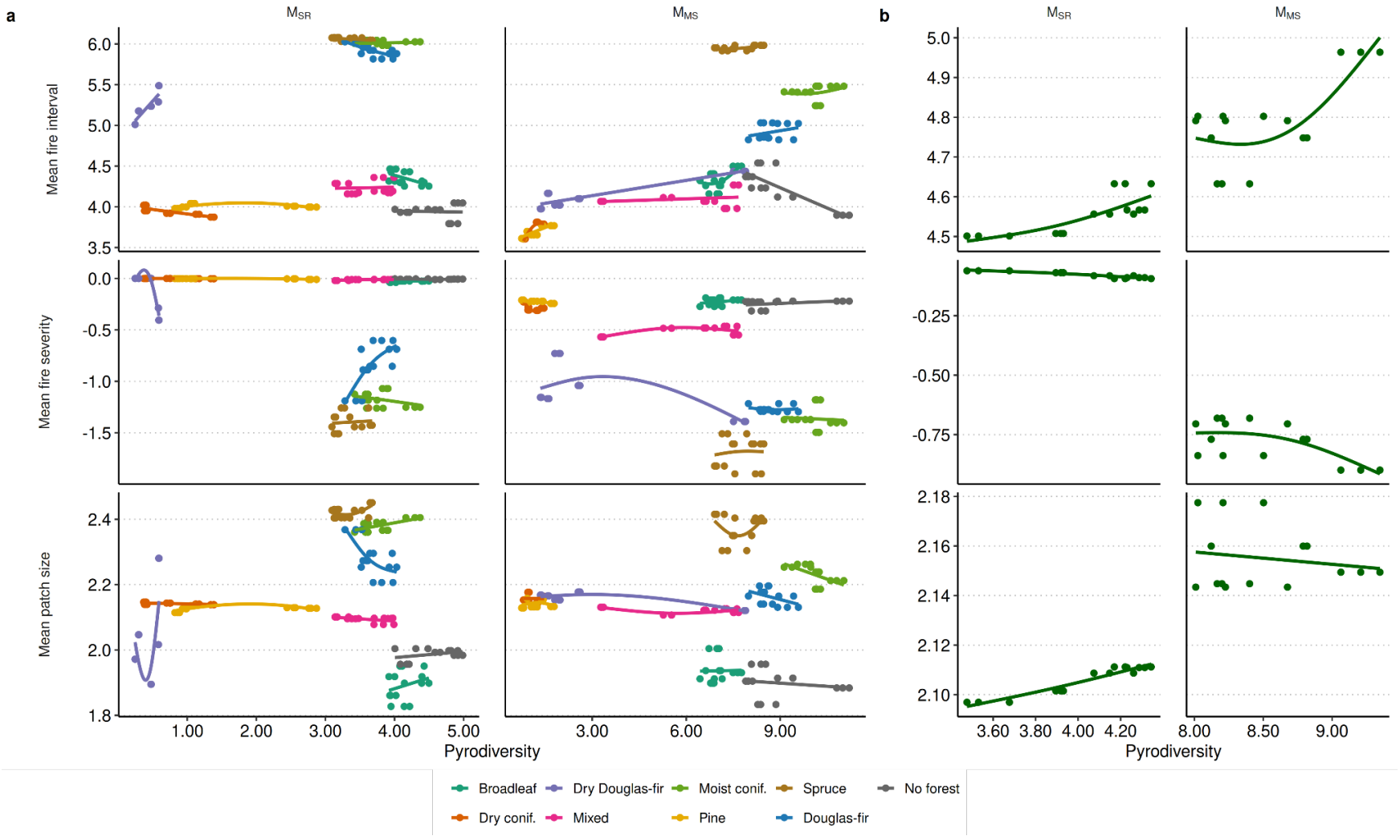
a
b
M_{SR}
M_{MS}
Mean fire interval
Mean fire severity
Mean patch size
Pyrodiversity
Broadleaf
Dry conif.
Dry Douglas-fir
Mixed
Moist conif.
Pine
Spruce
Douglas-fir
No forest

Figure A.6. Temporally integrated fire attribute values across the pyrodiversity gradient a) within forest types and b) in the entire landscape in each model. Here, fire attributes were averaged across pixels per model (per forest type, in panel a, or across the landscape, in panel b) and simulation replicate, and logged for visual clarity. Note that hypervolumes were on the pixel-level fire attribute values (not on the plotted logged averages). Pyrodiversity values are raw hypervolume sizes.

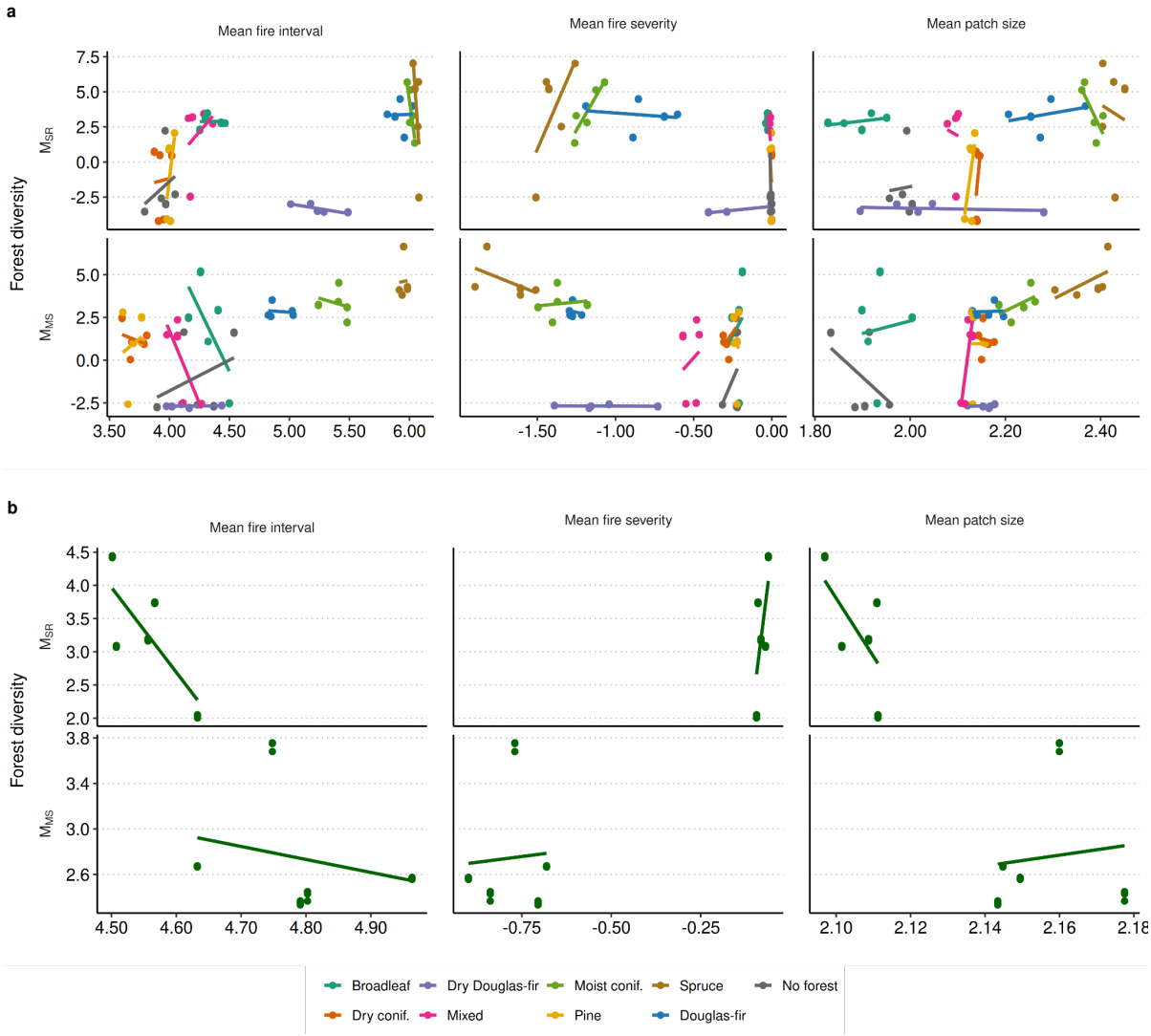

Figure A.7. Forest diversity values across all three fire attribute gradients a) within forest types and b) in the entire landscape in each model. See legend in Fig. A.6. for fire attribute had hypervolume calculation details. Forest diversity values are logged hypervolume sizes.

Appendix B

Data-driven parameter estimation and simulation of fire and regeneration

Supplementary tables and figures can be found in this or corresponding appendices (e.g. all tables starting Table A.* are found in Appendix A).

Estimation of vegetation parameters

Data inputs and model parameters for the simulation of vegetation dynamics were prepared by three modules: *Biomass_speciesData*, *Biomass_borealDataPrep* and *Biomass_speciesParameters* (Fig. 2, main text). Before estimating any traits/parameters and initialising the landscape, the data modules assess data quality and correct for any known issues (e.g., missing stand age data in a pixel with recorded species cover and biomass; Appendix C). We group parameters involved in simulating cohort dynamics into three main categories: i) invariant species traits, ii) spatially varying species traits, and iii) ecolocation-specific parameters. Invariant species traits are spatio-temporally constant for any given species, and influence growth, mortality, dispersal and recruitment dynamics, as well as responses to disturbances (i.e., fire). Invariant species trait values were compiled from published literature, default species trait tables used in LBSE and from our own statistical fitting using *Biomass_speciesParameters*. *Biomass_speciesParameters* estimates species-specific growth and mortality curve parameters ('growth curve' and 'mortality shape') by matching theoretical growth curves and observed growth curves from permanent sample plot data. All invariant species traits are listed in Table B.1. Spatially varying species traits varied by 'ecolocation' (combination of ecological zone from Natural Regions and Subregions of Alberta, and land-cover class from Land Cover of Canada 2010), but not through time. Spatially varying species traits were maximum biomass (maxB), maximum aboveground net primary productivity (maxANPP) and species establishment probability (SEP). All three were estimated by *Biomass_borealDataPrep* from available data on species cover, biomass and age and recalibrated by *Biomass_speciesParameters* (Table B.3). The only ecolocation-

specific parameter – i.e., values can vary across ecolocations, but not across species – is minimum relative biomass (minRelativeB). It determines the shade thresholds at the pixel-level that result in successful germination of a species given its shade tolerance. In this case, we took the minRelativeB values used in other applications of LBSE (which are constant across ecolocations; see source in Table A.1) and lowered them for the higher shade classes (Table B.4). This reflects lower shade levels observed in Western Canadian forests with respect to their Eastern counterparts at similar density levels (Messier et al., 1998), likely driven by higher resource (i.e., moisture) limitation in the west (Hogg et al., 2008; Peng et al., 2011). Given that we had no indication that shade levels for a given forest density varied across our study area (which is also relatively small), we used the same minRelativeB for all ecolocations.

Below, we detail further the estimation of several of the above-mentioned parameters.

Growth- and mortality curve parameters, maximum biomass and maximum aboveground net primary productivity adjustment factors (Biomass_speciesParameters module)

Cohort growth and mortality in LandR Biomass is essentially determined by four parameters: 'growth curve', 'mortality shape', maximum biomass (maxB) and maximum aboveground net primary productivity (maxANPP). The 'growth curve' and 'mortality shape' parameters (so called in LANDIS-II Biomass Succession Extension v3.2) are invariant species traits that modulate the shape of species growth curves. They were estimated using *Biomass_speciesParameters*, which matches theoretical species curves obtained by varying parameter values (namely, 'growth curve', 'mortality shape', 'longevity' and 'mANPPproportion') against observed species growth curves from permanent sample plot (PSP) data (see Appendix C for details on simulated and observed data, as well as the ranges of parameter values used). The parameter mANPPproportion reflects the relationship between maxB and maxANPP and was later used to adjust the values of maxANPP estimated by *Biomass_borealDataPrep*.

Before calculating the observed species growth curves, the PSP data was subset to stand ages below the 95th percentile (for each species), as records for larger age classes were limited and constituted statistical outliers. In addition, 50 points were added at the origin (age = 0 and biomass = 0), since very young trees (diameters < 10 cm) were not measured in the original data. This forced the intercept to be essentially 0 age and 0 biomass. Growth curves for each species were then modelled using a generalised additive mixed effects model (GAMM) that related species biomass (B) with stand age (standAge), accounting for the random effects of the measurement year (measureYear) and plot (plotID) on the intercept:

$$\mathrm{B} \sim \mathrm{f\_1}\,(\mathrm{standAge}) + (\sim 1\,|\mathrm{measureYear} + \mathrm{plotID}) \qquad \text{[Eq. B.1]}$$

where f1 denotes the smoother function. To avoid overfitting, we constrained the smoother on stand age to a maximum smoothing degree of 3 (i.e. 3 knots and a polynomial degree of 2) and a point constraint at 0 that attempted to force the intercept to 0. In addition, B was weighted with respect to species dominance. This consisted in 1) calculating the average biomass of each dominant species *i* (i.e. relative biomass in a plot > 0.5; $\mathrm{domSpeciesB_i}$), in each plot and measurement year, and 2) dividing the species average biomass by the average biomass across all n dominant species (allDomSpecies):

$$\frac{\overline{domSpeciesB_i}}{\overline{allDomSpeciesB}} \qquad \text{[Eq. B.2]}$$

For the added 0 age and 0 biomass data we used weights equal to 1. Some species did not have enough data to allow for model convergence, thus their growth and mortality curve parameters, together with mANPPproportion, were assigned LANDIS-II default values (see Table B.1). *Biomass_speciesParameters* generated a large number of curves (the "theoretical" curves) in a factorial simulation experiment with many growth curve and mortality shape values that span all reasonable values. Longevity is assumed to be an input by user as it was not possible to estimate using PSP data. After fitting the GAM curves to PSP data, *Biomass_speciesParameters* compared these to the theoretical curves and picked the best one for each species, using maximum likelihood. The user had the option to constrain the values of the growth and mortality curve parameters. We noted that the theoretical curves

never achieved the biomass indicated by maxB (set to 5000 for all simulations of theoretical species curves). This is because maxB is an asymptotic parameter that reflects the potential maximum biomass for a species in an ecolocation (here, the combination of ecological zone and land-cover that reflects a particular combination of biophysical characteristics and growth conditions for a species). Hence, we used the relationship between the achieved and potential maximum biomass in the theoretical species curves, to rescale the maxB parameter estimated from data (by *Biomass_borealDataPrep*; see below) so that species could achieve maximum observed biomasses during the simulations. Not all species had enough data to build an observed growth curve and find the best matching growth and mortality curve parameters. In this study, observed curves were successfully built for Picea engelmannii, P. glauca and Pseudotsuga menziesii. For the remaining species growth and mortality curve trait values were not changed, maxB was not rescaled and maxANPPproportion kept its default value (see below).

Maximum biomass (maxB) and maximum aboveground net primary productivity (maxANPP) are spatially varying species traits, which vary by ecolocation. *Biomass_borealDataPrep* statistically estimates maxB from observed data using a linear mixed effects model reflecting the response of species-specific biomass (B) to the interaction between age (on the log scale, logAge) and species, and the interaction between % cover and species, while accounting for the random effect of ecolocation on the calculated slopes (per species) and intercepts:

$$B \sim logAge * species + cover * species + (logAge + cover + species \mid ecolocation)$$

[Eq. B.3]

Where '*' denotes the inclusion of separate fixed effects and the interaction between them. Coefficients were estimated by maximum likelihood, and model fit was calculated as the proportion of explained variance explained by fixed effects only (marginal r2) and by the entire model (conditional r2), which was 0.45 and 0.62 respectively. We then predicted maxB by species and ecolocation combination, by setting cover to 100% and log age to log longevity and predicting biomass at that point value (i.e. log-longevity; Table B.3). As mentioned above,

maxB was rescaled so that species could achieve maximum observed biomasses during the simulation. maxANPP was calculated as maxB * mANPPproportion/100, where mANPPproportion came from the *Biomass_speciesParameters* module above. Only the species that had enough data to estimate growth and mortality curve parameters and maxANPPproportion were adjusted for maxB – in this case, *P. engelmannii*, *P. glauca* and *Pseudotsuga menziesii*. Others kept defaults from LANDIS-II (using mANPPproportion = 3.33) and a non-rescaled maxB.

Species establishment probability (Biomass_borealDataPrep module)

Species establishment probability (SEP) was estimated by modelling the probability of observing a given species in each ecolocation. For this, we used a generalised linear mixed model, whereby the probability of occurrence of a species (π) – calculated as the number of pixels with % cover > 0 divided by the total number of pixels, by ecolocation and species identity following a binomial distribution (with a logit link), while accounting for the random effect of ecolocation on the intercepts.

$$logit(\pi) \sim species + (1 \mid ecolocation) \quad \text{[Eq. B.4]}$$

where π is the probability of finding a species in an ecolocation. Model fit resulted in 0.99 for both the marginal r^2 and the conditional r^2. The fitted values were used as the spatially varying SEP trait values for each species and ecolocation combination (Table B.3)

Fire parameters, fire dynamics and forest responses to fire

Converting simulated biomass to fire fuels (Biomass_fuelsPFG module)

Each pixel was assigned a dominant fire fuel type based on simulated species composition and age structure in forested pixels and land-cover class in non-forested pixels. Fuel types followed the Canadian Forest Fire Behaviour Prediction System (hereafter 'FBP System') fuel classification and the conversion between simulated pixel composition and fuels was adapted to our study area. In forested pixels, species were initially assigned to a fire plant functional group (PFG) according to their identity and age (Table B.5). Species biomasses were summed

for each PFG and divided by the total stand biomass to obtain relative PFG abundance per pixel. The dominant PFG determined the final fuel type based on a minimum threshold of relative abundance (Table B.6). Fuel types that were characterised by more than one PFG needed to meet the minimum relative abundance thresholds of all PFGs. For instance, the mixed stand fuel type M2 required a minimum of 25% conifer species abundance and 26% broadleaf species abundance (PFGs 4 and 5, respectively), and the Douglas-fir dominated fuel type 'C7' required a minimum 50% abundance of Douglas-fir (Pseudotsuga menziesii) and at least 75% of conifer species abundance (PFGs 2 and 4, respectively; Table B.6). In cases where several fuel types filled the minimum requirements, the final fuel type was the one that had the most PFGs meeting the requirements or the highest thresholds of minimum relative biomass. In 'mixed' fuel types, we also calculated the relative abundance of conifers used to calculate fire behaviour properties in the *FireProperties* module.

Fuel types in non-forested pixels were based on pixel land-cover class (see Appendix C for non-forested land-cover classes and Table B.5 for conversion table). 'Open' fuel types can be associated with a degree of curing, important for the calculation of fire behaviour properties. For land-cover classes with a varying curing level (fixedCuring set to FALSE), the curing level was drawn for each pixel and each year from a skewed normal distribution, with a mean set to curingMean, variance and slant set to 10, and constrained between curingMin and curingMax levels (Table B.7). Values for curingMean, curingMin and curingMax were obtained from expert knowledge of common curing values and intervals observed in non-forested habitats of Alberta (D. Perrakis pers. comm.). Croplands and barren-lands (Land Cover of Canada 2010 classes 15 and 16, respectively) were not included in the simulation but are abundant in eastern areas of the study area (Fig. A.1).

Fire behaviour properties (FireProperties module)

We calculated five fire behaviour properties using the Canadian Forest Fire Danger Rating System, *cffdrs*, R package (Wang et al., 2017): crown fraction burned, CFB, equilibrium head fire rate of spread (ROS), critical spread rate for crowning (RSO), head fire intensity (HFI), and

total fuel consumption (TFC). This consists in first calculating Fire Weather Index (FWI) System components (fine fuel moisture code, FFMC and buildup index, BUI) from weather and geographical data (latitude, longitude, day, month, temperature, relative humidity, wind speed at 10m, precipitation). Together with topography (slope and aspect) and fuel conditions (fuel type, conifer cover for mixed fuel types and degree of curing for open fuel types), FWI components are then used as inputs to the Fire Behaviour Prediction (FBP) System, which calculates the above-mentioned fire behaviour properties. Both FWI and FBP outputs were calculated in a spatio-temporally varying manner, whereby both weather and fuel conditions varied at each time step per pixel. To vary fire weather, we randomly sampled a 'typical' fire day (fire weather index, FWI >= 19) from the daily weather data generated for the baseline climate period (Appendix C); similarly, fuel conditions were updated every time step at the pixel level by converting simulated cohort biomass into fire fuel types (see above). Finally, slope and aspect were calculated from a Digital Elevation Model subset to the study area (see source in Table A.2) using the *gdalUtils* R package (Greenberg & Mattiuzzi, 2020). Given that the *fbp* function of the *cffdrs* package does not accept the broadleaf 'D2 - Green Aspen' fuel type, we converted all pixels with this fuel type to the allowed 'D1 - Leafless Aspen'. The two differ in their ability to reach higher fire intensity classes, with D1 being able to reach the two highest classes under extremely dry and windy conditions, but not D2.

Probability of ignition (FireSense and FavierFireSpread modules)

The fire ignition probability depended on the estimated average number of fires per pixel, which were based on observed fire occurrence data from the climate baseline period between 1961-1990 (i.e. pre-climate change). We followed the approach described in Marchal, et al. (2017) (implemented in the *fireSense_IgnitionFit* and *fireSense_IgnitionPredict* SpaDES modules) and modelled fire occurrences as a function of weather and fuel conditions during the reference period (see Appendix C for fire and weather data details).

Fuel conditions used to fit the model were obtained by converting the species composition per pixel at the beginning of the simulation into a dominant fuel type, following

the FBP System fuel classification (see above; Fig. B.1). We then calculated the cover of each fuel type at 1 Km^2, by calculating the proportion of 250 m^2 pixels of each fuel type inside each 1 Km^2 pixel (Fig. B.2). We crossed each fire occurrence (usually just one per 1 Km^2 pixel) with the July mean drought code (julDC) of the fire year and with fuel composition. July mean drought code was calculated as the mean of July daily drought code. To balance the design, we added a number of fire absences equal to twice the number of fire occurrences for each fire year. Fire absences were randomly placed in pixels with no fire records and assigned their respective pixels' and years' julDC and fuel composition. The module *fireSense_IgnitionFit* then fit a piecewise generalised linear model that related the expected number of fires (Y_i) per pixel across years, as a function of the interaction between mean julDC (calculated across years) and each fuel type cover. As in Marchal et al. (2017) we modelled the intercept at 0 and allowed breakpoints to vary across fuel types. The model was fit with Negative Binomial distribution using an identity link, and θ = 1:

$$Y_i \sim Negative\ Binomial(\mu, \theta)$$

$$\mu \sim -1 + coniferous{:}julDC + D2{:}julDC + M2{:}julDC + O1b{:}julDC +$$

$$NF{:}julDC + coniferous{:}pw(julDC, k_{conif}) + D2{:}pw(julDC, k_{D2}) +$$

$$M2{:}pw(julDC, k_{M2}) + O1b{:}pw(julDC, k_{O1b}) + NF{:}pw(julDC, k_{NF}) \quad \text{[Eq. B.5]}$$

where 'coniferous' is the sum of all coniferous fuel types in a pixel, and remaining fuel types are broadleaf, 'D2', mixed, 'M2', open habitat, 'O1b', and non-fuel, 'NF'; ':' denotes the inclusion of predictor interactions but not their main effects, an '-1' denotes the zero-intercept. Note that θ is inverse of the dispersion parameter (α) of a Negative Binomial distribution. Model coefficients were estimated by direct minimization of the negative log-likelihood function, on a constrained optimization procedure ensuring that all coefficients were non-negative (see Marchal et al., 2017). We also bounded all coefficients between 0 and 20. Together, this means that we assumed a fire occurrence probability of 0, when julDC is 0, a strictly positive effect of MDC on the probability of fire ignition, but varying thresholds of effect changes (i.e. breakpoints) depending on fuel types. The model was then used by *fireSense_IgnitionPredict*

to spatially predict the average number of fires per pixel across the 1961-1990 period, which can be translated to a probability of fire occurrence, the λ parameter of a Poisson distribution (Marchal et al., 2017). Model performance was high, with fitted values matching the observed data both spatially and annually, with the exception of extreme years (Fig. B.3).

Fire escapement and spread (FavierFireSpread module)

Fire escapement depended on the probability of spread, *p*, and fire spread depended on *p* and *q*, the probability of persistence. Values of p and q were recalculated every year, on a pixel basis, in function of fire behaviour properties (thus annually varying as a function of weather, fuel and topography conditions). We chose three fire behaviour properties: ROS, HFI and TFC, calculated for each year and pixel by the *FireProperties* module. We assumed that 1) higher rates of spread and higher fire intensities will lead to higher probability of passing to a neighbour cell, 2) that the more fuel a fire consumes and the more intensity it has and the longer it burns at a given location, and 3) that these variables affect the probabilities of spread and persistence synergistically, rather than additively. Following this logic, we calculated *p* and *q* as:

$$p_i = ROS_i \times HFI_i$$

$$q_i = TFC_i \times HFI_i \qquad \text{[Eq. B.6]}$$

To convert *p* and *q* to probability values bounded to [0,1], we rescaled all *p* to values ranging 0.20-0.25 (values that were originally 0 were converted back to 0) and all *q* to values ranging 0-1. Bounding *p* between 0.20 and 0.25 ensured sensible fire sizes and perimeters (visually determined).

Vegetation responses to fire - Biomass_regenerationPM and Biomass_regeneration modules

Biomass_regenerationPM follows the LANDIS-II Dynamic Fire System v3.0 equations to kill entire cohorts as a function of the fire severity class in the pixel (varying between 1, very low severity, and 5, highest severity and complete stand mortality), cohort age and their fire tolerance (a species-level trait) (Sturtevant et al., 2018). The fire severity class is calculated

for each pixel as a function of three fire behaviour properties: CFB, ROS and RSO, which are in turn dependent on fuel, topography and weather conditions (see above). We varied weather conditions every timestep for every pixel, by randomly sampling a 'typical' fire weather day (fire weather index, FWI >= 19; Podur & Wotton, 2011) from daily weather data generated for the baseline climate period using BioSIM v11 (Régnière et al., 2017). Fuel conditions were also updated every time step by the *Biomass_fuelsPFG* module, which translated tree cohort biomass into fuel types used by *cffdrs*.

After calculating CFB, ROS and RSO in every burnt pixel (i.e., pixels where fire spread to, as simulated by the *FavierFireSpread* module), the fire severity class was determined as:

$$\text{severity}_i = \begin{cases} 1, & \text{if } \text{CFB}_i < 0.1 \wedge \text{ROS}_i < \frac{\text{RSO}_i + 0.458}{2} \\ 2, & \text{if } \text{CFB}_i < 0.1 \wedge \text{ROS}_i \geq \frac{\text{RSO}_i + 0.458}{2} \\ 3, & \text{if } 0.1 \leq \text{CFB}_i < 0.495 \\ 4, & \text{if } 0.495 \leq \text{CFB}_i < 0.9 \\ 5, & \text{if } \text{CFB}_i \geq 0.9 \end{cases} \quad \text{[Eq. B.7]}$$

A severity of class 5 constitutes a stand-replacing fire, killing all cohorts in that pixel. The remaining classes are compared against species fire tolerances, by subtracting fire tolerance from fire severity (severityToleranceDif), to determine the fire damage (i.e. which cohorts are killed; 'agesKilled' column in Table B.8). Cohorts whose ages relatively to longevity (age/longevity) are lower or equal to the fire damage are killed. From Table B.8 we can see that the more tolerant a species or the lower the severity of the fire, the lower will be 'severityToleranceDif' and the more the younger cohorts survive.

After killing cohorts, *Biomass_regenerationPM* calculates the total and relative biomass lost (the "actual" fire severity) and activates serotiny and resprouting mechanisms for the (partially) killed species. It follows the post-fire regeneration mechanisms in the LANDIS-II Biomass Succession Extension v.3.2.1 model (Scheller & Miranda, 2015; Scheller & Mladenoff, 2004), activating serotiny and resprouting depending on pre-fire species composition and age. Unlike LANDIS-II, we allow serotiny and resprouting to occur in the same pixel (although not for the same species) to simulate the competitive advantage of

resprouter species (e.g., trembling aspen, *Populus tremuloides* Michx.) with respect to serotinous species (e.g., lodgepole pine) (Greene & Johnson, 1999; Johnstone, 2005; Landhäusser et al., 2009), should they both be activated following a given fire event. *Biomass_regeneration* differs from *Biomass_regenerationPM* in that it always assumes stand-replacing fires (i.e., kills all cohorts). After removing cohorts and calculating the actual fire severity (i.e., raw and relative biomass lost), *Biomass_regeneration* activates serotiny and resprouting in the same way as *Biomass_regenerationPM*.

Table B.1. Invariant species traits. List of species trait values that are spatio-temporally constant. Most trait values were obtained from Dominic Cyr's publicly available LANDIS-II species trait tables (Table A.2). Simulated species were: *Abies sp* (Abie_sp), *Picea engelmannii* (Pice_eng), *P. glauca* (Pice_gla), *Pinus sp* (Pinu_sp), *Populus sp* (Popu_sp) and *Pseudotsuga menziesii*. Longevity ('long.') values were adjusted following Burton and Cumming (1995) and shade tolerance ('shadetol.') values were lowered to obtain a more realistic recruitment pattern. Mortality ('mortalityshape') and growth ('growthcurve') parameters, the adjustment factor for maxANPP ('mANPPprop.') and the inflation factor for maxB ('inflationFactor') were estimated from data where possible using LandR *Biomass_speciesParameters*, otherwise the default LANDIS-II values were kept. In this case, *Abies sp*, *Picea engelmannii*, and *Pseudotsuga menziesii* had enough data for the estimation of these parameters. maxB (an asymptotic parameter) was rescaled using 'inflationFactor' so that species could achieve the observed maximum biomass (derived from satellite data) during the simulation. See Appendices B and C for further detail on parameter estimation.

species	long.	sexual mature	shadetol.	firetol.	postfire regen	resprout prob	resproutage_min	resproutage_max	seed dist._eff	seeddistance_max	mortality shape	growth curve	mANPPprop.	inflationFactor
Abie_sp	200	20	2.3	1	none	0	0	0	25	100	21	0.7	4.518	1.102
Pice_eng	463	30	2.1	2	none	0	0	0	30	250	23	0.81	5.341	1.005
Pice_gla	400	30	1.6	2	none	0	0	0	100	303	22	0.75	5.27	1.037
Pinu_sp	150	15	1	2	serotiny	0	0	0	30	100	22	0.75	5.27	1.037
Popu_sp	140	20	1	1	resprout	0.5	10	70	200	5000	22	0.75	5.27	1.037
Pseu_men	525	25	2	3	none	0	0	0	100	500	23	0.74	5.946	1.003

Table B.2. Probability of germination for species shade tolerance and shade level combinations. Species shade tolerances ('shadetolerance') can take any value between 1-5 and pixel shade levels can vary between X0 (no shade) and X5 (maximum shade). If a species' shade tolerance is a non-integer, the resulting probability of germination in a given pixel (with a given shade level) is interpolated between the corresponding lower and upper shade tolerance values. Table values were taken from publicly available LANDIS-II input data (Table A.1).

shadetolerance	X0	X1	X2	X3	X4	X5
1	1	0	0	0	0	0
2	1	1	0	0	0	0
3	1	1	1	0	0	0
4	1	1	1	1	0	0
5	0	0	1	1	1	1

Table B.3. Spatially varying species traits. Species establishment probability (SEP), maximum biomass (maxB) and maximum aboveground net primary productivity (maxANPP) varied across species and by ecolocation. Ecolocations were defined as the combination of ecological zone (digits before "_") and land-cover (the digits after "_"), where the Natural Regions and Subregions of Alberta were used as ecological zones and land-cover followed the Land Cover Map of Canada 2010 (Fig. A.1). For *Picea engelmannii*, *P. glauca* and *Pseudotsuga menziesii*, maxB and maxANPP were adjusted using the adjustment factors estimated by LandR *Biomass_speciesParameters* (see Table B.1 and Appendix B). See Table B.1 for species names.

ecolocation	species	SEP	maxB	maxANPP
1_1	Abie_sp	0.950	10949	495
1_5	Abie_sp	0.778	8106	366
1_6	Abie_sp	0.838	9304	420
3_1	Abie_sp	0.100	11202	506
3_5	Abie_sp	0.099	8435	381
3_6	Abie_sp	0.069	12920	584
4_1	Abie_sp	0.900	7379	333
4_2	Abie_sp	0.847	2951	133
4_5	Abie_sp	0.960	8259	373
4_6	Abie_sp	0.880	8777	397
5_1	Abie_sp	0.609	12439	562
5_2	Abie_sp	0.530	6718	304
5_5	Abie_sp	0.733	10991	497
5_6	Abie_sp	0.607	12422	561
6_1	Abie_sp	0.705	11678	528
6_2	Abie_sp	0.849	4757	215
6_5	Abie_sp	0.815	9370	423
6_6	Abie_sp	0.822	10747	486
1_1	Pice_eng	0.296	11152	596
1_5	Pice_eng	0.106	7682	410
3_1	Pice_eng	0.555	11322	605
3_5	Pice_eng	0.219	7941	424

3_6	Pice_eng	0.279	14300	764
4_1	Pice_eng	0.994	6961	372
4_2	Pice_eng	1.000	2137	114
4_5	Pice_eng	0.996	7842	419
4_6	Pice_eng	0.993	8825	471
5_1	Pice_eng	0.818	11573	618
5_2	Pice_eng	0.968	6063	324
5_5	Pice_eng	0.600	10792	576
5_6	Pice_eng	0.703	12933	691
6_1	Pice_eng	0.971	10583	565
6_2	Pice_eng	0.997	3761	201
6_5	Pice_eng	0.934	8747	467
6_6	Pice_eng	0.958	10262	548
1_1	Pice_gla	0.511	12990	685
1_5	Pice_gla	0.437	9561	504
1_6	Pice_gla	0.983	11078	584
3_1	Pice_gla	0.993	13176	694
3_5	Pice_gla	0.747	9835	518
3_6	Pice_gla	0.989	16004	843
4_1	Pice_gla	0.952	8827	465
4_2	Pice_gla	0.847	3985	210
4_5	Pice_gla	0.941	9723	512
4_6	Pice_gla	0.972	10649	561
5_1	Pice_gla	0.914	13586	716
5_2	Pice_gla	0.915	7952	419
5_5	Pice_gla	0.912	12687	669
5_6	Pice_gla	0.944	14752	777
6_1	Pice_gla	0.931	12616	665
6_2	Pice_gla	0.910	5665	299
6_5	Pice_gla	0.908	10675	563
6_6	Pice_gla	0.916	12193	643
1_1	Pinu_sp	0.511	10382	547
1_5	Pinu_sp	0.437	8021	423
3_1	Pinu_sp	0.285	10642	561
3_5	Pinu_sp	0.181	8344	440

3_6	Pinu_sp	0.330	11755	619
4_1	Pinu_sp	0.703	7358	388
4_2	Pinu_sp	0.439	3470	183
4_5	Pinu_sp	0.450	8158	430
4_6	Pinu_sp	0.575	8462	446
5_1	Pinu_sp	0.951	12119	639
5_2	Pinu_sp	0.866	6839	360
5_5	Pinu_sp	0.760	10565	557
5_6	Pinu_sp	0.852	11612	612
6_1	Pinu_sp	0.947	11510	607
6_2	Pinu_sp	0.752	5179	273
6_5	Pinu_sp	0.798	9242	487
6_6	Pinu_sp	0.856	10444	550
1_1	Popu_sp	0.658	8982	473
1_5	Popu_sp	0.745	6696	353
1_6	Popu_sp	0.737	7623	402
2_5	Popu_sp	0.750	6703	353
3_1	Popu_sp	0.736	9247	487
3_5	Popu_sp	0.750	7023	370
3_6	Popu_sp	0.749	10240	540
4_1	Popu_sp	0.010	6037	318
5_1	Popu_sp	0.541	10799	569
5_2	Popu_sp	0.126	5544	292
5_5	Popu_sp	0.732	9198	485
5_6	Popu_sp	0.706	10175	536
6_1	Popu_sp	0.091	10214	538
6_2	Popu_sp	0.024	3928	207
6_5	Popu_sp	0.452	7925	418
6_6	Popu_sp	0.190	9104	480
1_1	Pseu_men	0.992	13408	797
1_5	Pseu_men	0.985	9805	583
1_6	Pseu_men	0.838	11421	679
3_1	Pseu_men	0.813	13569	807
3_5	Pseu_men	0.497	10057	598
3_6	Pseu_men	0.401	16764	997

4_1	Pseu_men	0.189	9076	540
4_2	Pseu_men	0.094	4137	246
4_6	Pseu_men	0.323	11031	656
5_1	Pseu_men	0.817	13679	813
5_2	Pseu_men	0.915	8134	484
5_5	Pseu_men	0.752	12985	772
5_6	Pseu_men	0.738	15256	907
6_1	Pseu_men	0.588	12644	752
6_2	Pseu_men	0.333	5755	342
6_5	Pseu_men	0.823	10854	645
6_6	Pseu_men	0.790	12407	738

Table B.4. Minimum relative biomass values used to determine the shade level in each pixel. All ecoregions (ecoregionGroup) shared the same values. Shade levels of X0 had 0 biomass. Values taken from publicly available LANDIS-II input data (https://github.com/LANDIS-II-Foundation/Extensions-Succession-Archive/blob/master/biomass-succession-archive/trunk/tests/v6.0-2.0/biomass-succession_test.txt). Initial runs revealed excessive recruitment of moderately shade intolerant species even as stand biomass increased, so we adjusted values for shade levels X4 and X5 downwards (X4: 0.8 to 0.75; X5: 0.90 to 0.85) to reflect higher competition for resources in Western Canadian forests with regards to Eastern Canadian forests.

ecoregionGroup	X1	X2	X3	X4	X5
all	0.15	0.25	0.5	0.75	0.85

Table B.5. Fire plant functional groups (PFGs), used to attribute a fire fuel type to pixels, based on species ages and biomass. In each pixel, the total biomass of each PFG is calculated by summing the cohorts that constitute it. A fire fuel type is later assigned to the pixel depending on the relative biomass of its PFGs (see Table B.6). See Table B.1 for species names

PFG	Name	Species	ageMin	ageMax
1	Mature Flammable Pines	Pinu_sp	60	1000
2	Non-Flammable Conifer	Pseu_men	40	1000
3	Immature Flammable Pines	Pinu_sp	15	60
4	All conifers, all ages	Abie_sp	15	1000
		Pice_eng	15	1000
		Pice_gla	15	1000
		Pinu_sp	15	1000
		Pseu_men	15	1000
5	All broadleaves, all ages	Popu_sp	15	1000
6	Open, all species	Abie_sp	0	15
		Pice_eng	0	15
		Pice_gla	0	15
		Pinu_sp	0	15
		Popu_sp	0	15
		Pseu_men	0	15

Table B.6. Correspondence table between plant functional groups (PFGs) and fire fuel types (FTs). The dominant FT of each pixel is determined based on the relative biomass of the pixel's PFGs. PFGs must meet the minimum threshold of relative abundance in order to apply a particular fuel type to a stand. When two PFGs are listed for a fuel type, they must both meet the minimum threshold of relative abundance (e.g. M2 needs at least 25% of any conifer and 26% of any broadleaf species). See Table B.5 for PFG definitions and their species. FTs were adapted (in terms of species composition) from the Canadian Forest Fire Behaviour Prediction System fuel type classification (Taylor & Alexander, 2016). The M2 fuel type was converted to M1 (Boreal Mixed - leafless) when calculating fire properties, since the *cffdrs* R package functions do not recognise M2.

FT	Name	PFG	Threshold
C2	Boreal spruce	4	0.76
C3	Mature Jack or Lodgepole pine	1	0.8
C4	Immature Jack or Lodgepole pine	3	0.8
C7	Ponderosa pine/Douglas-fir	2	0.5
		4	0.75
M2	Boreal Mixedwood – green	4	0.25
		5	0.26
D2	Green Aspen	5	0.76
O1b	Grass - standing	6	0.8

Table B.7. Non-forest fuels. Pixels with non-forested land-cover classes (according to Land Cover of Canada 2010) were assigned fire fuel types (FTs) following the Canadian Forest Fire Behaviour Prediction System (REF), to allow fire dynamics (ignition and spread) to occur in these pixels. For land-cover classes with a varying curing level (*fixedCuring* set to FALSE), the curing level was drawn each year from a skewed normal distribution, with the location value (i.e. mean) set to *curingMean*, and scale (i.e. variance) and slant set to 10, and constrained between *curingMin* and *curingMax* levels. All values were obtained from expert knowledge of common curing values observed in non-forested habitats of Alberta (D. Perrakis pers. comm.).

Land cover	FT	Name	fixedCuring	curingMean	curingMin	curingMax
8	O1b	Grass - standing	FALSE	60	50	80
10	O1b	Grass - standing	FALSE	60	50	80
12	O1b	Grass - standing	FALSE	60	50	80
11	O1b	Grass - standing	FALSE	60	50	80
13	O1b	Grass - standing	TRUE	30	30	30
16	NF	Non-fuel	NA	NA	NA	NA

Table B.8. Fire damage table. The difference between fire 'severity' (sensu Sturtevant et al., 2018) and species fire tolerances (see Table B.1) determines which cohorts of a species will be killed. If age / longevity ≤ agesKilled, then the cohort is killed. The more tolerant a species or the lower the severity of the fire, the more younger cohorts survive.

severityToleranceDif	agesKilled
< -2	0
-2	0.2
-1	0.5
0	0.85
≥ 1	1

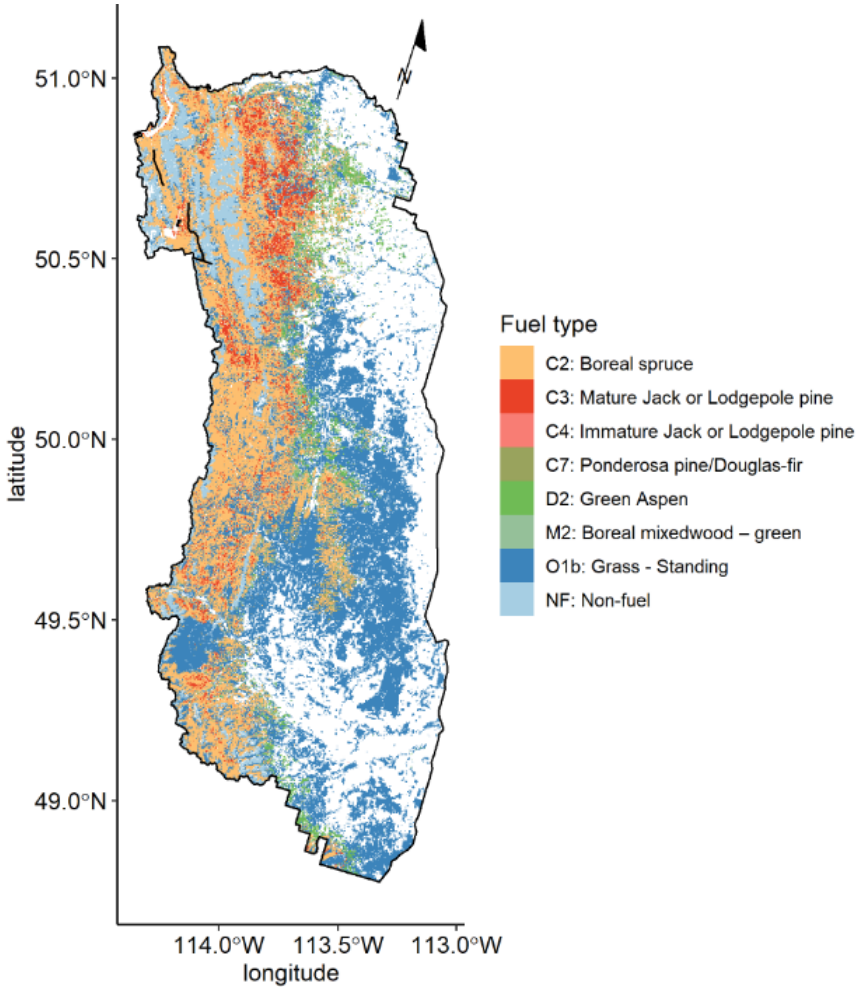

Figure B.1. Map of dominant fuel type per pixel at the start of the simulation (i.e. initial conditions). Fuel types follow the Canadian Forest Fire Behaviour Prediction System, adapted to the study area (see above). Areas in white were not simulated. See Table B.6 for fuel type names.

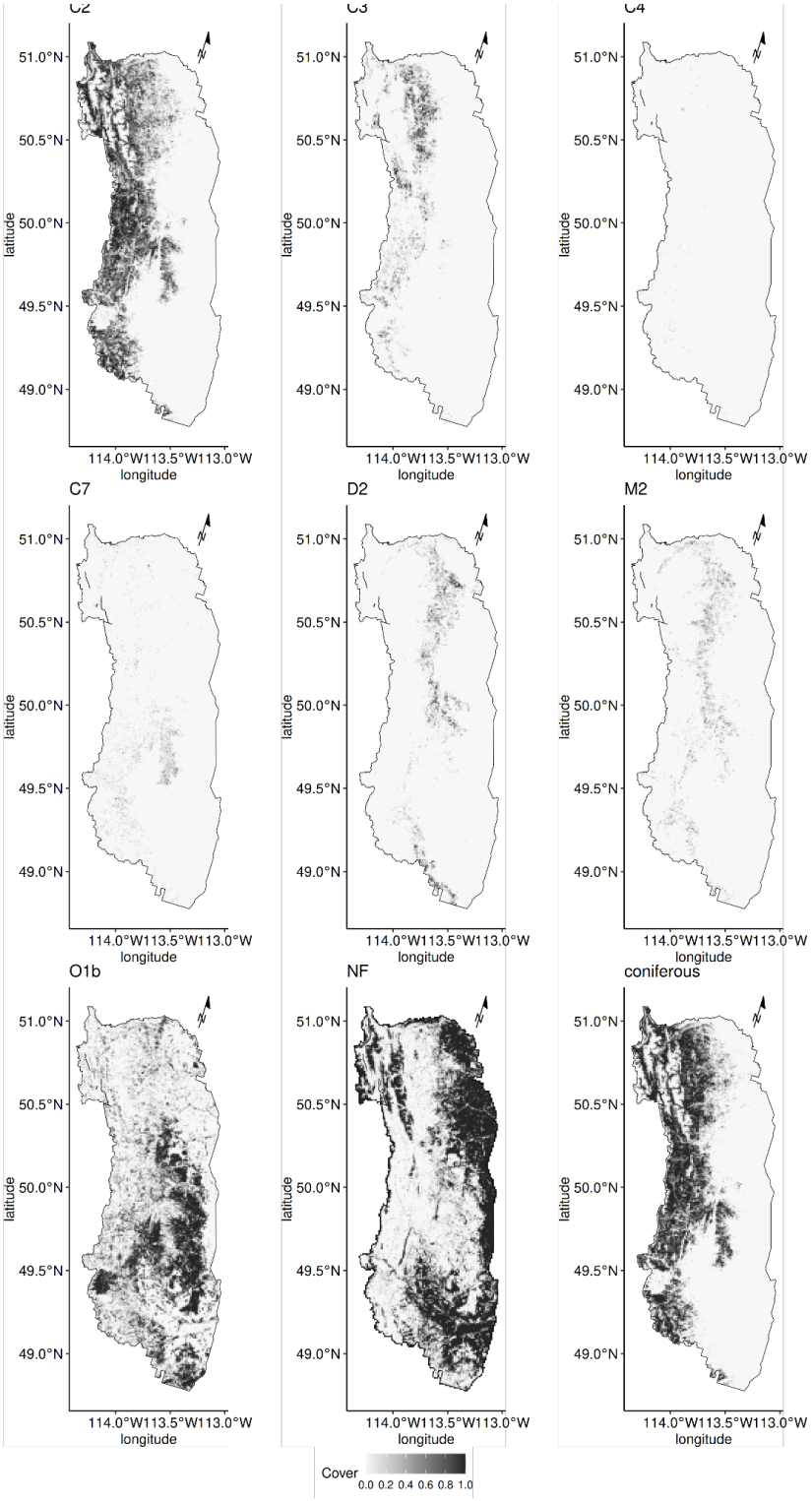

Figure B.2. Maps of fuel type cover per pixel. Cover was calculated as the proportion of 250 m^2 pixels inside each larger 1 Km^2 pixel. Fuel types follow the Canadian Forest Fire Behaviour Prediction System, adapted to the study area. The cover of coniferous fuel types (C2, C3, C4 and C7) was summed into a general “coniferous” fuel type, which was used to fit fire

occurrence models. Fire properties used to influence spread during the simulation used the separate conifer fuel classes. See Table B.7 for fuel type names.

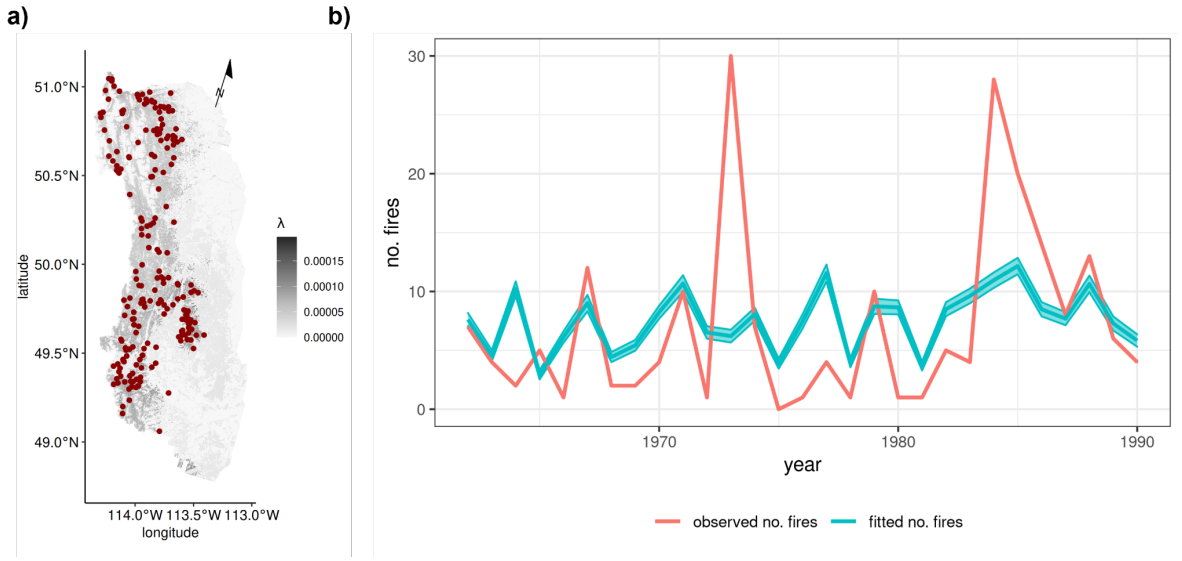

Figure B.3. Observed and modelled fire ignitions. Locations of lightning-caused fires between 1961-1990 in the study area are shown in a) as red points (see Table A.2 for data source) with predicted fire occurrence probabilities (lambda in grey scale). The model used to calculate lambda, related fire occurrences in a) with climate data from 1961-1990 and fuel cover conditions at the start of the simulation (Figure B.2). The model showed good fit with respect to a) where fires are more likely to occur spatially and b) the total number of fires per year across the landscape.

Appendix C

Model input data treatment

Supplementary tables and figures can be found in this or corresponding appendices (e.g. all tables starting Table A.* are found in Appendix A).

The LandR Biomass metamodel carries out a semi-automated, on-the-fly parametrization. The only object that the user must supply is a shapefile that defines the study area. If this study area is within western Canada, the model is able to parametrize itself, provided that it finds enough data. In this work, we also used proprietary datasets to complement the freely available, but often of poorer quality, datasets that are used by default by the modules.
Our study area in the SW Alberta Foothills of the Rocky Mountains range was rasterized using a 250 m^2 grid. Hence, after sourcing the data, spatial objects were subset and reprojected to match the study area perimeter, geographical coordinate system and resolution.

Land cover data (*Biomass_borealDataPrep* module)

Land cover data was used to define the pixels where vegetation and fire dynamics would be simulated (forested pixels), pixels where only fire dynamics were simulated (non-forested, but vegetated pixels - 'non-forested pixels' hereafter) and pixels that were excluded entirely from the simulation. We used land-cover classes from the Land Cover Map of Canada 2010 (Table A.2, Fig. A.1) product. Pixels with classes 1, 2, 5 and 6 were included as 'forested pixels'; non-forested but vegetated classes 8 and 10-12, as well as the naturally non-vegetated class 16 were included as 'non-forested pixels' where fire spread dynamics were allowed. Other land-cover classes that existed in the study area but were completely excluded from the simulation were: 14 - wetland, 15 - cropland, 17 - urban, 18 - water and 19 - snow and ice. Croplands, in particular, were abundant in eastern parts of the study area but were excluded as they do not reflect pre-industrial land-cover and would be too influential on fire spread (Fig. A.1).

Vegetation data

Species cover (Biomass_speciesData module)

Species percent cover (% cover) data were obtained from open and proprietary sources (Table A.2, Fig. A.2) and pre-processed by the *Biomass_speciesData* module. This module ensures 1) that all data use the same geospatial geometries, 2) that these match the study area, and 3) attempts to fill-in and replace the lower quality datasets with higher quality datasets, in increasing order of quality. For this work, we used the freely available species % cover rasters derived from MODIS satellite imagery from 2011, prepared by the National Forest Inventory, Natural Resources Canada Canadian Forest Service (NRCan), (hereafter 'NFI species data'; Beaudoin et al., 2017), as the lowest quality dataset and filled it with better quality proprietary data (in order of lower to higher quality): vegetation inventory data from the Common Attribute Schema for Forest Inventories, spanning years 1990 to 2016 (CASFRI v4, 2016; Cosco, 2011), LandSat-derived data from (Pickell & Coops, 2016) using satellite images from 1990, and species % cover rasters derived from forest inventories by SilvaCom in 2018. After overlaying these four datasets, we selected the species that would be included in the simulation based on a minimum threshold of cover in the study area. The species need to be present in at least 5% of the study area and have at least one pixel with 10% cover). This resulted in a total of six species or species groups: *Abies sp* ('Fir', comprising both *A. lasiocarpa* and *A. balsamea*), *Picea engelmannii* (Engelmann's spruce), *Picea glauca* (White spruce), *Pinus sp* ('Pine', comprising *P. albicaulis*, *P. contorta*), a 'Deciduous' group (comprising *P. tremuloides*, *P. balsamifera* and *Betula papyrifera*) and *Pseudotsuga menziesii* (Douglas-fir).

Stand age and species aboveground biomass (Biomass_borealDataPrep module)

Stand age and stand aboveground biomass (hereafter 'biomass') were obtained and prepared by the *Biomass_borealDataPrep* module (Table A.2). Like the NFI species data, stand age and biomass were rasters derived from MODIS satellite imagery from 2011 prepared by the

National Forest Inventory, NRCan (Beaudoin et al., 2017). *Biomass_borealDataPrep* directly downloads this data and performs a number of data cleaning operations to treat pixels with data inconsistencies. For instance, we detected pixels where species cover was > 0 but biomass was 0, or, inversely, where stand biomass was > 0 but cover was 0. Both age and biomass required fidelity to species % cover, as cover is presumed to be the most accurately estimated variable (especially after the afore-mentioned overlays). We considered age to be the least accurate. In cases with data mismatches, e.g. biomass = 0, cover = 0 and stand age > 0, or where age was missing, we imputed species ages using a linear mixed effects model relating age with the interaction between the log of stand biomass (logStandB), species % cover (cover) and species identity (species), while accounting for the random effect of ecolocation (ecological zone and land cover combination) on intercepts and the slope of the interaction between log standB and species.

$$age \sim logStandB * cover * species + (logStandB * species \,|ecolocation) \quad \text{[Eq. C1]}$$

where '*' denotes the inclusion of separate fixed effects and the interaction between them. Predicted ages were subsequently bounded to 0 on the lower limit.

Species biomass (B) was estimated for each species present in a given pixel by multiplying its relative cover by stand biomass. Since we used satellite-derived species cover data, the allocation of biomass to deciduous species cohorts was adjusted to reflect the fact that broadleaf canopies will typically have higher cover values for the same amount of biomass as coniferous species. Deciduous species cover was then multiplied by an adjustment factor of ≅ 0.84, before being multiplied by stand biomass to obtain the species biomass in the pixel. This value comes from a Gaussian generalised linear model (GLM) relating deciduous species biomass (B) with an interaction term between the log of stand age (logAge), standB, species and land cover (LC):

$$log(B/100) \sim logAge * log(standB/100) * species * LC \quad \text{[Eq. C2]}$$

where '*' denotes the inclusion of separate fixed effects and the interaction between them. The model was parameterized using similar data covering the entire Northwest Territories Province, Canada, and an optimization routine that searched for the best conversion factor

between deciduous cover and B, by minimizing AIC. The best conversion factor was found by refitting the model on different sets of B values (the response), recalculated by changing deciduous relative cover values between 0.1 and 1.

Permanent sample plot data and simulated species data (Biomass_speciesParameters module)

The *Biomass_speciesParameters* module used permanent sample plot (PSP) and simulated data to estimate species traits associated with growth and mortality. The PSP were obtained from the Canadian provinces of British Columbia, Alberta and Saskatchewan, treated for errors and standardized into a single dataset. The data include individual species and diameter at breast height (DBH) measurements for each tree in a plot, as well as stand age. As part of the standardization process, dead trees were removed from the dataset, and a minimum DBH of 10 cm was applied to ensure a consistent measurement cut-off. Tree biomass was then derived from DBH using the model by Lambert and colleagues (2005) and summed by plot. Lastly, the proportional biomass of each species was calculated for every individual measurement of each plot. General additive mixed effect models (GAMMs) were then used to model the annual biomass of the real species in the PSP dataset. For a given species, observations were excluded from the data if the corresponding species proportional biomass did not exceed 50% (e.g. for P. tremuloides, plots were only included if 50% of the biomass was composed of P. tremuloides). Measurement year and plot ID were random variables, and the proportional biomass was used to weight observations.

The simulated data came from runs of LandR Biomass used to create over 200,000 growth curves of theoretical species that differed in terms of growth and mortality traits (growth curve and mortality shape), longevity, and maximum aboveground net primary productivity (maxANPP). The annual biomass of each theoretical species (i.e. growth curves) was simulated using LandR Biomass with no reproduction, competition, disturbance, or dispersal, and only one cohort. These theoretical species growth curves were later used to find the most

likely combination of species traits by comparing the simulated growth curves and the PSP-derived GAMMs (see Appendix B).

Invariant species traits (Biomass_borealDataPrep and Biomass_speciesParameters modules)

Most species traits that did not vary spatio-temporally were obtained from available species trait tables used in LANDIS-II (Table A.2). Some were then adapted to our study using published literature and statistical models using LandR *Biomass_speciesParameters* (see Appendix B). Only a few invariant species traits needed to be adjusted "manually" to obtain more realistic successional dynamics in the study area.

The LANDIS-II species trait table contains species trait values for each Canadian Ecozone (NRCan, 2013), which we filtered to the Boreal Shield West (BSW), Boreal Plains (BP) and Montane Cordillera (MC) Canadian Ecozones. Most trait values did not vary across these ecozones, but when they did, we took the minimum value. Longevity values were adjusted to match the values in Table 2 of Burton & Cumming (1995) for the BSP and BP ecozones, and Tables 1 and 2 of Burton & Cumming (1995) corresponded to the MC ecozone depending on the species considered. These adjustments resulted in higher longevity for most species. As first runs revealed an excessive recruitment of young cohorts even after several decades of biomass accumulation, we lowered shade tolerance values (shade tolerance in Table B.1) to decrease cohort recruitment as stand biomass increased (*Abies sp*. from 4 to 2.3, *Picea engelmannii* from 4 to 2.1, *P. glauca* from 3 to 1.6, *Pseudotsuga menziesii* from 3 to 2). The relative ranking of species shade tolerances was maintained, except for *Picea glauca* and *Pseudotsuga menziesii*, the first becoming slightly less shade tolerant than the second. This aims at reflecting *P. glauca's* ability to recolonize disturbed sites alongside *Pinus contorta*, while *P. menziesii* is successional to *P. contorta* (Steinberg, 2002; Abrahamson, 2015). *Pinus sp* and *Populus sp* remained unchanged, with the lowest shade tolerance possible, 1.0.

Fire data (*fireSense_DataPrep* module)

We used fire point data to estimate the average number of fires across the landscape during a reference period. Fire point data were directly downloaded by the *fireSense_DataPrep* module from the National Fire Database available at Canadian Wildland Fire Information System database (Canadian Forest Service; see Table A.2). The module then filtered the fire occurrences to lightning-caused fires that occurred between 1961-1990, resulting in a total of 213 fire locations in the study area (Fig. B.3a). Although this period does not reflect 'pre-industrial' conditions (i.e. pre-1940's), it provides good-confidence data on both fire occurrences and climate, while still being commonly accepted as a baseline with regards to climate change.

Weather data (*fireWeather* module)

Weather data used to determine fire ignitions across the landscape, fire spread and fire severity, came from simulations of 'historic' daily weather using the software BioSIM v11 (Régnière et al., 2017). To generate these simulations, we provided BioSIM with a digital elevation model raster layer of the LIM study area at 1 Km2 resolution and Canada-US climate normals between 1961-1990 to generate daily values of average air temperature, total precipitation, relative humidity and wind speed at 10m high, for each pixel (see Table A.2 for data sources). The generated daily weather data are kept in a private online storage (GoogleDrive) and imported automatically by the *fireWeather* module if the user has permission to access it. The module then summarises the data in two ways. Into a table of July's average monthly drought code (MDC) for each year and each pixel, used by FireSense modules to estimate the average number of fires in the landscape; and into a table of daily weather values per pixel subset for 'fire days' only. We considered a day to be a 'fire day' if the fire weather index (FWI) was >= 19, a value considered to define a potential fire spread day (Podur & Wotton, 2011). Both July's MDC and FWI were calculated using the cffdrs R package (Wang et al., 2017), using default initial values for fine fuel moisture code, duff moisture code and drought code: 85, 6 and 15, respectively.

Field age data

We compared our simulated results with a dendroecological dataset of species ages collected in a smaller region within the LIM study area. The data was collected and analysed as part of the "fire regime reconstruction" subproject of the Landscapes in Motion Project, during three summer field campaigns in 2017, 2018 and 2019. The age data was built from crossdated increment cores collected from trees in plots distributed in the Montane subregion (Fig. 1, main text). Plot distribution followed a stratified sampling approach that aimed at maximising the range of forest types sampled within the Montane subregion. Small trees (< 4 cm of diameter at breast height, DBH) were not sampled. To restrict analyses to the pre-industrial period, all tree samples taken from stands estimated to having been established after 1940 (considered the turning point for industrialisation in the area, with the advent of the railway; REF) were excluded. The remainder of the data included a total of 51 distinct patches, with the number of cores sampled per patch varying between 10 and 79, and reconstructed tree ages varying between 77 and 449 years.

To compare between simulated cohort ages and field-based ages, we filtered the simulated data so that it best matched the field methods applied. This meant excluding simulated pixels that did not experience fires during the quasi-equilibrium period (last 500 years of the simulations), and excluding cohorts that would be too young/small to be sampled in the field, i.e. those smaller than minimum DBH (4cm). Given that none of the sampled trees had a DBH = 4cm and for many species the smallest DBHs were more than double the minimum DBH (e.g. the smallest *Abies lasiocarpa* before any filtering was applied had DBH = 12.8 cm), we modelled age as a function of DBH and species to estimate age at minimum DBH. For this we used a zero-intercept logarithmic model with an interaction between DBH and species, but no main effect of species to maintain a zero-intercept across all species (Eq. C3, Fig. C.2).

$$age \sim -1 + log(DBH) : species \quad \text{[Eq. C3]}$$

We then estimated age at DBH = 4 for each species and used it to exclude young simulated cohorts when comparing between simulated and observed ages.

Table C.1. Estimates of species ages at minimum DBH (4 cm). Note that indicated species follow the species names and groups used in the simulation, to which these estimates were applied to filter data used for comparisons with observations.

Species	Estimated age at min. DBH
Abies spp	51
Picea engelmannii	46
Pinus spp	49
Populus spp	47
Pseudotsuga menziesii	53

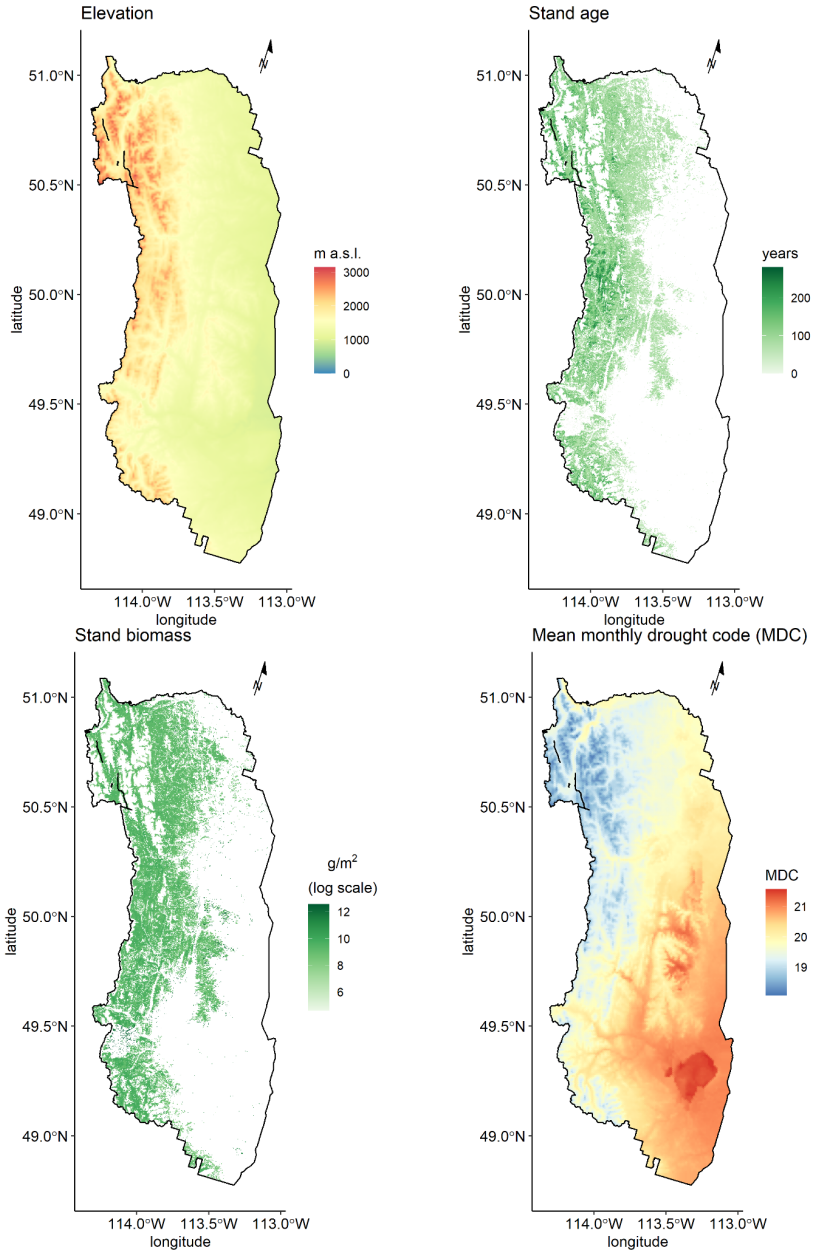

Figure C.1. Elevation, stand age, stand biomass and mean monthly drought code across the study area. Stand age and stand biomass values refer to the start of the simulation. Mean monthly drought code values were averaged across the climate period of 1961-1990. Please see Table A.2 for data sources.

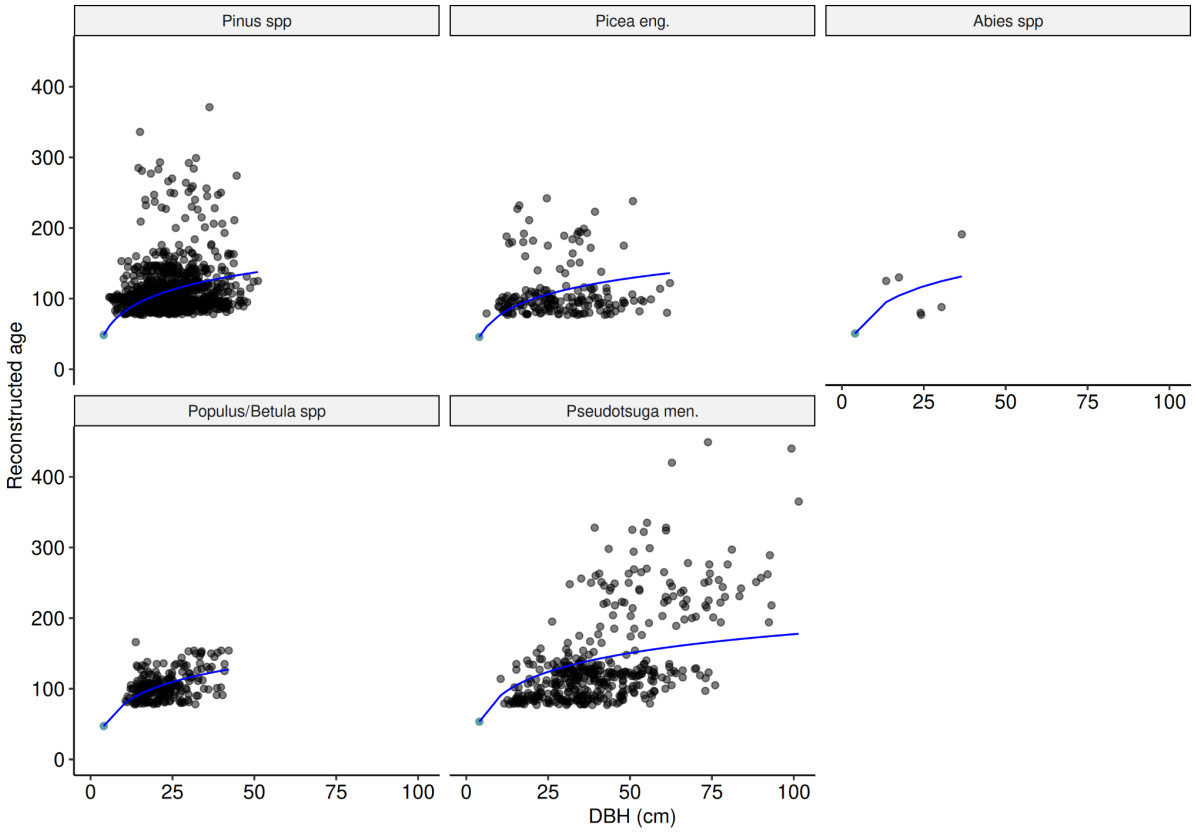

Figure C.2. Logarithmic model predictions (blue line) of tree-ring derived ages (reconstructed age) as a function of diameter at breast height (DBH) by species. Light blue point indicates prediction at minimum DBH = 4cm; black points are the observed data used to fit the model.

Appendix D

Measuring pyrodiversity and forest diversity

&

Forest cover type classification

Fire attributes for pyrodiversity

Pyrodiversity was based on fire frequency, mean patch size and mean actual fire severity, calculated at the end of the simulation for each pixel following the approach by Steel et al. (2021). Fire frequency was calculated as the mean fire-interval, with fire interval being the number of years between subsequent fires in a pixel, and including start and end years of the simulation period. To calculate mean patch size, we first calculated the patch size (i.e., number of pixels) of each fire severity class within each simulated fire. Then, for each pixel, we calculated average patch size across all severity classes and all fires that intersected that pixel. Mean actual fire severity was calculated as the mean proportional biomass burnt across all fires that the pixel intersected.

Hypervolume calculations

Hypervolume calculations largely followed Barros et al. (2016). We ensured the orthogonality of the dimensions (i.e., variables) entering the hypervolumes and the comparability between different hypervolumes of the same kind (i.e., pyro- or forest diversity), by calculating hypervolumes on the axes of a Principal Components Analysis (PCA). Pyrodiversity hypervolumes were calculated using the three axes of a PCA calculated on the dataset of scaled pixel-level fire attributes (fire frequency, mean patch size and mean fire severity) pooled across all forest types, scenarios and repetitions. Forest diversity hypervolumes were calculated using the first four axes of a PCA calculated on the dataset of pixel-level forest attributes (species relative abundances and mean and standard deviation of age) pooled across all forest types, years (first and last), scenarios and repetitions. In the case of forest

diversity hypervolumes, using a PCA resulted in a dimensionality reduction from the initial eight variables (relative biomass of six species plus two age variables), which is highly recommended (Barros et al., 2016; Blonder et al., 2014).

Hypervolumes were estimated using a one-class support vector machine (SVM) learning model, which "1) [transforms] the input data into a high-dimensional nonlinear space in which the data points can be optimally separated from background by a single hyperplane, 2) [back-transforms] the hyperplane into the original space, 3) [delineates] an adaptive grid of random points near the original data points, and 4) [uses] the SVM to predict if each of these points is in or out" (Blonder, 2019; Blonder et al., 2018). We used default values for all parameters, except *svm.gamma* which partly influences the wrapping of the hypervolume shape to the data. In this case, we changed its value from 0.5 to 0.01, which increased the influence radius of data points on defining the hypervolume. Each hypervolume (i.e., each combination of scenario, replicate and forest type where applicable) was calculated three times to account for variability generated by the hypervolume estimation algorithm.

Forest cover type classification

The age data obtained from field campaigns in the LIM study area was organised into sampling plots that were classified in terms of forest type. This forest type classification was based on a series of rules evaluating the basal area densities of different species and functional groups in the plot. In order to compare our simulated ages with those observed in the field, we classified our pixels using a similar approach based on relative biomass (*relB*) of different species grouped into the same functional types. Here, we detail the ruleset behind this classification. Several of the species (and forest types) included in this classification are not relevant in the study area, were not captured in the field sampling, or were not simulated by the model, or weren't explicitly simulated but could be seen as part of a simulated group of species (e.g. *Pinus* species were collapsed to genus level). In the latter case, we considered that the simulated "species" represented either of the corresponding species in the field. When no species were present in a pixel, the forest type was classified as 'No forest'.

Species codes and names, with correspondences to simulated species in brackets:

- PIPO: *Pinus ponderosa* (not simulated)
- QUGA: *Quercus garryana* (not simulated)
- PIED: *Pinus edulis* (not simulated)
- PIMO2: *Pinus monophyla* (not simulated)
- PIMO: *Pinus monticola* (not simulated)
- PIFL: *Pinus flexilis* (Pinu_sp)
- PICO: *Pinus contorta* (Pinu_sp)
- PIEN: *Picea engelmannii* (Pice_eng)
- PIGL: *Picea glauca* (Pice_gla)
- ABLA: *Abies lasiocarpa* (Abie_sp)
- JUSC, JUOC and JUOS: *Juniperus scopulorum*, *J. occidentalis*, *J. osteosperma* (not simulated)
- POTR5: *Populus trichocarpa* (not simulated)
- POTR, POBA: *Populus tremuloides, P. balsamifera* (Popu_sp)
- BEPA: *Betula papyrifera* (Popu_sp)
- PSME: *Pseudotsuga menziesii* (Pseu_men)
- THPL: *Thuja plicata* (not simulated)

Forest cover type codes and names (* indicates forest types present in this study, simulated or observed):

- Oak: Garry oak woodland
- PJ: Pynion juniper woodland
- purePIPO: relatively pure Ponderosa pine
- DMCPIPO: Dry mixed conifer (DMC) with Ponderosa pine
- *dryPSME: Dry Douglas-fir-dominated (simulated only)
- *PSME: Douglas-fir dominated (dry species absent)

- *DMCPSME: Dry mixed conifer (dominated by Douglas-fir and can contain patches of broadleaf species)
- *PICO: relatively pure Lodgepole pine
- *PIEN: Spruce-dominated
- *Broadleaf: relatively pure broadleaf
- *Mixedwood: relatively even broadleaf and conifer mix.
- *MMC: Moist mixed conifer (can contain patches of broadleaf species)

Parameters used in classification:

- *pure.cutoff*: threshold of relative biomass defining species (of functional group) dominance. Set to 0.8.
- *drySpp*: a vector of species considered to be indicators of dry site conditions. Set to {PSME, PIPO, PIFL, JUSC, QUGA}.
- *moistSpp*: a vector species considered to be indicators of moist site conditions. Set to {ABLA, BEPA, PIEN, PIGL, PIMO, POBA, THPL}.

Ruleset

Relative biomass (*relB*) was calculated per simulated species in a pixel, by dividing the sum of cohort biomasses by the total stand biomass. When a simulated species corresponded to several species codes the relative biomass was only counted once for summing purposes. For example, $S(relB_{POTR}, relB_{BEPA})$ was actually just $S(relB_{POTR})$, as POTR and BEPA were not simulated independently. The rules are a series of hierarchical decisions (which we numbered here), whereby if the first condition applies the pixel/stand is classified as that forest type and following conditions are not evaluated. See full list of rules in Table D.1.

Table D.1. List of hierarchical conditions constituting the rules used to classify pixels according to forest types used in the age dataset collected in the field. *S(...)* stands for sum of '…' elements. See forest type meanings above.

Order	Conditions	Forest type
1	$relB_{QUGA}$ >= pure.cutoff AND S($relB_{PIPO}$, $relB_{PSME}$, $relB_{PIED}$, $relB_{PIMO2}$, $relB_{JUSC}$, $relB_{JUOC}$, $relB_{JUOS}$) < 0.05	Oak
2	S($relB_{PIED}$, $relB_{PIMO2}$, $relB_{JUSC}$, $relB_{JUOC}$, $relB_{JUOS}$, $relB_{QUGA}$) >= pure.cutoff AND S($relB_{PIPO}$, $relB_{PSME}$) < 0.05	PJ
3	S($relB_{PIPO}$) >= pure.cutoff AND S($relB_{PSME}$, $relB_{PIFL}$, $relB_{PIED}$, $relB_{PIMO2}$, $relB_{JUSC}$, $relB_{JUOC}$, $relB_{JUOS}$, $relB_{QUGA}$) < 0.30	purePIPO
4	$relB_{PIPO}$ >= 0.10 AND $relB_{PIPO}$ < pure.cutoff AND S($relB_{PSME}$, $relB_{PIPO}$, $relB_{PIFL}$, $relB_{PIED}$, $relB_{PIMO2}$, $relB_{JUSC}$, $relB_{JUOC}$, $relB_{JUOS}$, $relB_{QUGA}$) >= 0.50	DMCPIPO
5	$relB_{PSME}$ >= pure.cutoff AND S(moistSpp) < 0.10 AND S($relB_{JUSC}$, $relB_{JUOC}$, $relB_{JUOS}$, $relB_{PIFL}$, $relB_{PIED}$, $relB_{PIMO2}$, $relB_{QUGA}$) > 0.05	dryPSME
6	$relB_{PSME}$ >= pure.cutoff AND S(moistSpp) < 0.10 AND S($relB_{JUSC}$, $relB_{JUOC}$, $relB_{JUOS}$, $relB_{PIFL}$, $relB_{PIED}$, $relB_{PIMO2}$, $relB_{QUGA}$) <= 0.05	PSME
7	S (drySpp) >= 0.50 AND S(moistSpp) < 0.10	DMCPSME
8	$relB_{PICO}$ >= 0.50	PICO
9	S($relB_{PIEN}$, $relB_{PIGL}$, $relB_{ABLA}$) > 0.50	PIEN
10	S($relB_{POTR}$, $relB_{POTR5}$, $relB_{POBA}$, $relB_{BEPA}$) >= pure.cutoff	Broadleaf
11	S($relB_{POTR}$, $relB_{POTR5}$, $relB_{POBA}$, $relB_{BEPA}$) >= 0.25 AND S($relB_{POTR}$, $relB_{POTR5}$, $relB_{POBA}$, $relB_{BEPA}$) < pure.cutoff	Mixedwood
12	If none of the above conditions apply	MMC